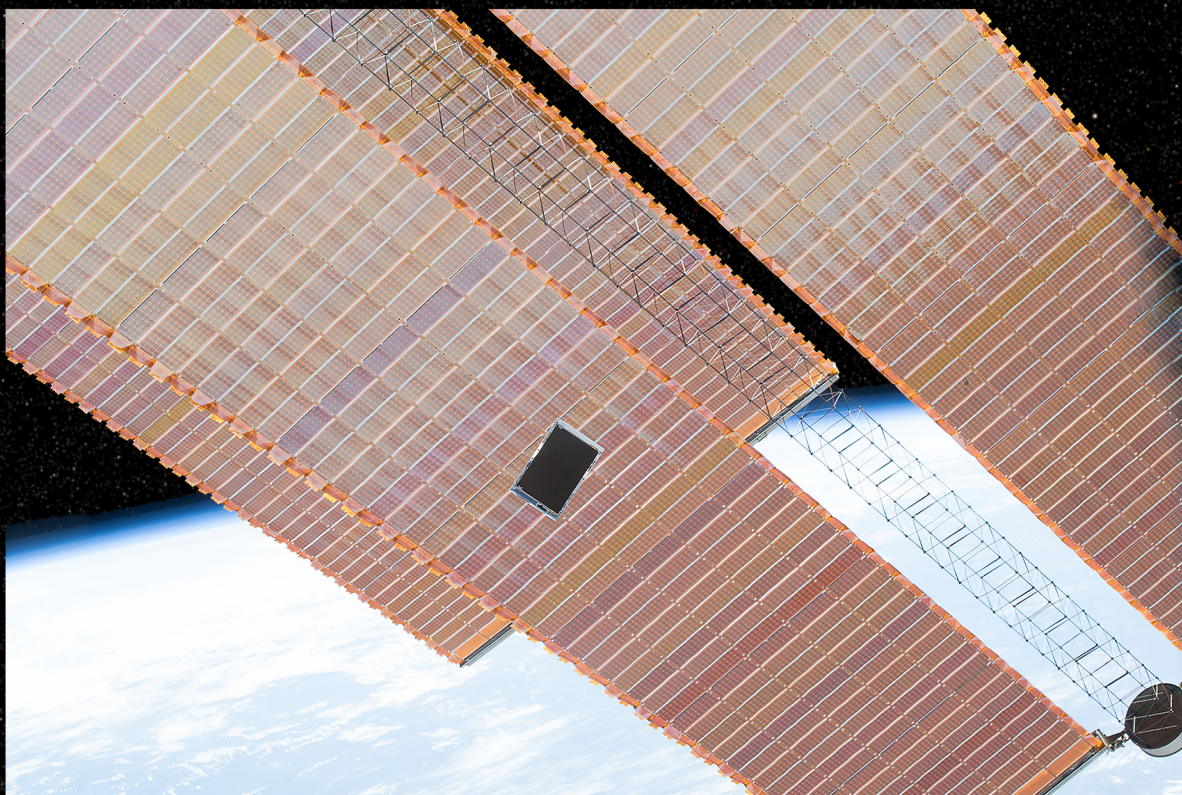




Arcsecond Space Telescope Enabling Research in Astrophysics (ASTERIA) Telecommunications

*Alessandra Babuscia, Peter di Pasquale,
Matthew W. Smith, Jim Taylor*



June 2019

Jet Propulsion Laboratory
California Institute of Technology

DESCANSO
Deep Space Communications and Navigation Systems
Center of Excellence

Near Earth Design and Performance Summary Series

The Cover

The ASTERIA satellite, launched in August 2017 to the International Space Station, was deployed from there into low-Earth orbit on November 20, 2017. ASTERIA is an abbreviation for Arcsecond Space Telescope Enabling Research in Astrophysics.

ASTERIA is a CubeSat, a type of small satellite consisting of “units” that are 10 centimeters cubed, or about 4 inches on each side. ASTERIA is the size of six CubeSat units, making it roughly 10 centimeters by 20 centimeters by 30 centimeters¹. With its two solar panels unfolded, the satellite’s longest dimension is just over 60 cm (about two feet). ASTERIA, weighs 10.2 kilograms (about 22 pounds). The spacecraft utilized commercially available CubeSat hardware where possible, thus contributing to a general knowledge of how those components operate in space. ASTERIA is the first CubeSat mission to be operated out of JPL.

The photograph shows the ASTERIA spacecraft (center) a few seconds after deployment from the International Space Station. ASTERIA is traveling from the upper-right corner of the frame toward the lower-left corner. The ISS solar arrays and supporting truss structure are visible in the background.

ASTERIA carries a payload for measuring the brightness of stars, which allows researchers to monitor nearby stars for orbiting exoplanets that cause a brief drop in brightness as they block the starlight. This approach to finding and studying exoplanets is called the transit method, the same as NASA’s Kepler Space Telescope uses.

The payload also employs a control system to reduce “noise” in the data created by temperature fluctuations in the satellite, allowing the instrument to carefully monitor stellar brightness. The temperature of the controlled section of the detector fluctuates by less than 0.02 degree Fahrenheit (0.01 Kelvin, or 0.01 degree Celsius) during observations.

¹ Measured dimensions are $37 \times 24 \times 12$ cm (before solar panel deployment).



Near Earth Design and Performance Summary Series

Article 2

Arcsecond Space Telescope Enabling Research in Astrophysics (ASTERIA) Telecommunications

Alessandra Babuscia

Peter di Pasquale

Matthew W. Smith

Jim Taylor

*Jet Propulsion Laboratory
California Institute of Technology
Pasadena, California*

**National Aeronautics and
Space Administration
Jet Propulsion Laboratory
California Institute of Technology
Pasadena, California**

June 2019

This research was carried out at the Jet Propulsion Laboratory, California Institute of Technology, under a contract with the National Aeronautics and Space Administration.

Reference herein to any specific commercial product, process, or service by trade name, trademark, manufacturer, or otherwise, does not constitute or imply endorsement by the United States Government or the Jet Propulsion Laboratory, California Institute of Technology.

Copyright 2019 California Institute of Technology.
Government sponsorship acknowledged.

NEAR EARTH DESIGN AND PERFORMANCE SUMMARY SERIES

Issued by the Deep Space Communications and Navigation Systems

Center of Excellence

Jet Propulsion Laboratory

California Institute of Technology

Jon Hamkins, Editor-in-Chief

Articles in This Series

***Article 1*—“Soil Moisture Active Passive (SMAP) Telecommunications”**

Jim Taylor, William Blume, Dennis Lee, and Ryan Mukai

***Article 2*—“Arcsecond Space Telescope Enabling Research in Astrophysics (ASTERIA)**

Telecommunications”, Alessandra Babuscia, Peter di Pasquale, Matthew W. Smith, Jim Taylor

Foreword

This Near Earth Design and Performance Summary Series, issued by the Deep Space Communications and Navigation Systems Center of Excellence (DESCANSO), is a companion series to the Design and Performance Summary Series and the JPL Deep Space Communications and Navigation Series. Authored by experienced scientists and engineers who participated in and contributed to near-Earth missions, each article in this series summarizes the design and performance of major systems, such as communications and navigation, for each mission. In addition, the series illustrates the progression of system design from mission to mission. Lastly, the series collectively provides readers with a broad overview of the mission systems described.

Jon Hamkins
DESCANSO Leader

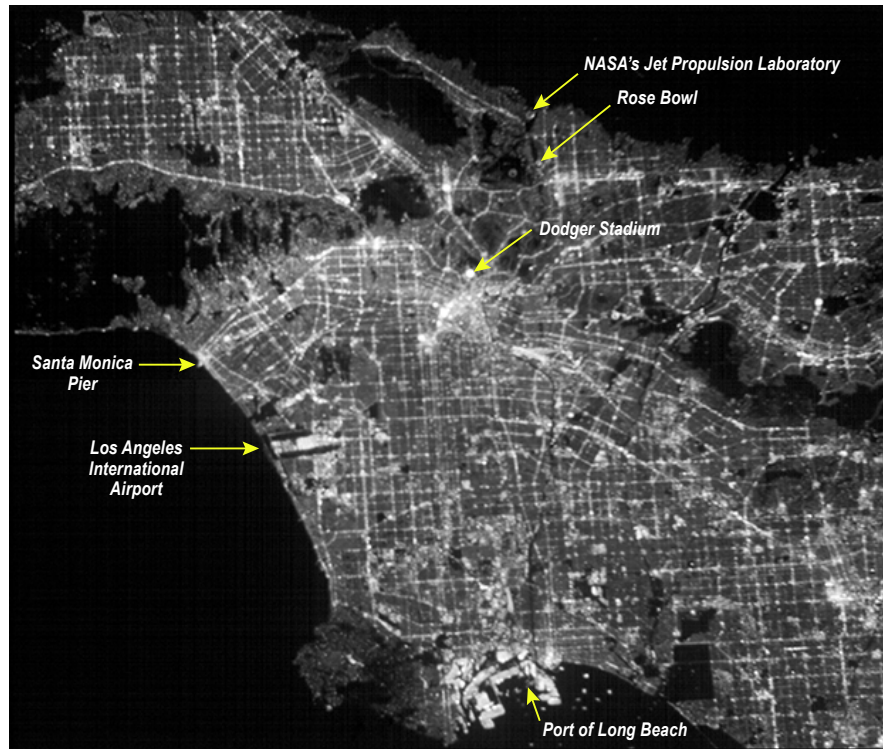
Near Earth and Deep Space Missions

Near Earth and deep space communications differ from each other in several ways. The ASTERIA spacecraft/Earth station communications links operate at much shorter distances than those deep space missions that communicate with the Deep Space Network. Additionally, ASTERIA is a CubeSat which is different from other missions because it is much smaller and has many more constraints.

Mission Status

As of May 2019 [1]

Shortly before this article was posted and continuing in its extended mission orbit, ASTERIA looked down at Earth to capture several images of the greater Los Angeles region in California. The mission team took the images to further test the capabilities of the satellite. The images, taken March 29, 2019, reveal a massive grid of illuminated city streets and freeways. The image below shows a region of about 43.5 square miles (70 square kilometers) with a resolution of about 100 feet (30 meters) per pixel.



Annotated image of Los Angeles area from ASTERIA, March 29, 2019. Credit: NASA/JPL-Caltech

Many orbiting small satellites can take higher-quality pictures of Earth than this one. But ASTERIA is the only CubeSat in orbit that can also look for exoplanets, or planets orbiting stars other than our Sun. Its primary mission objective was to demonstrate precision-pointing technology in a small satellite.

As of January 2019

Since this Descanso article went into final editing September 2018, ASTERIA has continued operating nominally and it is currently in its third extended mission. Passes are scheduled and executed regularly with the Morehead State University ground station, and they are on a cadence of 1–2 passes per day.

In addition to the nominal mission activities, an experiment was performed in January 2019 using an Amazon Web Service (AWS) ground station. Specifically, while ASTERIA was performing its regular downlink operations with the Morehead State ground station at its nominal data rate (1 Mbps), the AWS station was also listening to attempt to lock on the transmitted signal. The experiment was successful as the AWS station locked on the signal and frames were received. The experiment is significant as it shows the

possibility for future CubeSat missions to use AWS stations, hence increasing telecommunication options and providing additional flexibility in operations.

As of September 2018 [2–4]

As of September 2018, ASTERIA had accomplished all of its primary mission objectives, demonstrating that the miniaturized technologies on board can operate in space as expected. This marks the success of one of the world’s first astrophysics CubeSat missions, and shows that small, low-cost satellites could be used to assist in future studies of the universe beyond the solar system.

The ASTERIA team demonstrated that the satellite’s payload can point directly and steadily at a bright source for an extended period of time, a key requirement for performing the precision photometry necessary to study exoplanets via the transit method. ASTERIA achieved the first detection of a transiting exoplanet by measuring the known transit of the super-Earth exoplanet 55 Cancri e [3].

Holding steady on a star while in Earth orbit is difficult because there are many things that subtly push and pull on the satellite, such as Earth’s atmosphere and magnetic field. ASTERIA’s payload achieved a pointing stability of 0.5 arcseconds RMS, the amount the payload wobbles away from its intended target over a 20-minute observation period. The pointing stability was repeated over multiple orbits, the stars positioned on the same pixels on each orbit.

The ASTERIA mission earned the Small Satellite Mission of the Year award from the Small Satellite Technical Committee of the American Institute of Aeronautics and Astronautics (AIAA). The award is given to a mission that has “demonstrated a significant improvement in the capability of small satellites,” according to the award description. The award was presented in August 2018 at the annual Small Satellite Conference in Logan, Utah [4].

Acknowledgments

The authors would like to acknowledge all the ASTERIA team members and mentors who have supported the design, integration, testing, and operation of the mission throughout the years. Additionally, the authors are thankful for the support of the ground operation team at Morehead State University. Finally, the authors would like to acknowledge Sarah Gavit and the JPL Phaeton Program for early career hires, which has supported the mission from the very beginning.

Table of Contents

Foreword.....	iv
Near Earth and Deep Space Missions.....	v
Mission Status	vi
Acknowledgments	viii
1 ASTERIA Mission and Overview.....	1
1.1 ASTERIA Mission Objectives	1
1.2 Mission Phases	1
1.2.1 Launch and Deployment from ISS.....	1
1.2.2 Deployment.....	1
1.2.3 Spacecraft Initial Acquisition.....	2
1.2.4 Checkout.....	2
1.2.5 Technology Demonstration.....	3
1.2.6 Photometric Demonstration	3
1.2.7 Photometric Observation	3
1.2.8 Decommissioning.....	3
1.3 Orbit.....	4
2 ASTERIA Spacecraft Overview	5
2.1 Structure	6
2.2 Power	6
2.3 Command and Data Handling	6
2.4 Flight Software	6
2.5 Thermal	7
2.6 Attitude Determination and Control	7
2.7 Science Payload.....	7
3 Telecommunications Subsystem.....	9
3.1 Overview	9
3.2 Telecom Block Diagram and Subsystem Design.....	11
3.3 Antennas.....	12
3.4 Transceiver	14
3.5 Telecom Subsystem Mass and Power.....	15
3.6 Communication Module.....	15
3.6.1 Boot and Configuration	16
3.6.2 Antenna Switching.....	17
3.6.3 Radio Duty Cycle.....	18
4 Tracking Station and Data System.....	19
4.1 Morehead State University Ground Station	19
4.1.1 Downlink Processing.....	21
4.1.2 Uplink Processing	21
4.2 Compatibility Test at Morehead State University	22
4.3 ASTERIA Ground Data System (GDS).....	30
4.3.1 GDS Overview	30
4.3.2 WTCCS	30
4.3.3 OpenMCT	32

4.3.4	Custom Scripts and Webpages.....	33
4.3.5	Third-party Tools	35
5	Link Performance.....	36
5.1	Link Analysis.....	36
5.1.1	Uplink Performance	36
5.1.2	Downlink Performance.....	39
5.2	Orbital Analysis.....	41
5.2.1	Passes Statistics.....	41
5.2.2	Doppler Analysis.....	44
5.3	Spectrum Considerations and License Process.....	45
6	Flight Operations.....	47
6.1	Overview of the Operations Cycle.....	47
6.2	Operations Planning.....	49
6.2.1	Deployment and Initial Acquisition	49
6.2.2	Planning and Sequencing Following Initial Acquisition	49
6.2.3	Flight Rules.....	49
6.2.4	Contingency Planning	50
6.3	Execution.....	50
6.4	Lessons Learned	53
7	In-flight Performance	54
7.1	Spacecraft Deployment	54
7.2	Telecommunication Acquisition.....	54
7.3	Radio Checkout and Link Performance Achieved.....	54
8	References	61
9	Abbreviations, Acronyms, and Nomenclature.....	62

List of Figures

Annotated image of Los Angeles area from ASTERIA, March 29, 2019. Credit: NASA/JPL-Caltech	vi
Figure 1: ASTERIA deployment from dispenser on the International Space Station.	2
Figure 2: Beta angle and eclipse duration during the ASTERIA prime mission.....	4
Figure 3: ASTERIA flight vehicle with solar array deployed.....	5
Figure 4: ASTERIA internal components.....	5
Figure 5: ASTERIA communication links and data rates.....	9
Figure 6: ASTERIA telecommunication system block diagram.	11
Figure 7: ASTERIA interior computer-aided design (CAD) model.....	12
Figure 8: Patch antenna. (Courtesy of Vulcan Wireless Inc.)	13
Figure 9: Antenna pattern. (Courtesy of Vulcan Wireless Inc.).....	13
Figure 10: Return loss. (Courtesy of Vulcan Wireless Inc.)	14
Figure 11: CSR-SDR-S/S radio. (Courtesy of Vulcan Wireless Inc.)	15
Figure 12: Boot sequence and operational behavior for the radio.....	17
Figure 13: Flight software concept of operation for the radio.....	18
Figure 14: Radio power cycle behavior.	18
Figure 15: Morehead State University ground station location and ASTERIA orbit.....	19

Figure 16: Morehead State University 21-m antenna.	20
Figure 17: ASTERIA downlink diagram.	21
Figure 18: ASTERIA uplink diagram.	22
Figure 19: Test 1 uplink configuration (cabled, Project modem and server to CSR radio).	23
Figure 20: Test 1 downlink configuration (cabled, CSR radio to Project modem and server).	23
Figure 21: Test 2 uplink configuration (cabled, Morehead modem and server to CSR radio).	24
Figure 22: Test 2 downlink configuration (cabled, CSR radio to Morehead modem and server).	24
Figure 23: Test 3 uplink configuration (wireless, Project modem and server to CSR radio).	25
Figure 24: Test 3 downlink configuration (wireless, CSR radio to Project modem and server).	25
Figure 25: Test 4 uplink configuration (wireless, Morehead modem and server to CSR radio).	26
Figure 26: Test 4 downlink configuration (wireless, CSR radio to Morehead modem and server).	26
Figure 27: Compatibility test setup.	27
Figure 28: Ground station setup at Morehead State University.	27
Figure 29: ASTERIA GDS Overview. (Note that the testbed is not shown.)	30
Figure 30: ASTERIA WTCCS Operator’s Console.	31
Figure 31: Web architecture for ASTERIA.	32
Figure 32: OpenMCT plot for ASTERIA.	34
Figure 33: ASTERIA uplink product generation tools.	35
Figure 34: ASTERIA coverage map in 2D on a Mercator map.	41
Figure 35: ASTERIA accesses simulated for one year (daylight-only tracking).	42
Figure 36: ASTERIA accesses simulated for one year (daylight and nighttime tracking).	43
Figure 37: Simulated Doppler shift during the 4 October 2017 telecommunication contact.	44
Figure 38: Simulated Doppler shift during the 7 November 2017 telecommunication contact.	44
Figure 39: ASTERIA measured radio spectrum. The red line indicates the NTIA mask.	46
Figure 40: ASTERIA Command Product Life Cycle.	48
Figure 41: Deployment pass planning from the ASTERIA Operational Readiness Review.	51
Figure 42: Real time telecom monitoring by spacecraft operator during initial ASTERIA acquisition.	52
Figure 43: Real-time telemetry values during Pass 30 (Antenna 1 used).	57
Figure 44: Real-time telemetry values during Pass 30 (radio processor temperature).	57
Figure 45: Real-time telemetry values during Pass 30 (oscillator temperature).	58
Figure 46: Real-time telemetry values during Pass 30 (power amplifier voltage).	58
Figure 47: Real-time telemetry values during Pass 30 (lock status).	59
Figure 48: Approximate value of E_b/N_0 for high-rate downlink per weeks of operation.	59
Figure 49: Number of radio crash events per week of operations.	60

List of Tables

Table 1: ASTERIA telecommunication signal parameters.	10
Table 2: Telecom configuration plan for each mission phase.	10
Table 3: Antenna characteristics.	12
Table 4: Transceiver characteristics.	14
Table 5: ASTERIA telecom subsystem mass and power input.	15

Table 6: S-band ground station characteristics [from Ref. 8].	20
Table 7: Results of Test 1 through Test 4.	28
Table 8: Uplink design table (32 Kbps data rate).	37
Table 9: Uplink design table (4 Kbps data rate).	38
Table 10: Downlink design table (1 Mbps data rate).	39
Table 11: Downlink design table (10 Kbps data rate).	40
Table 12: Tracking and acquisition bandwidth for the ASTERIA radio over temperature.	45
Table 13: ASTERIA ORT activities and activity leads.	47
Table 14: Real-time telecommunication telemetry values during Passes 2 and 3.	55
Table 15: Real-time telecommunication telemetry values during Pass 4.	55
Table 16: Real-time telecommunication telemetry values during Pass 5.	56

1 **ASTERIA Mission and Overview**

ASTERIA [5] (Arcsecond Space Telescope Enabling Research in Astrophysics) is a 6U CubeSat designed, integrated, and operated by JPL. Developed under the JPL Phaeton Program for training early career engineers, the goal of ASTERIA is to demonstrate high-precision pointing control and thermal control, and to conduct opportunistic photometric measurements of bright, nearby stars to seek transiting exoplanets.

The project commenced in December 2014 and delivered a completed spacecraft in June 2017. ASTERIA launched in August 2017 as pressurized cargo on a Commercial Resupply Services (CRS) mission to the International Space Station (ISS). ASTERIA deployed into low-Earth orbit in November 2017 and as of February 2018 had successfully completed the technology demonstration objectives planned for the 90-day prime mission. Since then, ASTERIA has undertaken an extended mission to search for transiting exoplanets and obtain additional operational performance and health data on hardware and software components. ASTERIA successfully measured the transit of 55 Cancri e, a known transiting super-Earth exoplanet orbiting a Sun-like star with a visual magnitude of $V = 5.95$. As of this writing September 2018, ASTERIA has been operating in space for over 280 days.

1.1 **ASTERIA Mission Objectives**

The overall technical objective of ASTERIA is to demonstrate capabilities that enable stellar photometry, that is, the measurement of star brightness over time. Specifically, the mission seeks to:

1. Demonstrate optical line-of-sight pointing stability of 5 arcseconds root mean square (RMS) over a 20-minute observation, and pointing repeatability of 1 arcsecond RMS from one observation to the next;
2. Demonstrate thermal stability of ± 0.01 K at a single location on the focal plane over a 20-minute observation;
3. Demonstrate an ability to conduct at least ten 20-minute observations per day and transmit the windowed star images to the ground for post-processing.

A secondary goal of ASTERIA is to conduct opportunistic photometric observations of bright stars in an effort to seek exoplanet transits.

1.2 **Mission Phases**

The ASTERIA mission consists of the phases described below. The baseline objective of the 90-day prime mission (November 2017 through February 2018) was to accomplish all activities up to and including the Technology Demonstration Phase. Later phases such as Photometric Demonstration and Photometric Observation were undertaken as part of an extended mission (February 2018 through September 2018).

1.2.1 **Launch and Deployment from ISS**

Instead of launching as a traditional secondary payload and deploying directly into orbit from the upper stage of a launch vehicle, ASTERIA was launched to the ISS as pressurized cargo. The launch occurred at 9:31 AM PDT on 14 August 2017 aboard a SpaceX Falcon 9 launch vehicle from Kennedy Space Center as part of NASA's 12th Commercial Resupply Services mission (CRS-12).

1.2.2 **Deployment**

After a stay lasting several weeks at the ISS, ASTERIA was deployed into low-Earth orbit via a spring-loaded dispenser furnished by NanoRacks and affixed to the end of the Japanese Experiment Module (JEM) robotic arm. Deployment occurred at 12:25:01 UTC (4:25:01 PST) on 20 November 2017 (see Figure 1).

Thirty minutes after deployment from the ISS, an onboard timer expired, deploying the solar arrays, and activating the attitude determination and control subsystem (ADCS) to detumble the spacecraft and acquire the Sun. Several hours later, the radio turned on (radio power-on was delayed to preserve battery state of charge under worst-case detumble scenarios).

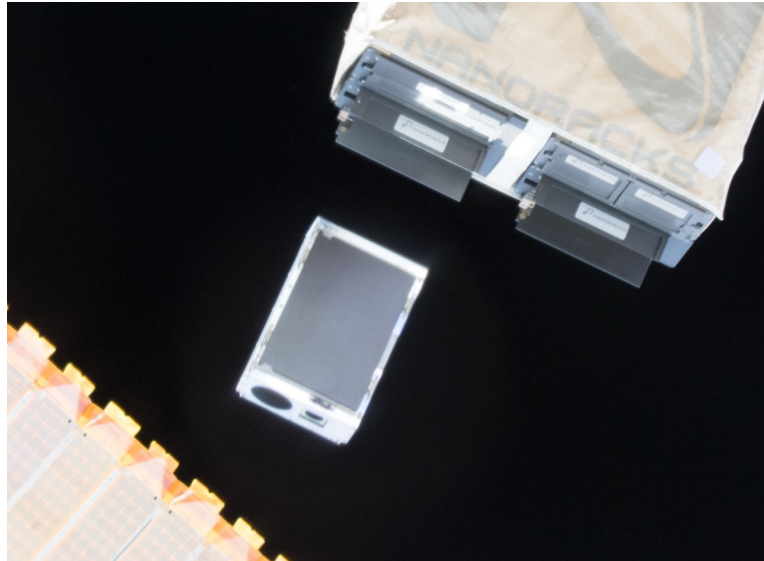


Figure 1: ASTERIA deployment from dispenser on the International Space Station.

1.2.3 Spacecraft Initial Acquisition

Spacecraft tracking is carried out by the Joint Space Operations Center (JSpOC) as part of their routine monitoring and cataloging of space borne objects. JSpOC produced a North American Aerospace Defense Command (NORAD) two-line element set² (TLE) that contains the orbital ephemerides for ASTERIA. During the initial acquisition phase, the ASTERIA team used published TLEs to predict ground station overflight times. First acquisition was accomplished about 1-1/2 days after deployment at 01:14 UTC on 22 November 2017. The acquisition required tracking the spacecraft in the sky using TLE predictions, radiating a carrier using the ground station, and observing the receipt of downlink carrier, frames, and real-time telemetry. Commandability was confirmed by sending a no-op (no operation) command and observing the response in the real-time event verification record (EVR) stream.

1.2.4 Checkout

The checkout phase consisted of sequentially activating and characterizing the performance of the spacecraft subsystems and payload. Checkout activities included transitioning the radio to its high data-rate mode, demonstrating file downlink and uplink, characterizing the orbit-to-orbit battery state of charge cycle, and transitioning the ADCS [6] from Coarse Sun Point Mode to the higher performance Fine Reference Point Mode. Payload commissioning activities occurred during this time and started by activating the camera system in full-frame mode. After confirming the full-frame capability, a calibration image was acquired. This image, along with knowledge of the attitude at the time of acquisition, was used to calibrate several optical parameters, including the relative alignment of the star tracker and payload reference frames. Once the camera system was checked out, the piezo stage of the payload's optical telescope was activated

² A NORAD two-line element set is a data format encoding a list of orbital elements of an Earth-orbiting object for a given point in time, the epoch. (https://en.wikipedia.org/wiki/Two-line_element_set)

and exercised in open loop and closed loop modes. The final checkout was an end-to-end demonstration of the closed loop pointing control system, which involved successful coordinated operation of the ADCS, camera system, and piezo stage.

1.2.5 Technology Demonstration

The technology demonstration phase was devoted to performing the observation activities needed to achieve the technology demonstration objectives outlined above. The full Level 1 (L1) requirements outline the durations over which the various levels of performance must be met. Specifically, pointing stability had to be demonstrated by an observation lasting 20 minutes or more; pointing repeatability had to be demonstrated over five or more sets of observations—each set consisting of three consecutive observations—distributed over a minimum of eight days; and thermal stability had to be demonstrated five times over a minimum of eight days. Furthermore, the system had to demonstrate an ability to perform ten observations in a 24-hour period. When these objectives were satisfied, the technology demonstration phase was complete.

1.2.6 Photometric Demonstration

The photometric demonstration phase consisted of observations of a known photometric signal to determine if ASTERIA had sufficient end-to-end capabilities to make quality science measurements. The observation target for the photometric demonstration phase was 55 Cancri e, a two-Earth-radius exoplanet already known to transit its host star. The transit depth³ is approximately 410 parts per million (ppm), the transit duration⁴ is approximately 92 minutes, and the orbital period is approximately 18 hours. A transit detection of 55 Cancri e by ASTERIA provided an end-to-end validation of the system's potential to detect small exoplanets.

1.2.7 Photometric Observation

The photometric observation phase is dedicated to seeking previously undetected transits. There are generally two classes of targets during this phase. The first is the set of stars known to harbor exoplanets discovered via the radial velocity method, but whose exoplanets are not known to transit. These targets are attractive because the radial velocity measurements constrain the predicted transit times, providing guidance on when to observe. The second class of targets during the photometric observation phase is stars without known exoplanets. These targets are nearby, bright Sun-like stars that would be prime targets for follow-on observation by space-based spectrographs. Long duration monitoring would permit the detection of exoplanets with longer orbital periods and larger semi-major axes that are better aligned with the likely habitable zones of these targets. The ultimate duration of the photometric observation phase will be limited by spacecraft lifetime and available funding.

1.2.8 Decommissioning

After September 2018, ASTERIA is predicted to remain in a viable orbit until late 2019, when aerodynamic drag will cause a loss of momentum control and subsequent atmospheric re-entry. ASTERIA requires no passivation prior to the end of mission (EOM). Therefore decommissioning will consist mainly of allowing the spacecraft to re-enter the atmosphere naturally due to drag. Orbital debris analysis shows that no components are expected to survive re-entry.

³ Transit depth is the fraction of the surface area of the star blocked by the planet's disk.

⁴ Transit duration is the amount of time it takes for the exoplanet to traverse the stellar disk, as viewed from the observer.

1.3 Orbit

ASTERIA has no onboard propulsion and resides in a similar orbit to the ISS—approximately 400 km altitude, 51.6° inclination. The orbital period is 92.6 minutes, and the eclipse duration varies as a function of the beta angle (β), the angle between the orbit plane and the Earth-Sun vector. Eclipse duration reaches a maximum of 35.8 minutes when $\beta=0^\circ$ and the orbit plane is coincident with the Earth-Sun vector. Conversely, no eclipse occurs, and ASTERIA is in sunlight for the entire orbit when $\beta=\pm 75^\circ$. Figure 2 shows the variation in β and eclipse duration for the 90-day prime mission.

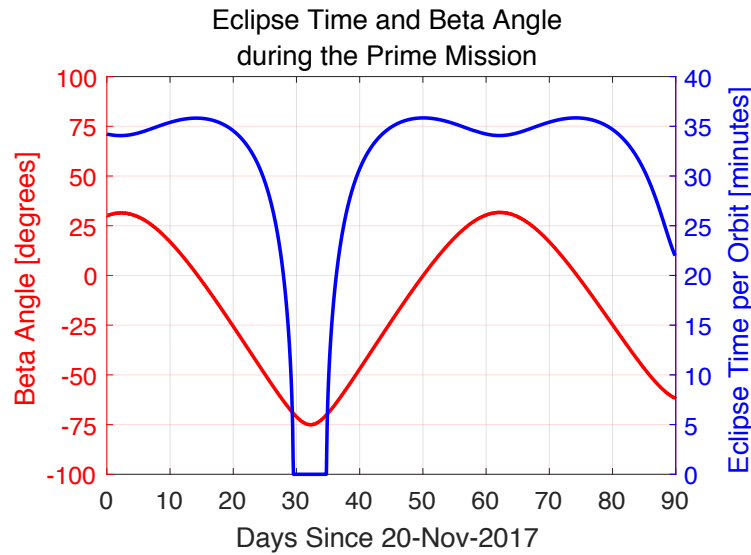


Figure 2: Beta angle and eclipse duration during the ASTERIA prime mission.

2 ASTERIA Spacecraft Overview

ASTERIA is a 6U CubeSat measuring approximately $37\text{ cm} \times 24\text{ cm} \times 12\text{ cm}$ with a mass of approximately 10.2 kg. It was designed and built at JPL using a combination of commercial-off-the-shelf (COTS) components—often customized or modified—and components that were developed in-house at JPL. Figure 3 shows the completed flight vehicle with the solar arrays in the deployed configuration. Figure 4 shows the internal spacecraft components.

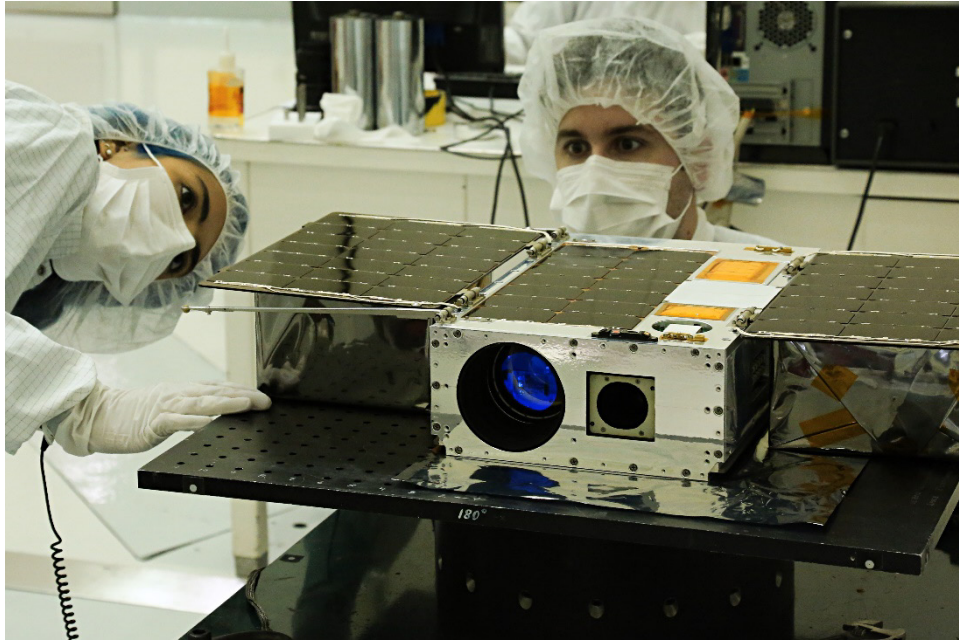


Figure 3: ASTERIA flight vehicle with solar array deployed.

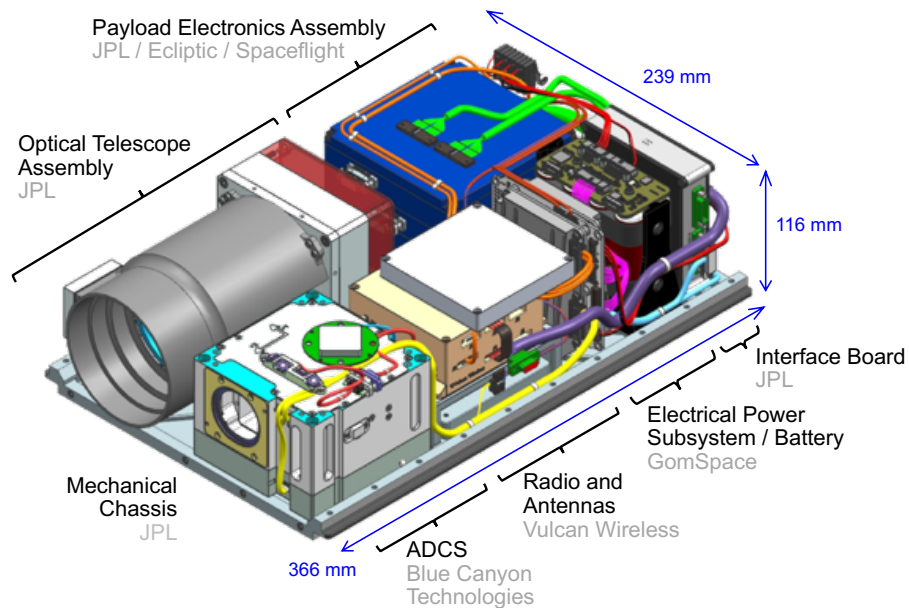


Figure 4: ASTERIA internal components.

2.1 Structure

The spacecraft mechanical chassis was designed at JPL and consists of six aluminum side-walls with a rib structure to minimize weight. Nearly all of the internal components are mounted to the bottom plate (as shown in Figure 4). This provided a convenient mounting surface for spacecraft integration. It also provides a thermal path for removal of heat from the internal components (see Section 2.5).

The ASTERIA structure complies with the NanoRacks 6U deployer interface control document (ICD). Instead of the four rails on each corner of the chassis—used by the classic P-POD (Poly-Picosatellite Orbital Deployer) design—the NanoRacks deployer uses a pair of C-shaped channels that guide two tabs, one on each edge of the bottom plate.

2.2 Power

Power is provided by a solar array that consists of eight strings, each string containing seven cell-interconnect-coverglass (CIC) modules. The CICs use Spectrolab ultimate triple-junction (UTJ) cells, which have a theoretical efficiency of 28.3%. The solar array has two deployable wings with three cells each, plus two strings affixed to the spacecraft top panel. The array system was developed by MMA Design LLC. The deployable panels are spring-loaded and held in place using dedicated constraints that do not rely on the side walls of the dispenser to maintain the stowed configuration. Deployment occurs when a current is passed through a wire that cuts through a plastic rod, allowing the restraints to release under spring-loaded action.

Energy is stored in a battery assembly consisting of eight lithium-ion 18650 cells⁵ wired in series for a bus voltage that nominally varies between 30 V and 32.8 V. The projected battery capacity at end of life (EOL) is 47 Whr. The battery assembly was sourced from GomSpace⁶ and the cells underwent lot-level vibration, thermal, and electrical testing to verify compliance with ISS safety requirements.

Power is regulated and distributed using an electrical power subsystem (EPS) card, also sourced from GomSpace. The EPS card is responsible for conditioning the solar array input, regulating the battery charge/discharge cycles, and distributing power to the subsystems via a set of commandable output switches. The EPS outputs the unregulated raw battery voltage along with regulated channels at 3.3, 5, and 12 V.

2.3 Command and Data Handling

Command and data handling (C&DH) is carried out by a single-board flight computer manufactured by Spaceflight Industries. It has a Xilinx Virtex 4FX FPGA⁷ (field-programmable gate array) with an embedded PowerPC processor running at 400 MHz. The flight computer interfaces with peripheral components using RS-485, SPI (Serial Peripheral Interface), and GPIO (general purpose input/output). It also has an Ethernet interface used as a data connection during development and laboratory testing.

2.4 Flight Software

The ASTERIA flight software (FSW) uses F Prime [7], a free and open-source FSW framework developed at JPL, designed to support small-scale systems such as CubeSats and instruments. The F Prime framework uses an architecture in which discrete units of FSW functionality—i.e., components—are connected

⁵ An accumulator cell 18650 is a lithium-ion battery. The battery shape is cylindrical. The battery's size is in its name 18650. The battery is 18 mm in diameter and its length is 65.0 mm (with protection, 66.5 mm). One 18650 has an output voltage of 3.7 V. Ref. <https://all-spares.com/en/technical-articles/what-does-18650-battery-mean.html>

⁶ GomSpace, name and history ref. <https://gomspace.com/the-story.aspx>

⁷ See https://www.xilinx.com/support/documentation/data_sheets/ds112.pdf for an overview

together via ports. Components correspond to spacecraft functions such as attitude control, communication, fault protection, power management, etc., and together constitute the overall spacecraft behavior. The ASTERIA software is written mostly in C++ (drivers for interacting with hardware are written in C), and it contains approximately 200,000 lines of source code.

Fault protection is a set of behaviors residing within FSW designed to maintain system health and safety. ASTERIA has a set of monitors that periodically check critical parameters such as battery voltage, temperatures, and the health of the attitude control subsystem hardware. These monitors are linked to responses that execute when a monitor falls outside of an acceptable range. The two primary responses are (1) go to System Safe Mode—which powers off the payload and returns to a Sun-pointed attitude, among other things—or (2) perform a spacecraft reset in which all hardware components except the electrical power supply are power cycled. Both these responses were successfully tested in flight.

2.5 Thermal

The spacecraft thermal design uses passive means to maintain internal components within their allowable flight temperatures. Specifically, the internal components with high dissipation are bolted to the spacecraft bottom plate, which acts as a heat sink. Heat is then conducted through the mechanical chassis walls and radiated into space. The radiative effect is achieved from an external surface coating of 10-mil silver Teflon over nearly the entire spacecraft body. The telescope, batteries, and interface board (described below) are thermally isolated from the bottom plate to avoid temperature transients that affect performance and avoid excessively high temperatures that could damage components.

2.6 Attitude Determination and Control

ASTERIA uses the Blue Canyon Technologies (BCT) fleXible Attitude Control Technology (XACT) unit for attitude determination and control. It features a star tracker, inertial measurement unit (IMU), coarse sun sensor, magnetometer, reaction wheels, torque rods, a processing unit, and Attitude Control System (ACS) software in a self-contained assembly. The XACT software is capable of autonomously detumbling the spacecraft and pointing the solar arrays at the Sun. During observations, the XACT is commanded into a fine-pointing mode and slews the spacecraft to point at the target star. This fine-pointing mode is also used during sequenced passes, where the XACT is commanded to point the spacecraft antenna at the ground station throughout a pass. This significantly improves the strength of the downlink signal, resulting in greater downlink data volume due to fewer bad frames.

2.7 Science Payload

The ASTERIA payload is a compact, wide field-of-view optical telescope with specialized hardware to perform high-precision pointing and thermal control. These capabilities enable stellar photometry—i.e., measurement of a star’s brightness as a function of time—permitting the detection of transiting exoplanets around bright, nearby stars.

The optical telescope consists of a five-element refractive lens assembly with an 85-mm focal length and 60-mm effective aperture. The optics illuminate a complementary metal-oxide-semiconductor (CMOS) imager attached to a two-axis piezoelectric positioning stage that translates in the plane perpendicular to the optical axis. Operating within a 20-Hz pointing control loop based on the motion of guide stars, the piezo stage is used to maintain the relative position of the target star on the focal plane. This allows for optical line-of-sight pointing control beyond that which is possible with the attitude control system alone.

The payload also has active thermal control to maintain the temperature of the imager. A thermal strap is connected to the back of the imager at one end and the telescope baffle at the other. This allows heat to move from the imager to the baffle, where it is radiated into space. A closed-loop heater circuit resides at the back of the imager and on the baffle. Each circuit consists of a resistive heater and platinum resistance

thermometers (PRT) for measuring temperature. The temperature at the focal plane is maintained by a proportional-integral-derivative (PID) control loop for each heater circuit.

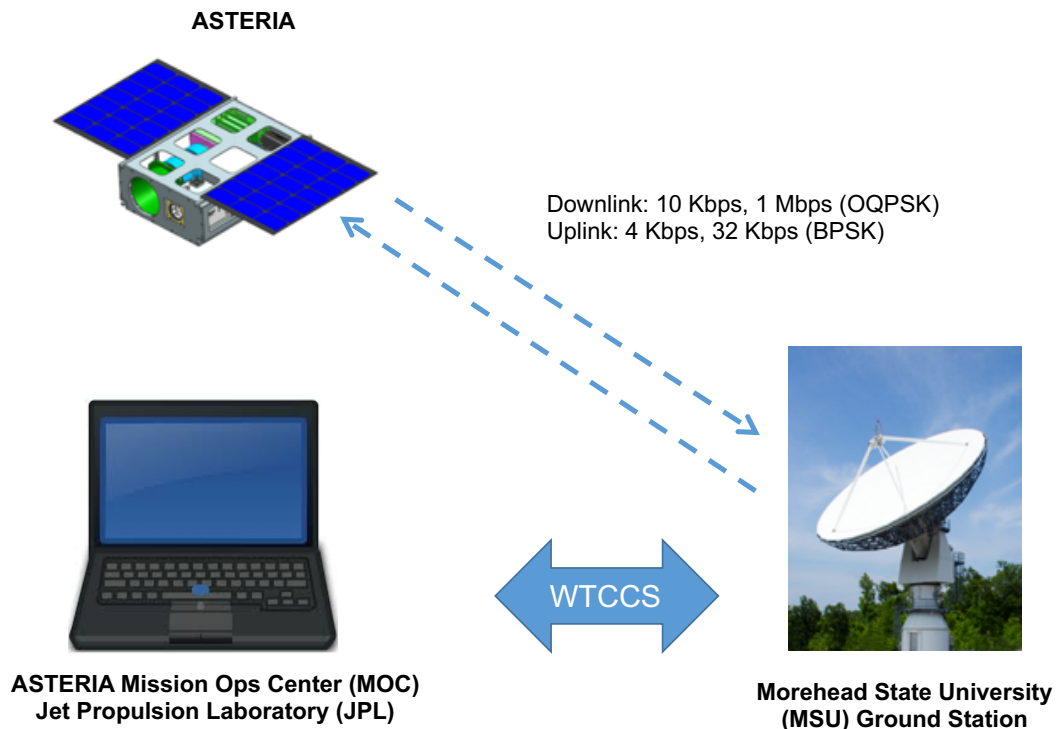
Observations occur during orbit night and typically last 20 minutes. During an observation, the pointing control and thermal control systems are active, and 20-Hz raw images are co-added onboard to a one-minute cadence. Instead of storing the entire full-frame image—much of which contains dark sky—up to eight windows, each measuring 64×64 pixels, are captured at each time step. Observations normally occur in multiple back-to-back orbits, yielding measurements that can span up to several days.

3 Telecommunications Subsystem

3.1 Overview

The telecommunications subsystem provides a single uplink and a single downlink at S-band. The S-band uplink provides the means to upload commands and files that are needed on-board to control the satellite. The S-band downlink returns both the telemetry data and the payload data.

Figure 5 summarizes the ASTERIA communication links and data rates. Commands originate from the ASTERIA Mission Operations Center (MOC) located at JPL. The commands are created, processed, and verified in the WTCCS. The validated commands go from the WTCCS client at JPL via a secure internet link to the WTCCS server at Morehead State University in Kentucky. There the commands are modulated onto an S-band uplink and transmitted to ASTERIA from the 21-m antenna at the ground station at the university. The uplink data rates are 4 Kbps (for safe mode used mainly in the acquisition mission phase) and 32 Kbps (nominal operations). The downlink data rates are 10 Kbps (also for safe mode used mainly in the acquisition mission phase) and 1 Mbps (nominal). Typical ground station contact durations range between 8 and 10 minutes. The ASTERIA team does not use contacts shorter than 8 minutes.



Abbreviations in Figure 5: BPSK = binary phase shift keying, Mbps = megabits per second, WTCCS=WISE (Wide-field Infrared Survey Explorer) Telemetry Command and Communications System, Kbps = kilobits per second, OQPSK = offset quadrature phase shift keying.

Figure 5: ASTERIA communication links and data rates.

Table 1 summarizes the S-band signal parameters.

Table 1: ASTERIA telecommunication signal parameters.

Parameter	Value
S-band carrier frequency	2062.9 MHz (uplink) 2271.395 MHz (downlink)
LGA polarization	Right-hand circularly polarized
Uplink/downlink data rates	4 and 32 Kbps (uplink) 10 Kbps and 1 Mbps (downlink)
Forward error correction (FEC) coding	Downlink: Reed Solomon (255, 223) Uplink: BCH (Bose-Chaudhuri-Hocquenghem) per CCSDS standards, followed by differential
Modulation	Uplink: BPSK (binary-phase-shift keying) Downlink: OQPSK (offset quadrature phase shift keying)
Data format	Non-return to zero level (NRZ-L)

The telecommunication system is a full duplex S-band telecommunication system that includes one S-band transceiver assembly and two low gain antennas (LGA). This article uses the term transceiver assembly interchangeably with the term radio. The transceiver assembly includes a switch to select one of the antennas, a diplexer to separate uplink and downlink, a solid state power amplifier (SSPA) for the downlink, and a low noise amplifier (LNA) for the uplink. The two LGAs are identical S-band patch antennas which operate at both transmitting and receiving frequencies. Hence, they are redundant, placed on opposite sides of the spacecraft to maximize coverage. The spacecraft attitude results in LGA 1 pointed toward Earth with an unobstructed FOV (field of view) to the Earth horizon during orbital day. LGA 2 is boresighted in the nadir direction and has an unobstructed FOV to the Earth horizon during orbital night.

Table 2 summarizes the S-band configuration during the different mission phases.

Table 2: Telecom configuration plan for each mission phase.

Phase	Timeline	Description	Telecom configuration
Deployment	L+60 days (D=0) (planned)	Spacecraft sequenced to be silent for 30 minutes (maximum time to detumble).	No telecom
Acquisition	D+5 hours to D+5 days (planned) D+36 hours (actual)	Using predicted trajectory and updated NORAD (North American Aerospace Defense Command) 2 line elements, the Morehead State ground station will try to uplink to the satellite and receive GPS (Global Positioning System) information. Up to 6 passes a day will be used to try to find the satellite.	S-band receiver is on periodically in a power cycle schedule. (See Section 3.6.3.) Safe mode data rates (4 Kbps in uplink, 10 Kbps in downlink) will be used.
Commissioning	D+5 days to D+30 days (planned)	Commissioning will start once link is established. Subsystems checkout and calibration will take place. 2–3 passes per day will be scheduled during this phase.	S-band receiver is on periodically in a power cycle schedule. Nominal data rates (32 Kbps uplink, 1 Mbps downlink) are used.
Technology Demonstration	L+30 days to L+60 days	The pointing control demo, thermal control demo, and photometric measurement demo will take place during this period.	S-band receiver is on periodically in a power cycle schedule. Nominal data rates (32 Kbps uplink, 1 Mbps downlink) are used.
Science	Beyond L+60 days	Opportunistic science pointing and photon counting at specific stars will occur. 2–3 passes per day will be scheduled during this phase.	S-band receiver is on periodically in a power cycle schedule. Nominal data rates (32 Kbps uplink, 1 Mbps downlink) are used.

Table 2: Telecom configuration plan for each mission phase.

Phase	Timeline	Description	Telecom configuration
Decommissioning	Estimated in late 2019 to early 2020	No preparation or burn. The ASTERIA orbit will naturally decay due to drag and re-enter the atmosphere. 1 pass per day (or less).	S-band receiver is on periodically in a power cycle schedule. Nominal data rates (32 Kbps uplink, 1 Mbps downlink) are used.

The transceiver is connected to the C&DH through a USB/RS-422 converter board⁸ to allow the FSW to control the radio, to set up a Point-to-Point Protocol Daemon (pppd) connection, to receive engineering data from the radio, and to receive/transmit the uplink/downlink data. The pppd request and pppd session that result from this connection are discussed in Section 3.6.1. The downlink processing that results from the connection is discussed in Section 4.1.1.

3.2 Telecom Block Diagram and Subsystem Design

Figure 6 is a block diagram of the telecommunication subsystem. Two identical low gain patch antennas (placed on opposite sides of the spacecraft) are connected through similar length coaxial cables to the antenna ports of the transceiver assembly. The transceiver assembly includes a switch among the two antenna ports, a diplexer to separate transmitting and receiving signals, two amplifiers, and a software defined radio (SDR). Figure 7 shows the location of the transceiver and antennas on the spacecraft.

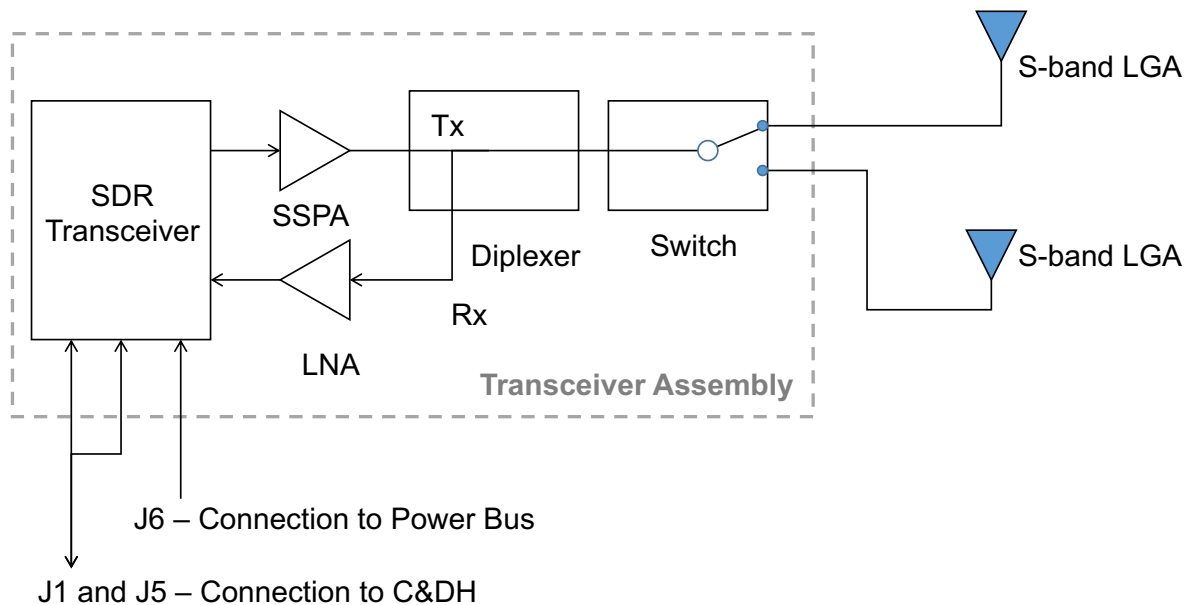


Figure 6: ASTERIA telecommunication system block diagram.

⁸ A universal serial bus (USB) is a common interface that enables communication between devices and a host controller such as a personal computer (PC). It connects peripheral devices such as digital cameras, keyboards, printers, scanners, and flash drives. <https://www.techopedia.com/definition/2320/universal-serial-bus-usb>. RS-422, RS-232, etc., are standards for binary serial communications between devices. RS-422 is the protocol or specification to be followed in order to allow two devices that implement this standard to communicate with each other. The RS-422 standard is an updated version of the original serial protocol standard known as RS-232. <http://www.futureelectronics.com/en/signal-interface/rs-422.aspx> RS-422 is the common short form title of American National Standards Institute (ANSI) standard ANSI/TIA/EIA-422-B Electrical Characteristics of Balanced Voltage Differential Interface Circuits. <https://en.wikipedia.org/wiki/RS-422>

In Figure 7, the transceiver assembly is shown in brown, and the two patch antennas are located on top and on the bottom of the radio (shown in grey).

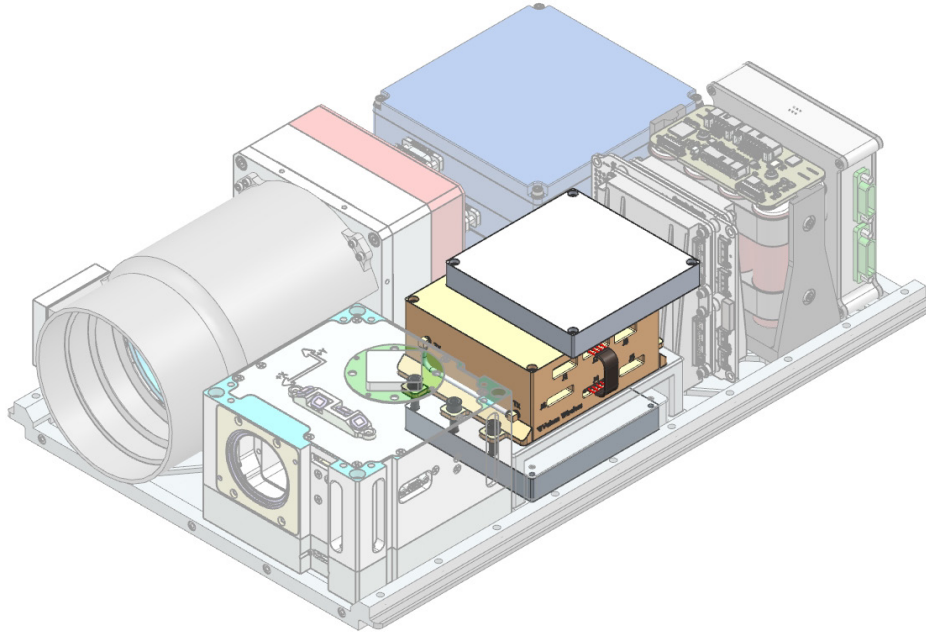


Figure 7: ASTERIA interior computer-aided design (CAD) model.

3.3 Antennas

The low gain patch antennas were provided to ASTERIA by Vulcan Wireless Inc. They are functional in full duplex mode over the entire Near Earth Frequency range.

Table 3 summarizes the key characteristics of the antenna, which are the same for both LGAs.

Table 3: Antenna characteristics.

LGA Characteristic	Value
Frequency passband	2.0–2.11 GHz (receive) 2.2–2.3 GHz (transmit)
Beamwidth	± 90 deg
Power handling	10 W
Impedance	50 Ohm
Return Loss bandwidth	275 MHz
Return Loss	> 13 dB
Polarization	RHCP
Axial Ratio	< 5 dB receive < 4 dB transmit
Peak gain	7.0 dBi
Minimum gain	–10 dBi
Half power beamwidth (double-sided)	70 deg
Temperature range	–40 deg C to +85 deg C
Volume	82 mm \times 82 mm \times 12 mm
Mass	76 grams
Vibration	GEVS-7000, 16.2 GRMS, each axis
Connector	MMCX-Jack

Figure 8 shows a picture of the antenna, Figure 9 shows the antenna radiation pattern, and Figure 10 shows the return loss.

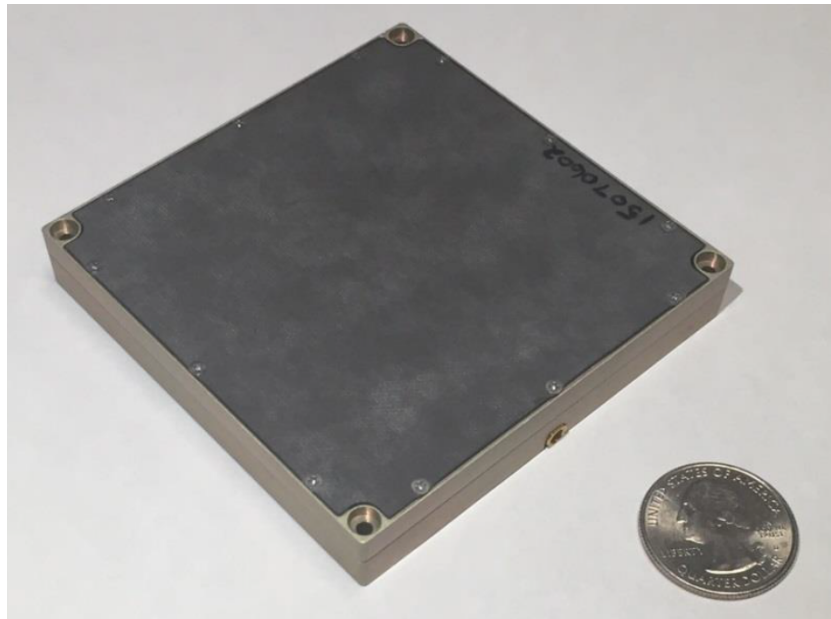


Figure 8: Patch antenna. (Courtesy of Vulcan Wireless Inc.)

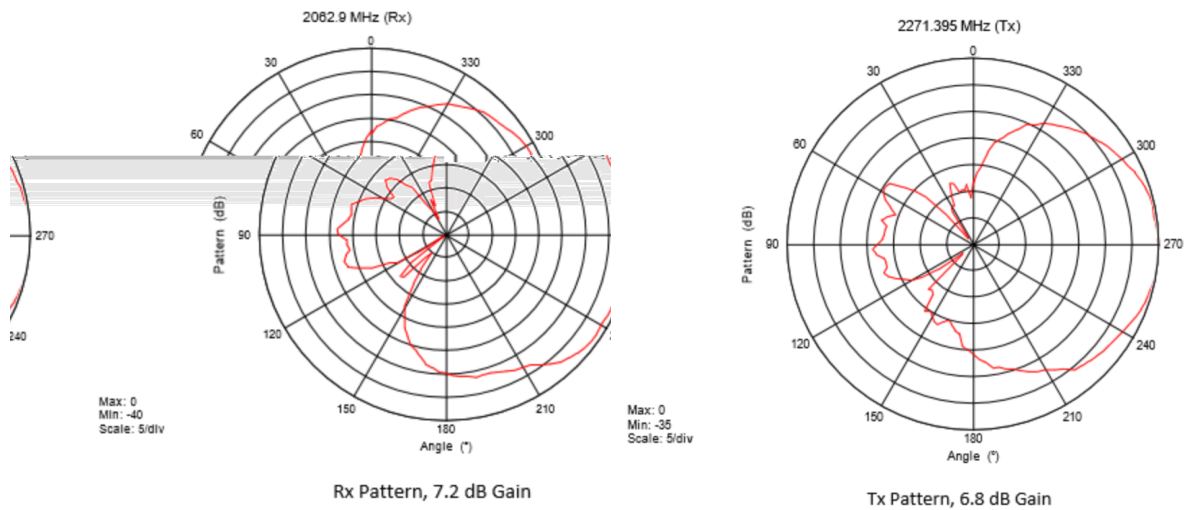
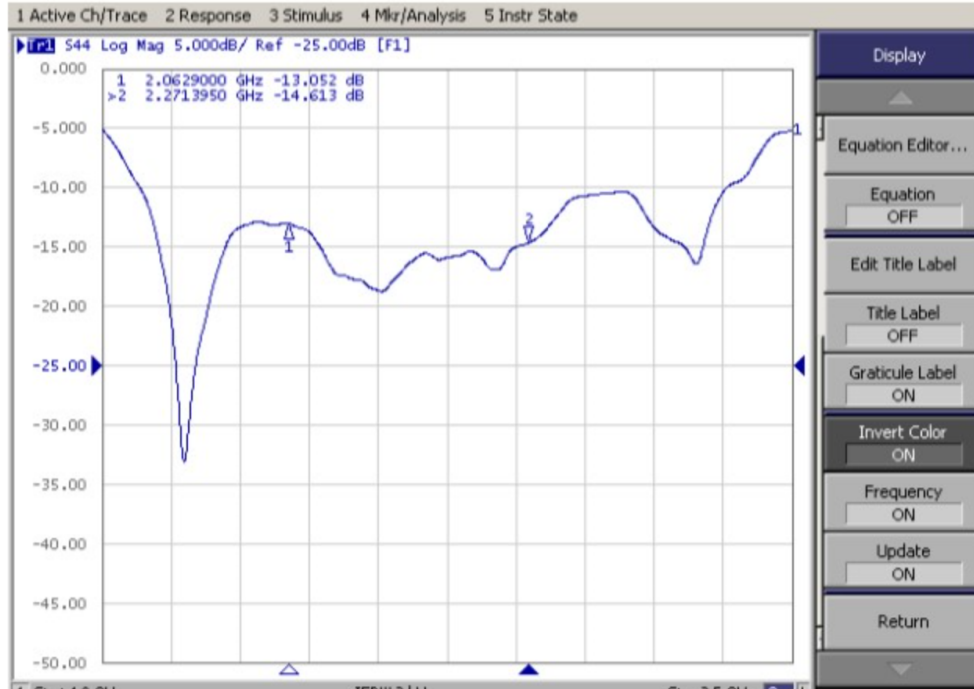


Figure 9: Antenna pattern. (Courtesy of Vulcan Wireless Inc.)



The y axis is in dB and the x axis in MHz (open, solid triangles mark 2063 MHz receive, 2271 MHz transmit carrier).

Figure 10: Return loss. (Courtesy of Vulcan Wireless Inc.)

3.4 Transceiver

The ASTERIA transceiver assembly includes a switch between the two antennas, a diplexer, an SSPA, an LNA, and a software-defined S-band transceiver. The transceiver is a full duplex radio which receives a direct carrier BPSK modulated signal at either 4 Kbps or 32 Kbps while transmitting a direct carrier OQPSK modulated signal at either 10 Kbps or 1 Mbps. The transceiver assembly (Figure 11) is provided by Vulcan Wireless Inc. and designated by them as CSR-SDR-S/S for CubeSat Radio-Software Defined Radio-S/S band. As shown in Figure 6, besides its two antenna ports, the transceiver assembly has a single interface with C&DH for radio telemetry and data and an interface for a 28 V line connected directly to the ASTERIA power system. Table 4 summarizes the key characteristic of the ASTERIA transceiver.

Table 4: Transceiver characteristics.

CSR Characteristic	Value
Transmit carrier frequency	2271.395 MHz
Receive carrier frequency	2062.9 MHz
Transmit FEC coding	Reed Solomon (255, 223)
Transmit RF output power	1 W
Transmit data format	Non-return to zero level (NRZ-L)
Transmit modulation	OQPSK
Transmit data rate	10 Kbps, 1 Mbps
Transmit modulation index	90 deg
Command modulation index	90 deg
Command data format	Non-return to zero level (NRZ-L)
Command modulation	BPSK
Command data rate	4 Kbps, 32 Kbps
Receiver noise figure	< 4.5 dB
Receiver acquisition frequency range	± 60 KHz

Table 4: Transceiver characteristics.

CSR Characteristic	Value
Receiver maximum input level	10 dBm
Receiver carrier level range	−126 dBm to −50 dBm
Receiver command threshold	−125 dBm (4 Kbps) −118 dBm (32 Kbps)
DC power consumption	3.2 W (receive only) 8.5 W (full duplex)
Flight allowable temperature range	−25 deg C to +60 deg C
Dimensions	82 × 82 × 38 mm
Data interface to C&DH	USB
Input direct current voltage	24–33.6 VDC



Figure 11: CSR-SDR-S/S radio. (Courtesy of Vulcan Wireless Inc.)

3.5 Telecom Subsystem Mass and Power

Table 5 summarizes the mass and power consumption of the ASTERIA telecom subsystem.

Table 5: ASTERIA telecom subsystem mass and power input.

Component	Number of units	Mass per Unit (g)	Total Mass (g)	Spacecraft Power (W)	Notes
Antennas	2	75	150		
Transceiver	1	400	400	3.5 8.78	Receive only Receive and transmit
Coaxial cables	2	10	20		
Data cable	1	10	10		
Power cable	1	10	10		
Total			590		

3.6 Communication Module

The communication module is a set of functions in FSW that are dedicated to managing the interface with the radio, requesting radio telemetry, sending data to the radio for downlink, and receiving data from the radio for uplink. Refer to Figures 12–14 with the following text. Figure 12 diagrams the boot sequence and the operational behavior for the radio. Figure 13 diagrams how the FSW controls selection between the two

antennas. And Figure 14 shows how the XACT interacts with radio fault indications to swap antennas or not.

3.6.1 Boot and Configuration

The radio has a relatively complex boot sequence and does not automatically boot into a state where radio frequency (RF) communication with the ground is possible. Therefore, it is the responsibility of FSW to ensure that the radio boots into and remains in a state where RF communication is possible. When power is applied to the radio, the radio operating system (OS) Linux begins its boot process. Once the OS boots, the radio configures a USB connection on the USB/RS-422 converter board, which must be powered on by FSW. When the USB connection is established, the radio starts a pppd in passive mode and sends a configuration packet via the transfer control protocol (TCP). Because pppd is in passive mode, the radio will wait indefinitely after sending the configuration packet to receive a configuration packet from the flight computer. Once the radio receives a pppd request from the flight computer and the pppd session is active, the radio is capable of receiving Application programming interface (API) communication packets. With the pppd session active, FSW will use API function calls to connect to the radio and implement the behavior. Note that Figure 12 does not show the fault that is triggered if there is a connection timeout between the radio and FSW. FSW monitors this connection and sends a fault to the system fault engine if the connection timeout (a configurable parameter) is exceeded.

When opening a link with the VW LinkOpen command (a C function in the radio API), the radio can be configured to send and receive data. When configured to receive, the radio will be capable of receiving data from the ground. Once the radio receives a modulated carrier with the ASTERIA idle sequence, the radio's full duplex mode will be triggered, and the radio will start transmitting idle packets until FSW starts transmitting data packets. FSW detects when the radio is in duplex mode and sends data packets accordingly at the appropriate downlink rate.

The radio only operates in its default mode, as shown in Figure 12. The only difference in radio operations between system modes is the selection between data rates, as performed by a FSW function.

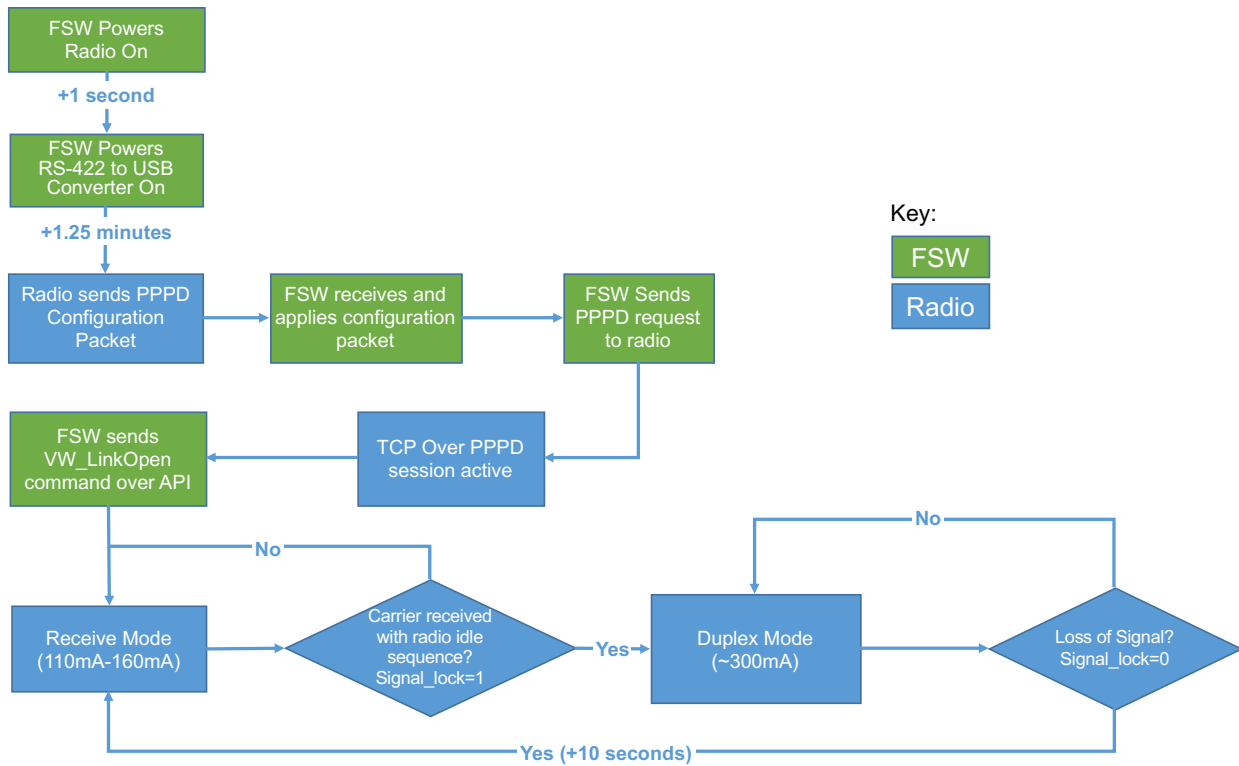


Figure 12: Boot sequence and operational behavior for the radio.

3.6.2 Antenna Switching

The radio is connected through an internal switch to two antennas on opposite sides of the spacecraft as shown in the block diagram (Figure 6) and the CAD model (Figure 7).

Only one antenna can be used at a time, and FSW uses an API function call to indicate to the radio which antenna to use. Operational antenna pointing is controlled when the XACT⁹ is in Fine Point mode (see Figure 13). The FSW selects the antenna on the side of the spacecraft whose unit normal vector has the larger component in the direction of the nadir vector.

The only scenario in which the System Safe Mode switches the antenna is in response to a fault when the radio is in Receive Only mode. When ASTERIA is in System Safe Mode, the XACT is in Sun Point Mode, and FSW selects the default antenna, Antenna 1.

The radio has two states: Receive and Duplex. The radio is detected by FSW based on the value of Signal Lock, which is 0.0 in Receive state and 1.0 in Duplex state. An additional indicator is the current radio monitor on the EPS. The radio will boot up in its Receive state, and the telecommunication subsystem will listen for commands to be uplinked from the ground. Depending on the system mode, the radio is configured for either the 4-Kbps or 32-Kbps uplink data rate. The ground shall send a carrier with the ASTERIA idle sequence, which, when received by the radio, will cause the radio to lock and start transmitting in its Duplex state. See Figure 12 for the boot and operational behavior of the radio. In Duplex state, the radio is capable of simultaneous receipt and transmission of data. Depending on the system mode, the radio is configured for either 10-Kbps or 1-Mbps downlink data rate.

⁹ XACT is the hardware system used to point the spacecraft. Antenna 1 is the antenna on the side of the spacecraft opposite to the solar panels.

FSW shall not switch antennas in System Safe Mode (XACT Sun Point Mode) while the radio is in its Duplex state (Signal lock telemetry value is one), as shown in Figure 13.

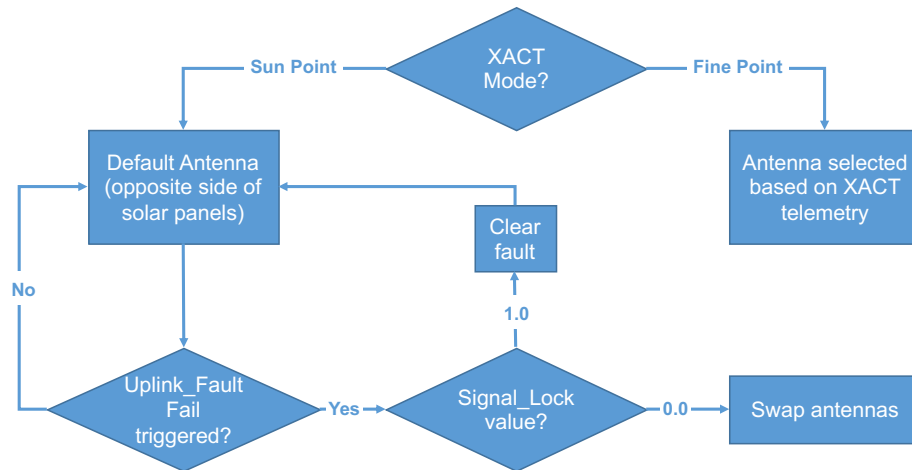


Figure 13: Flight software concept of operation for the radio.

3.6.3 Radio Duty Cycle

FSW implements the radio power cycle behavior shown in Figure 14 in order to allow flexibility in operations arising from unforeseen power constraints. The radio is ON for 30 minutes, then OFF for 10 minutes, then back on for 30 minutes, and so on. Each power-on of the radio shall include power-on of the radio followed by power-on of RS-422 to USB converter board, as demonstrated in Figure 12. However, if the radio is in its Duplex state (Signal_Lock==1.0)¹⁰, FSW will not turn off the radio for 10 minutes or until the radio loses lock (Signal_Lock==0.0), as shown in Figure 14.

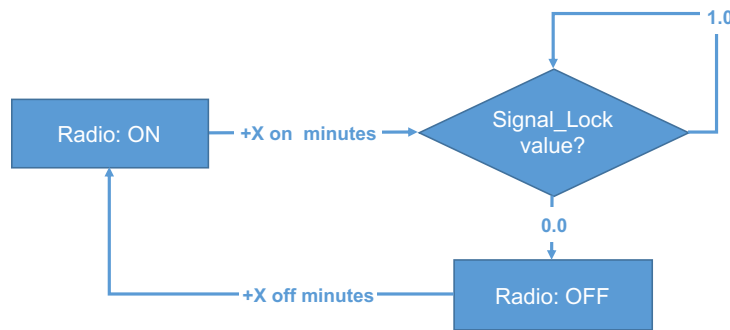


Figure 14: Radio power cycle behavior.

¹⁰ The assignment operator (=) is used to assign a value to a variable, element of an array, or property of an object. The equality operator (==) is used to compare two values or expressions. It is used to compare numbers, strings, Boolean values, variables, objects, arrays, or functions. The result is TRUE if the expressions are equal and FALSE otherwise. <https://www.quora.com/What-is-the-difference-between-and-operator-in-C++>

4 Tracking Station and Data System

ASTERIA communicates with the 21-m antenna station operated by Morehead State University in Kentucky. The station is located at a latitude of 38.1889 degrees north and at a longitude of 83.4312 degrees west. Figure 15 shows the location of the ground station with respect to the ASTERIA orbit.



Figure 15: Morehead State University ground station location and ASTERIA orbit.

4.1 Morehead State University Ground Station

The ground station at Morehead State University is composed of a 21-m dish antenna with functionalities from Ultra High Frequency (UHF) to Ku-band. Figure 16 shows the ground station dish. Table 6 is a summary of the antenna characteristics and RF performance capabilities at S-band¹¹.

¹¹ Ref. [https://www.moreheadstate.edu/getattachment/College-of-Science/Earth-and-Space-Sciences/Space-Science-Center/Satellite-Tracking,-Telemetry-Control-Services/satellite-\(2\).pdf.aspx?lang=en-US](https://www.moreheadstate.edu/getattachment/College-of-Science/Earth-and-Space-Sciences/Space-Science-Center/Satellite-Tracking,-Telemetry-Control-Services/satellite-(2).pdf.aspx?lang=en-US)



Figure 16: Morehead State University 21-m antenna.

Table 6: S-band ground station characteristics [from Ref. 8].

Ground Station Characteristic (S-band)	Value
Antenna diameter	21 meter
Receive polarization	RHCP, LHCP, VERT, HORZ
Travel range	AZ (azimuth) axis: ± 275 degrees from due South (180 degree) EL (elevation) axis: -1 to 91 degrees POL (polar) axis: ± 90 degrees
Velocity	AZ Axis: 3 deg/sec EL Axis: 3 deg/sec POL Axis: 1 deg/sec
Acceleration	AZ: 1 deg/sec/sec min EL: 0.5 deg/sec/sec min
Display resolution	AZ/EL: 0.001 degree POL: 0.01 degree
Encoder resolution	AZ/EL: 0.0003 deg (20 Bit)
Tracking accuracy	Maximum pointing error specified as 5% of the half-power beamwidth (about 0.02 deg)
Pointing accuracy	≤ 0.01 deg rms
Antenna gain	52.8 dBi
System noise temperature	215 K
Half-power (3-dB) beamwidth	0.37 degree

4.1.1 Downlink Processing

The S-band receiver used for the ASTERIA mission includes a Kratos RT Logic T400 modem and an AMERGINT server. The receiver is Consultative Committee for Space Data Systems (CCSDS) compatible with the Vulcan CubeSat Radio (CSR) radio. Figure 17 shows a functional diagram for the ASTERIA-to-ground downlink at the higher 1 Mbps rate. The scheme is identical for the downlink at the lower 10 Kbps rate. The link consists of a carrier modulated with telemetry and science data. On-board ASTERIA, the data signal coming from the flight computer is sent to the radio through the pppd connection. PPPD (or pppd) is the point-to-point protocol daemon which is used to manage network connections between two nodes on Unix-like operating systems. It is configured using command-line arguments and configuration files. The signal is then framed according to CCSDS framing scheme, the Reed Solomon (255, 223) encoding is added, the signal is randomized, and the CCSDS frame sync preamble is added. Then, the signal is OQPSK modulated, and the 2271.395 MHz RF passes through the radio diplexer and switches to one of the two antennas from which it is radiated. On the ground, the RF signal is received, amplified, downconverted, demodulated, and separated into I and Q channels. Symbol synchronization is removed, and the channels are multiplexed. The final step in the downlink processing at the Morehead ground station is to strip out the frame synchronization, apply the CCSDS de-randomization process, and perform Reed Solomon decoding. The decoded downlink output then enters the ASTERIA Mission Operations System (MOS). It is handled by MOS operational software for ASTERIA called the WISE Telemetry Command and Communications System (WTCCS). The WTCCS was first used for downlink and uplink processing for the Wide-field Infrared Survey Explorer (WISE) spacecraft.

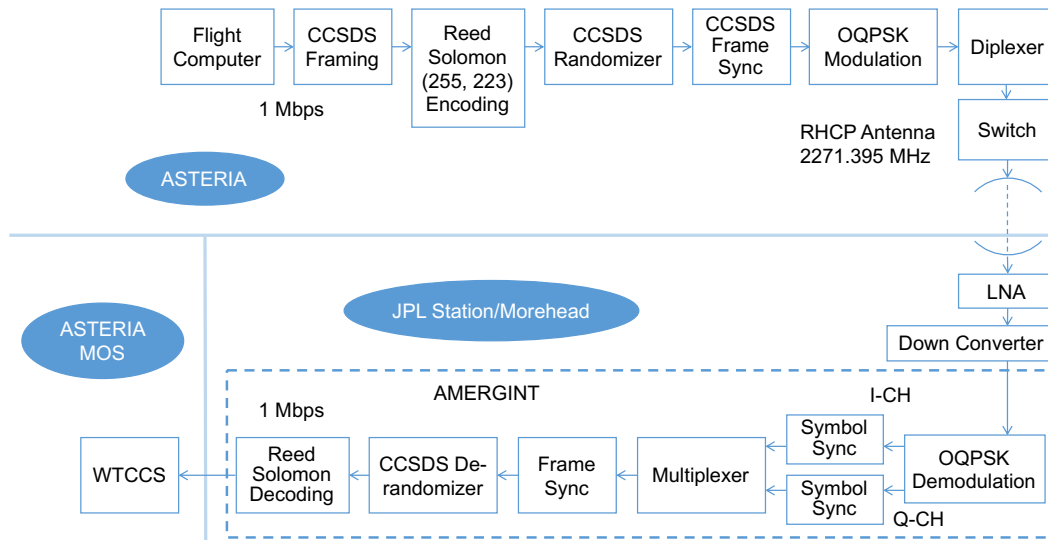


Figure 17: ASTERIA downlink diagram.

4.1.2 Uplink Processing

Figure 18 shows a functional diagram for the ground-to-ASTERIA uplink at the higher 32 Kbps rate. The scheme is identical for the uplink at the lower 4 Kbps rate¹². The commands are sent by WTCCS to a differential encoding block. The signal is then sent to the AMERGINT and T400 modem to be BPSK modulated. The modulated carrier at 70 MHz is then upconverted to 2062.9 MHz, amplified, and radiated by the antenna. On the spacecraft, the RF signal is received through the antenna, the switch, and the

¹² Two uplink bit rates (32 Kbps for nominal operations and 4 Kbps for safe mode) have been used in flight. A third uplink bit rate (64 Kbps for FSW update) was baselined into the ASTERIA spacecraft, but has not been used in flight.

diplexer. The signal is then BPSK demodulated, and the synchronization is removed. The signal is differentially decoded, the CCSDS frame is removed, and the commands are sent to the flight computer.

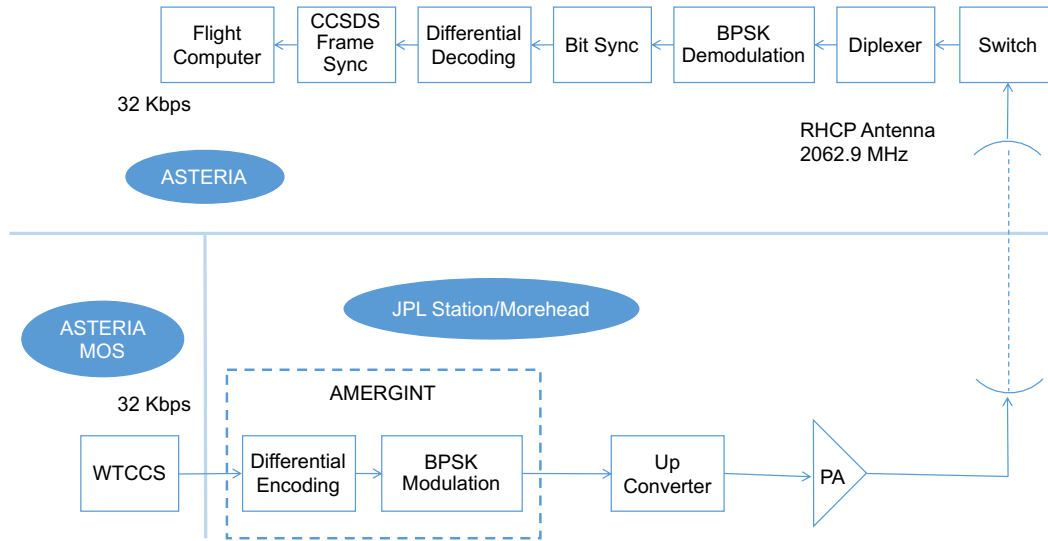


Figure 18: ASTERIA uplink diagram.

4.2 Compatibility Test at Morehead State University

Members of the ASTERIA team travelled to Morehead State University to test compatibility between the Vulcan CSR-SDR-S/S radio onboard ASTERIA and the Morehead State University 21-m ground station. For short, the radio is referred to in this section and its figures as the CSR radio.

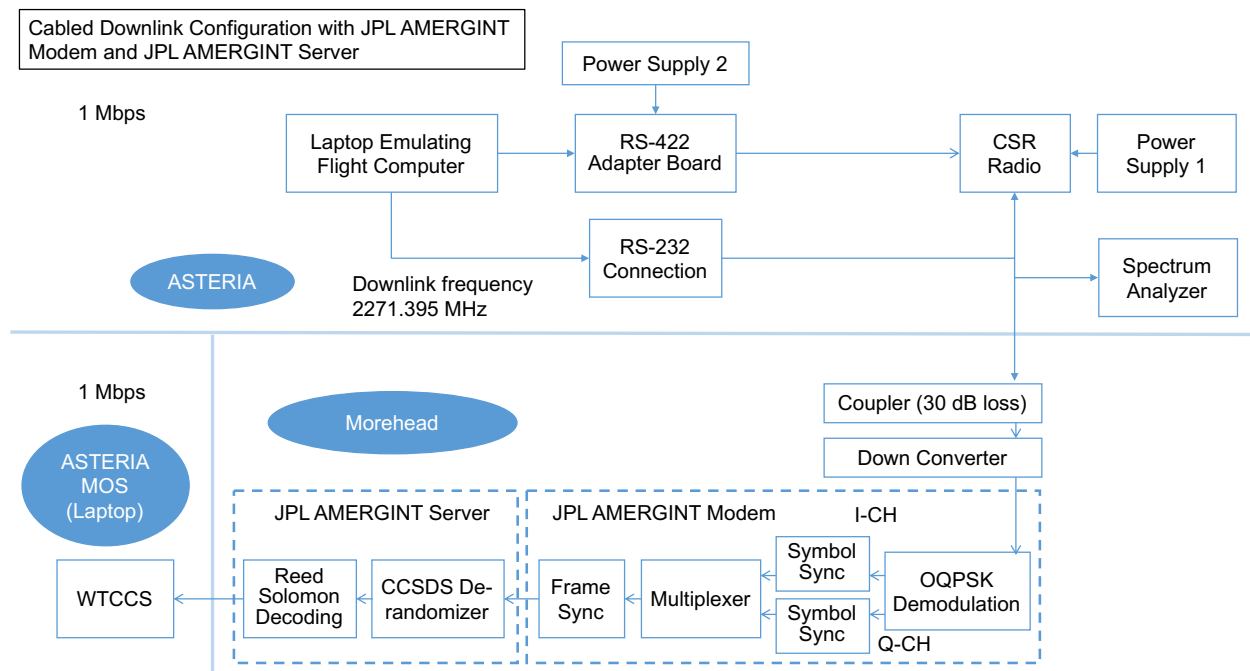
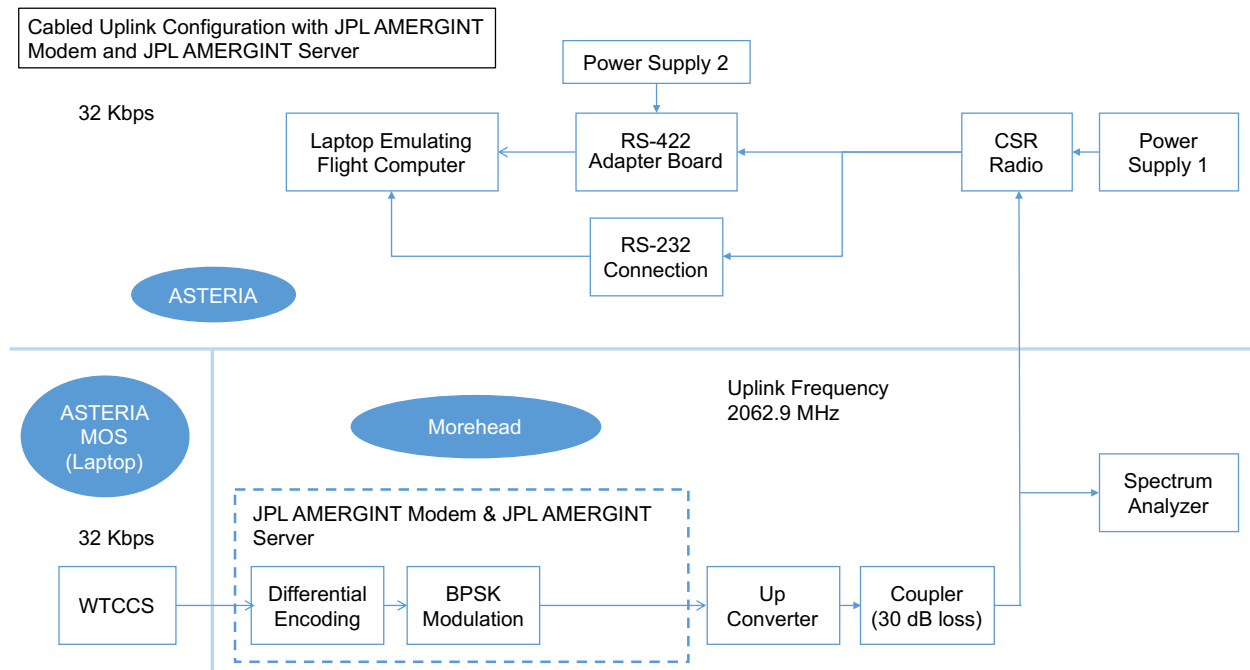
Four sets of tests were planned: CSR radio cabled to project uplink/downlink ground equipment; CSR radio cabled to Morehead ground equipment; CSR radio operating wirelessly with project equipment; and CSR radio operating wirelessly with Morehead equipment. Each test is shown below in one uplink block diagram and one downlink block diagram (Figures 19–20, 21–22, 23–24, and 25–26, respectively for the four tests).

Photographs of the test set-ups are in Figures 27–28.

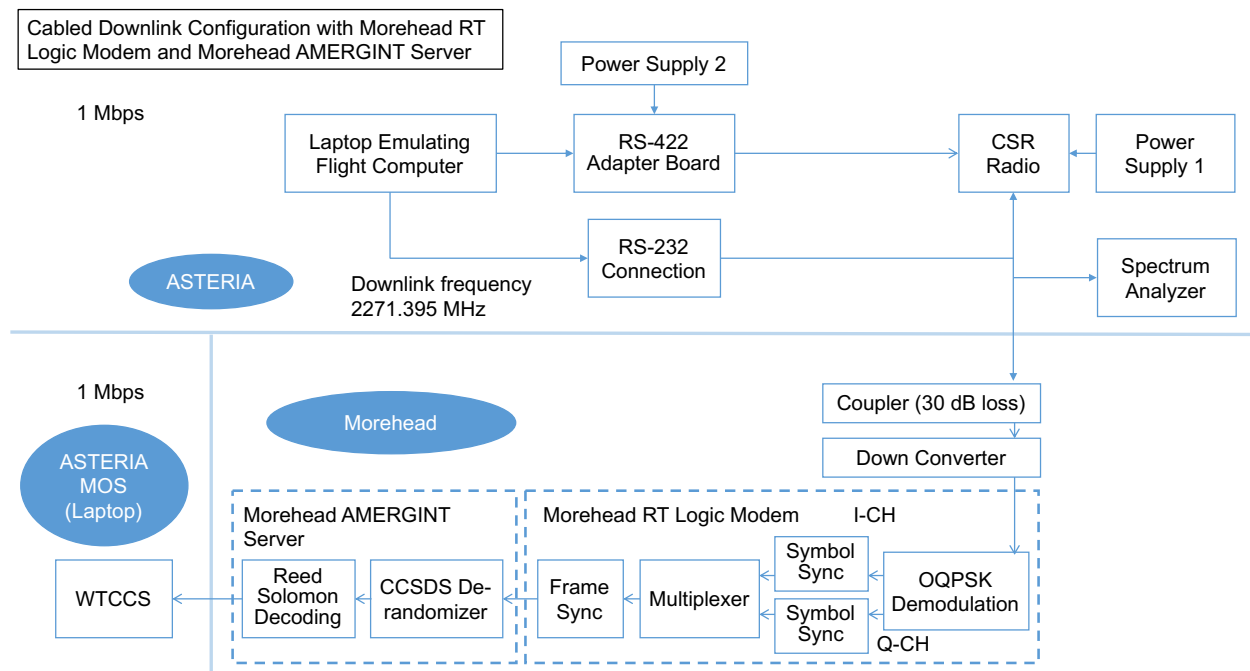
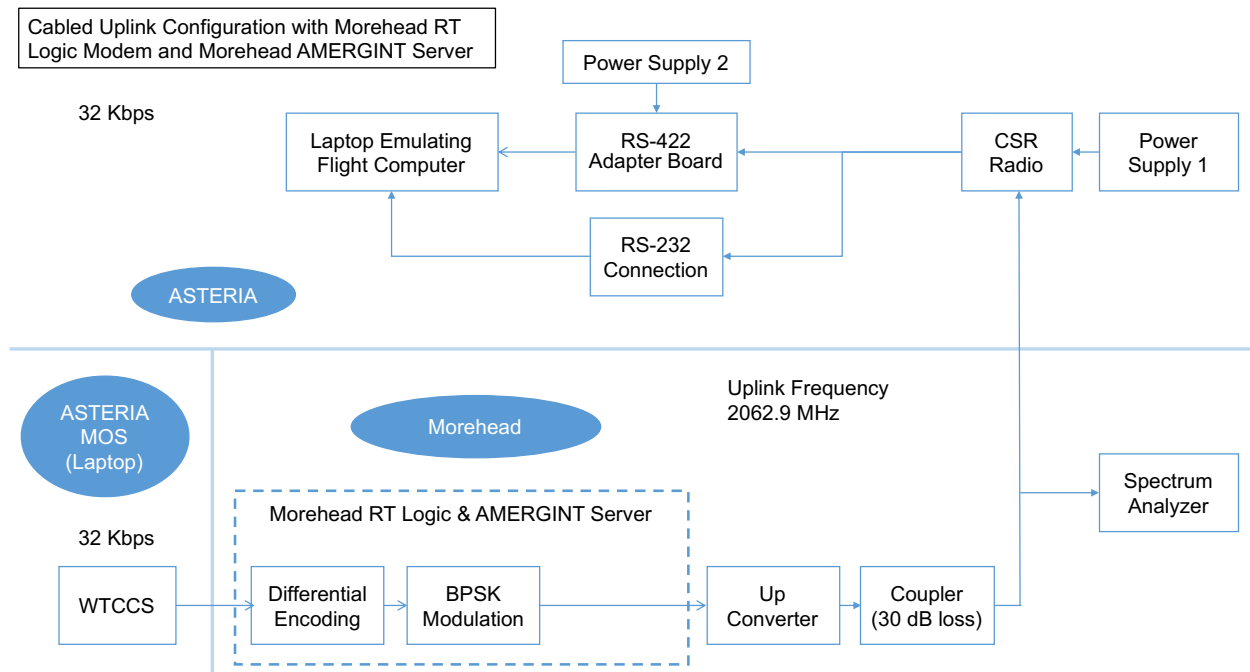
Because the ASTERIA team also owned an additional AMERGINT modem and server used as ground support equipment (GSE), this equipment was carried on at Morehead with the idea of using it as a backup during operation in case of issues with the primary Morehead T400 equipment. As a result, all the compatibility tests were performed with both the ASTERIA project-owned receiver and the Morehead-owned receiver.

The two sets of equipment were supposed to be identical and compatible with the on-board radio. However, tests showed that the Morehead equipment had some issues in the Reed Solomon and in the OQPSK ambiguity as explained in the paragraphs following Table 7 (test results).

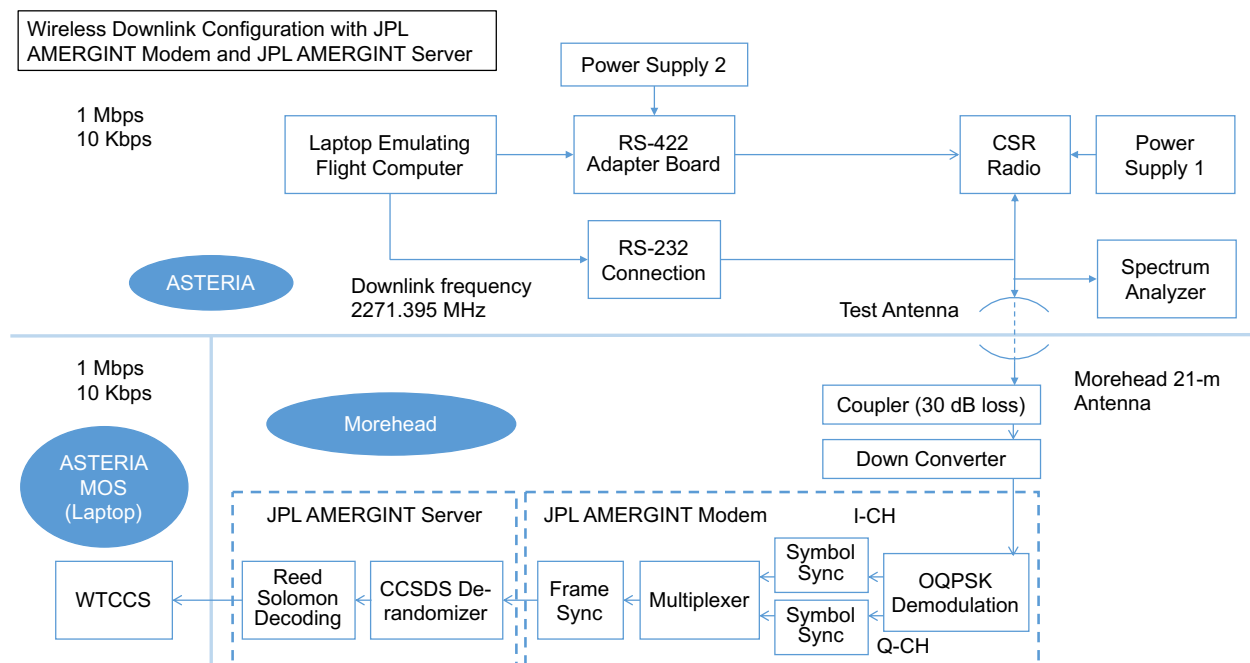
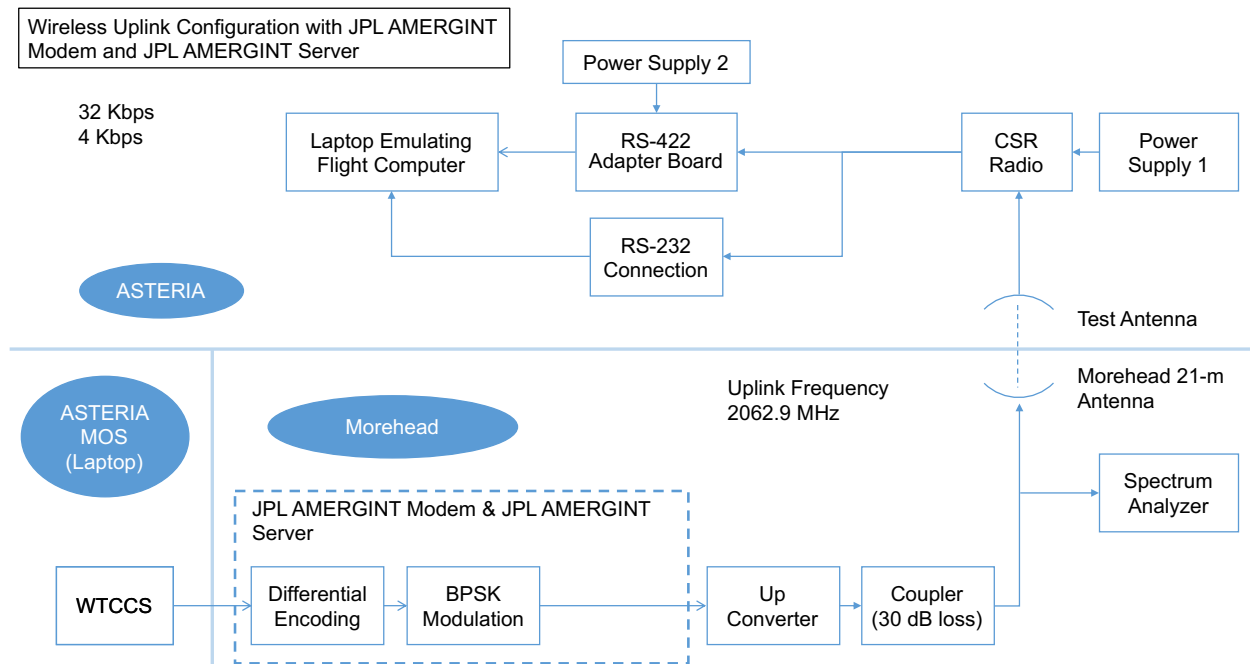
1. Cabled test between the CSR radio and the JPL AMERGINT (modem and server), uplink and downlink (see Figure 19 and Figure 20 for configuration).



2. Cabled test between the CSR radio and Morehead RT Logic T400 modem and AMERGINT server for both uplink and downlink (see Figure 21 and Figure 22 for configuration).



3. Wireless test between the CSR radio and JPL AMERGINT, uplink and downlink (see Figure 23 and Figure 24 for configuration).



4. Wireless test between the CSR radio and Morehead RT Logic modem and AMERGINT server, uplink and downlink (see Figure 25 and Figure 26 for configuration).

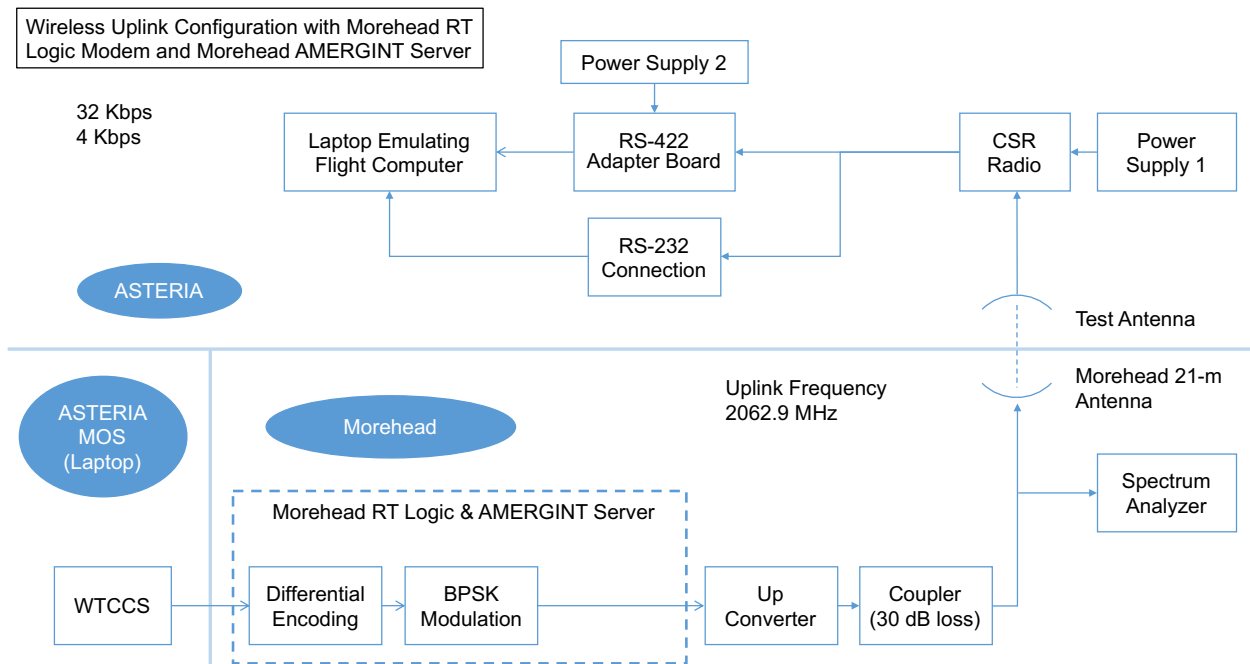


Figure 25: Test 4 uplink configuration (wireless, Morehead modem and server to CSR radio).

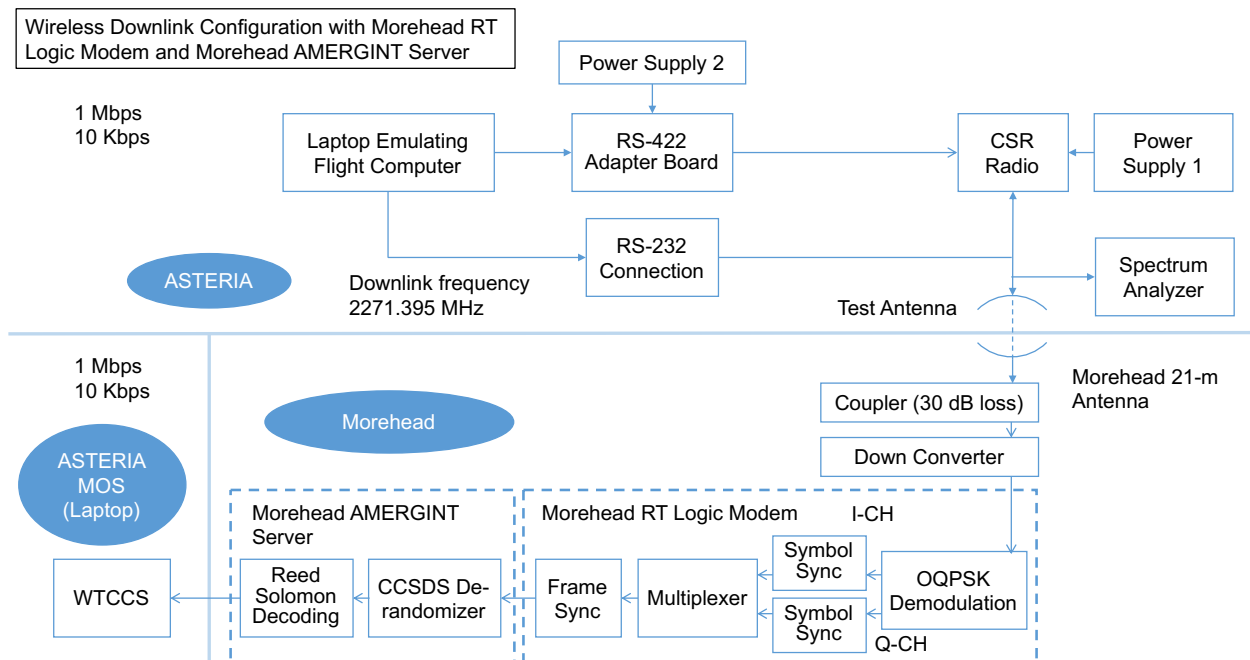


Figure 26: Test 4 downlink configuration (wireless, CSR radio to Morehead modem and server).

Figure 27 and Figure 28 show the setup of the compatibility test.

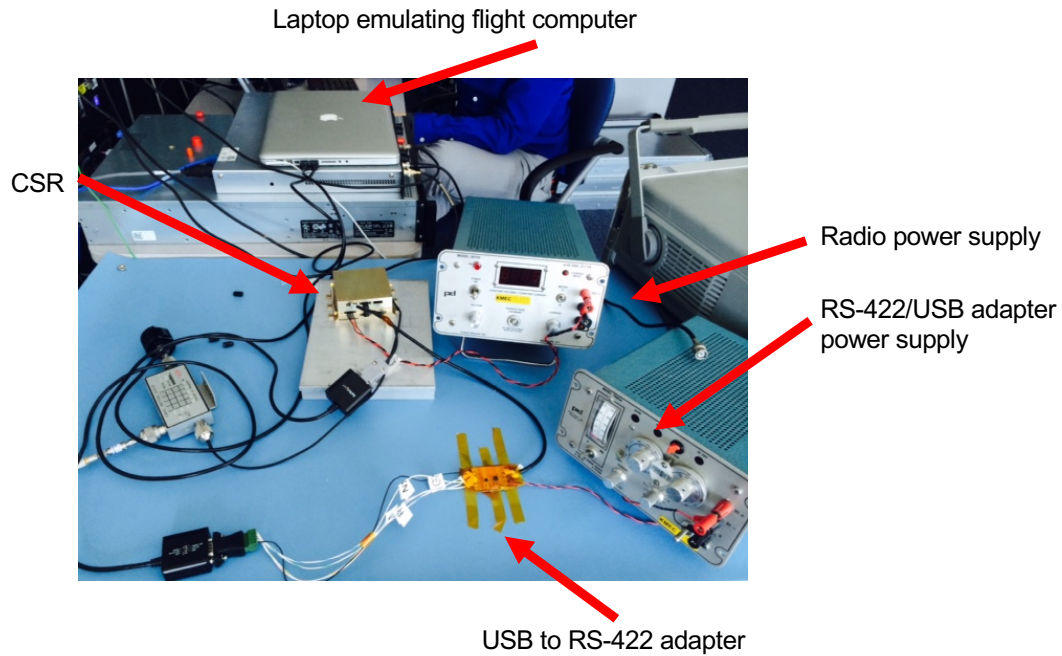


Figure 27: Compatibility test setup.

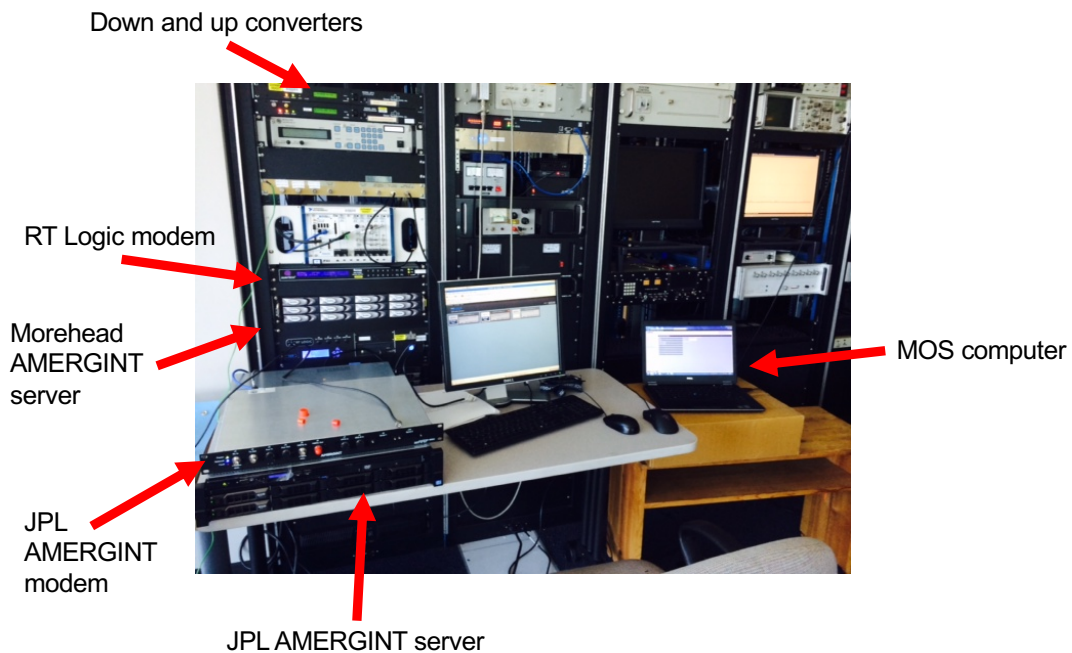


Figure 28: Ground station setup at Morehead State University.

Results for each of the tests are summarized in Table 7. Test outcomes are organized in the following categories:

- Success: the test worked without any particular issue that requires follow on.
- Partial success: the test was successful but one or more issues on the Morehead RT Logic T400 modem were discovered.
- Failure: the test was not successful.

Table 7: Results of Test 1 through Test 4.

Test	Data rates	Flight model used	Test result	Notes
Cabled uplink using JPL AMERGINT modem and server (Test 1, uplink)	32 Kbps	FM2	Success	Data were received on the flight computer. Frames were checked to verify that they were in fact identical to those sent from the WTCCS software. The transmitted signal was observed on the spectrum analyzer and resembled the one obtained in the laboratory at JPL.
Cabled uplink using Morehead RT Logic modem and AMERGINT server (Test 2, uplink)	32 Kbps	FM2	Partial Success	The test was partially successful for the following reason: 1) Configuration issues on the RT Logic T400 modem were affecting the generation of the modulation. 2) Header issues on the Morehead AMERGINT server turned out to be different from the JPL AMERGINT server. WTCCS software had to be modified to eliminate that particular header.
Cabled downlink using JPL AMERGINT modem and server (Test 1, downlink)	1 Mbps	FM2	Success	Data were received on the WTCCS. Frames were checked to verify that they were in fact identical to those sent from the flight radio. The transmitted signal was observed on the spectrum analyzer and resembled the one obtained in the laboratory at JPL.
Cabled downlink using Morehead RT Logic modem and AMERGINT server (Test 2, downlink)	1 Mbps	FM2	Partial success	This test was partially successful for the following reasons: 3) RT Logic seems to have a problem resolving the phase ambiguity in the OQPSK, and it requires rotation of the constellation until lock is achieved. 4) The RS (255, 223) on the Morehead AMERGINT server does work properly. Another important event during this test session was that while the test was in progress, lightning hit one of the campus buildings causing an electrical power shutdown. The shutdown lasted only a few minutes but: <ul style="list-style-type: none"> • The event triggered OVC (over voltage current) protection on the radio power supply. The radio seems to not have had any damage: it was inspected and checked by the Vulcan Wireless Inc. staff. • The same event affected the RT Logic modem by corrupting the uplink configuration setup of the prior day.
Cabled full duplex test using JPL AMERGINT modem and server (Test 1, uplink and downlink simultaneously)	1 Mbps down, 32 Kbps up.	FM2	Success	Downlink data from the radio were received on the WTCCS. Frames were checked to verify that they were in fact identical to those sent from the flight radio. Uplink data were received on the flight computer. Frames were checked to verify that they were in fact identical to those sent from the WTCCS software.
Cabled full duplex test using Morehead RT Logic and AMERGINT server (Test 2, uplink and downlink simultaneously)	1 Mbps down, 32 Kbps up	FM2	Partial success	The power shutdown of the prior day had corrupted the RT Logic settings in uplink, so the receiver had to be reconfigured. After that, the test was successful, frames were received on the flight radio (uplink) and on the WTCCS (downlink). However, the same bugs and problems previously discussed for the RT Logic and AMERGINT server remained.

Table 7: Results of Test 1 through Test 4.

Test	Data rates	Flight model used	Test result	Notes
Wireless full duplex test using JPL AMERGINT modem and server (Test 3)	1 Mbps down, 32 Kbps up	FM2, FM1	Success	Downlink data from the radio were received on the WTCCS. Frames were checked to verify that they were in fact identical to those sent from the flight radio. Uplink data were received on the flight computer. Frames were checked to verify that they were in fact identical to those sent from the WTCCS software.
Wireless full duplex test using Morehead RT Logic modem and AMERGINT server (Test 4)	1 Mbps down, 32 Kbps up	FM2, FM1	Partial success	Frames were received on the flight radio (uplink) and on the WTCCS (downlink). However, the same bugs and problems previously discussed for the RT Logic and AMERGINT server remained.
Wireless full duplex test using JPL AMERGINT modem and server (Test 3) at lower data rates	10 Kbps down, 4 Kbps up	FM1	Success	Downlink data from the radio were received on the WTCCS. Frames were checked to verify that they were in fact identical to those sent from the flight radio. Uplink data were received on the flight computer. Frames were checked to verify that they were in fact identical to those sent from the WTCCS software.
Wireless full duplex test using Morehead RT Logic modem and AMERGINT server (Test 4) at lower data rates	10 Kbps down, 4 Kbps up	FM1	Failure	The uplink was successful. The RT Logic bandwidth settings needed to be reconfigured. This test was descope and repeated later at JPL.

After compatibility tests, the following issues were identified:

1. Uplink modulation setting in the RT Logic T400 modem (RT Logic): the user is forced to turn on and off the modulation a couple of times before the system starts working.
2. OQPSK ambiguity: the RT Logic does not seem to be able to resolve the phase ambiguity in the OQPSK.
3. RS (255, 223): the Reed Solomon decoder on the Morehead AMERGINT server does not seem to work properly.
4. RT Logic low data rate lock: the RT Logic seems to have problem locking at 10 Kbps.

As a follow-up action, the Morehead State University staff allowed the ASTERIA team to bring their receiver from JPL for further tests and troubleshooting. The following results were accomplished:

1. Uplink modulation setting in the RT Logic: a workaround procedure in the operations was developed.
2. OQPSK ambiguity: a workaround procedure in the ground station operations was developed.
3. RS (255, 223): the Reed Solomon could not be fixed. Hence, the receiver was configured to bypass the coding scheme.
4. RT Logic low data rate lock: the correct settings were identified, and the RT Logic is now functional to receive at the lower data rates.

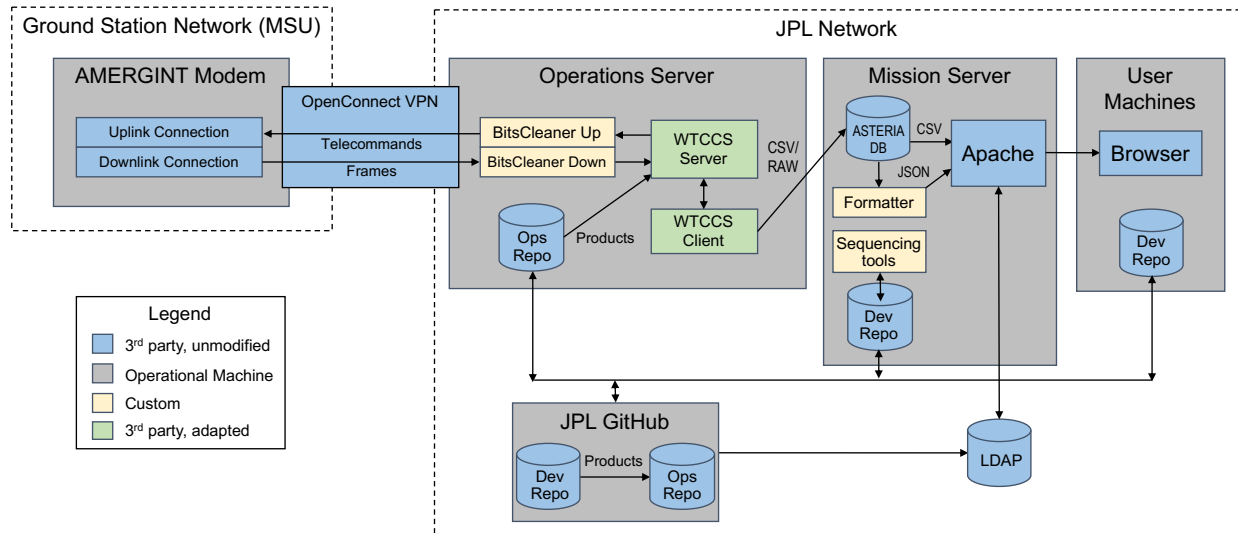
However, despite the work performed on the RT Logic modem, a decision was made to use the JPL Project-owned AMERGINT receiver as the primary receiver for the mission during operation. This decision was taken in order to minimize risks, because the project receiver did not have the Reed Solomon encoding issue. Also, the ASTERIA team was more familiar with this system.

4.3 ASTERIA Ground Data System (GDS)

Part of this section is taken from [9].

4.3.1 GDS Overview

The ASTERIA GDS is based on software and interface heritage from WISE, as well as additions meant to streamline operations. For Commanding and Telemetry, the WISE Telemetry Command and Communications Subsystem (WTCCS) is used. For web viewing, Open Mission Control Technologies (OpenMCT) is used to display recorded telemetry. All other operation tools are either unmodified software (Apache, GitHub) or custom Python tools designed for interface compatibility or operations streamlining. The basic GDS for ASTERIA can be seen in Figure 29.



4.3.2 WTCCS

WTCCS, the primary GDS software for ASTERIA, is a command and control software that supports translating and transmitting CCSDS telecommands; decommutating CCSDS frames and packets; reporting of hazards, EVRs, and alarms; providing CCSDS file delivery protocol for both uplink telecommands and downlink frames; viewing of real-time telemetry; and automating through a Tool Command Language (TCL) API. WTCCS is used by the Mission Operations Team spacecraft operator and the Mission Manager to monitor and command the ASTERIA spacecraft during passes and to export post-pass real-time and recorded downlink data. During operations, there is one typically WTCCS server instance running and one WTCCS client for each spacecraft operator and Mission Manager console.

A typical operator's console screen is shown in Figure 30.

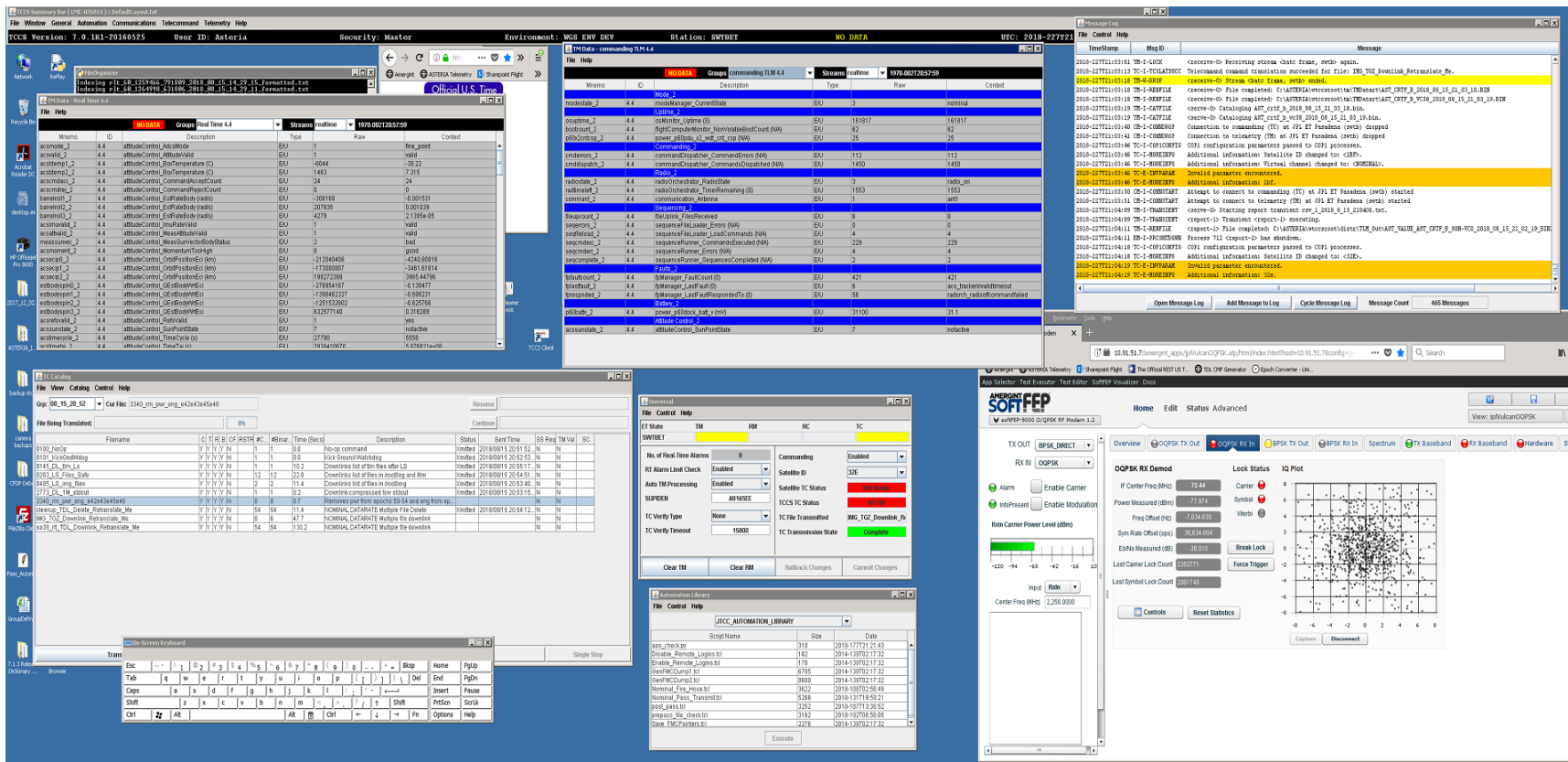


Figure 30: ASTERIA WTCCS Operator's Console.

4.3.3 OpenMCT

For typical ASTERIA operations, the ASTERIA team will not access data directly through WTCCS. Instead, OpenMCT is used via a web browser. OpenMCT is a next-generation mission control framework being developed at NASA's Ames Research Center in partnership with Advanced Multimission Operations System (AMMOS). OpenMCT provides a web front end for missions to use with plugins and back end databases. OpenMCT provides the following capabilities to ASTERIA:

- Plotting historical telemetry by date in the following plot formats:
 - Individual channel
 - Stacked channel
 - Overlaid channel
- Table views of telemetry that can be combined for channels, then exported in a comma-separated values (CSV) format
- Export of plots as images, either as a lossless (PNG) formatted file or a lossy (JPG) formatted file
- Historical telemetry displays configurations that can be customized and saved by individual users
- Simple combined access of other ASTERIA webpages

Figure 31 shows details of the OpenMCT architecture.

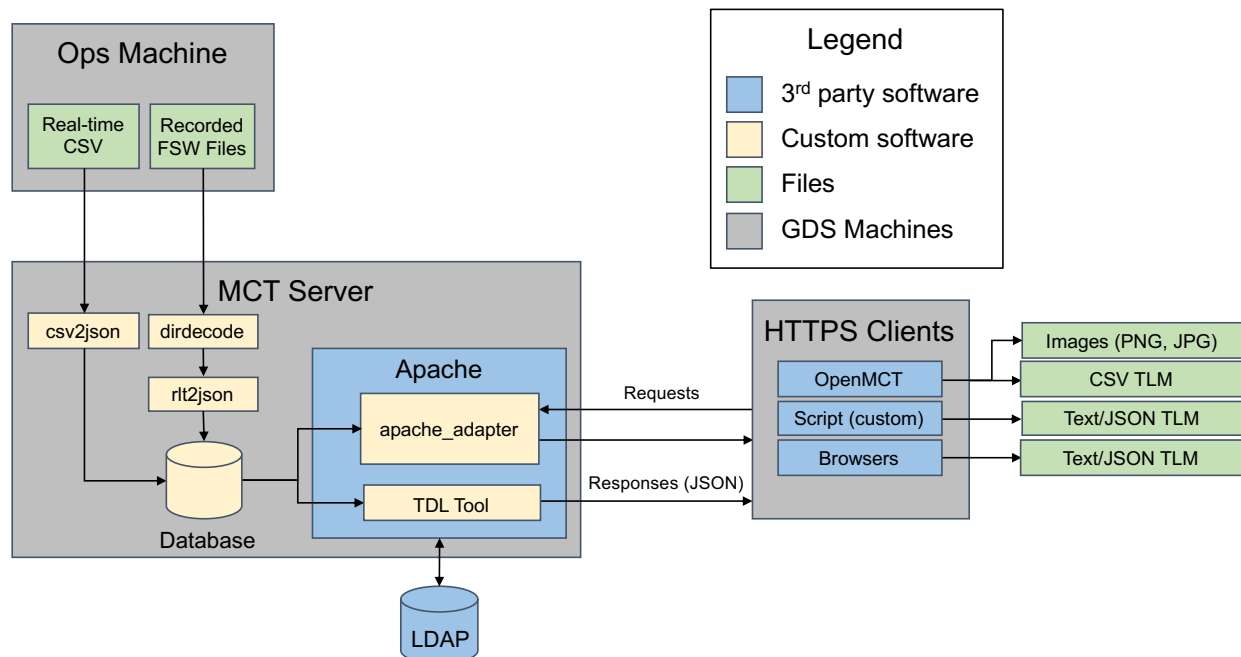


Figure 31: Web architecture for ASTERIA.

The backend for OpenMCT has been written to take advantage of native downlink formats for ASTERIA. Recorded telemetry is stored on board the spacecraft in files that are named according to when they were created. After receipt on the ground, the recorded telemetry files are ingested according to their names and the data are indexed by time. The ingested telemetry is then separated in CSV format and indexed by the flight system epoch. Since each flight system epoch is relative to its boot, the backend corrects timestamps to the spacecraft event time (SCET) based on an epoch file that tracks each spacecraft boot time. Once times are formatted, the corrected file is written out, and the filename is indexed. A second script then is responsible for interpreting queries received from OpenMCT, opening the applicable files, and returning the requested channel data in JavaScript Object Notation (JSON). Query and database access are controlled through basic authentication provided by Lightweight Directory Access Protocol (LDAP) and Apache. In addition to OpenMCT, users can format their own queries through script or browser to receive telemetry in either text or JSON formats.

Figure 32 displays a typical ASTERIA plot provided by OpenMCT.

4.3.4 Custom Scripts and Webpages

In addition to WTCCS and OpenMCT, ASTERIA is operated with the assistance of custom scripts. The operational scripts for ASTERIA are written in a variety of languages, the most common being Python. Operational scripts for ASTERIA provide the following capabilities:

- Pass automation
- Historical downlink automation
- Downlinked file deletion automation
- Onboard file compression, downlink, and removal automation
- Compatibility layers with ground station modem and WTCCS
- Post-pass server synchronization

Most of the ASTERIA scripts are run via shortcuts as needed during operations. Some, however, include web views. One such web view, available in OpenMCT, shown in Figure 33, provides for the generation of uplink products. Other OpenMCT views assist in downlinking, compressing, or deleting files.

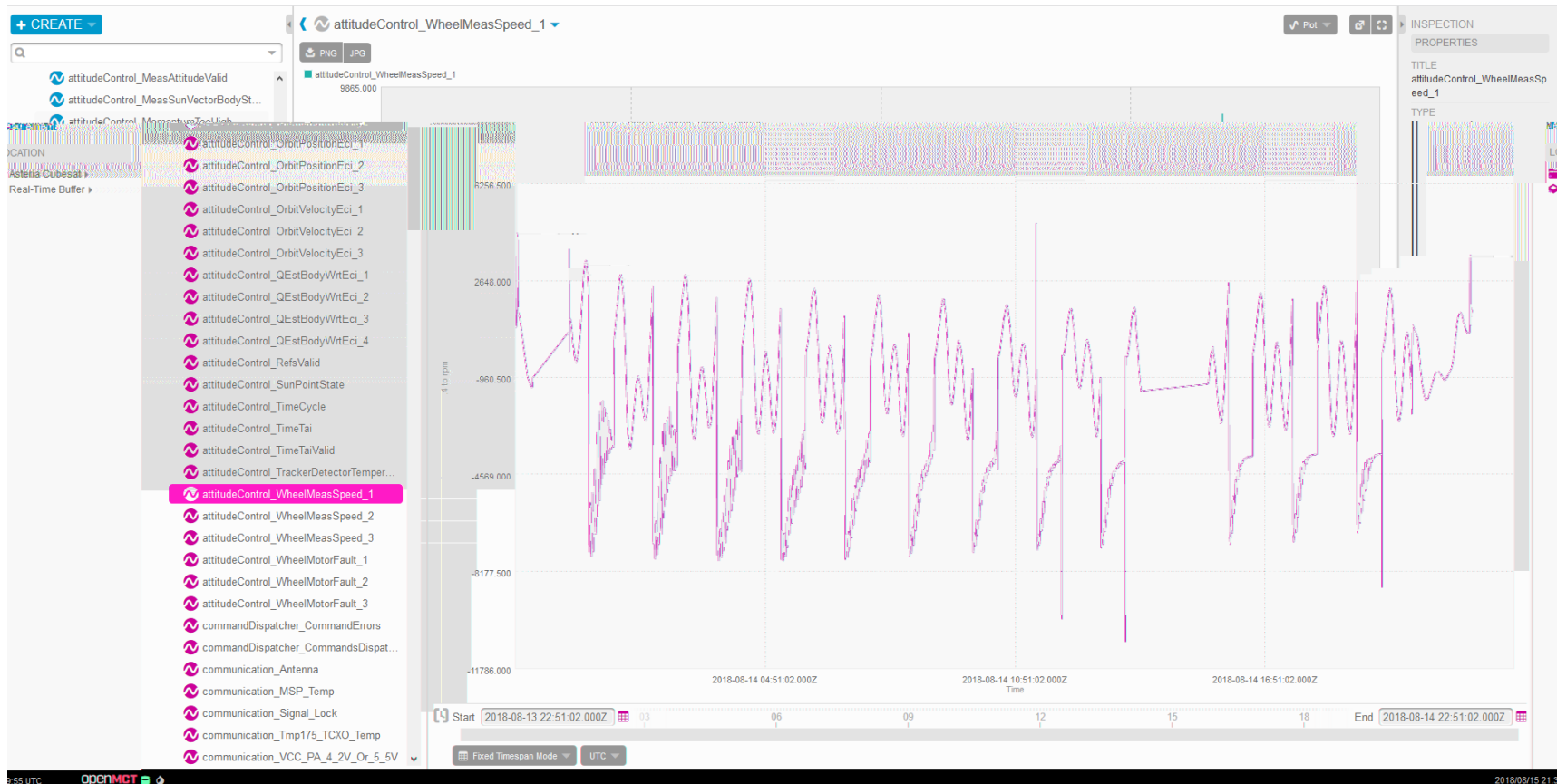


Figure 32: OpenMCT plot for ASTERIA.

Generate TDL CMF

Expand the folders you want, then select the files to downlink and hit save to download a CMF.

Downlink CMF	Delete CMF	Compression Seq	Refresh Zipfiles
Log Files			
<input type="checkbox"/> log_61_78427_066585.com 3.0s			
RLT Files			
IMG Files			
TGZ Files (Except in IMG)			
PCS Files			
ACS Files			
THM Files			
ENG Files			
PWR Files			
COM Files			

Figure 33: ASTERIA uplink product generation tools.

The usage of custom scripts on ASTERIA is at the Mission Manager's discretion. The scripts have been validated to produce uplink products that are safe for the spacecraft, and can be used as needed to downlink specific files during passes, to kick off compression sequences, or to remove specific files from the flight system.

4.3.5 Third-party Tools

In addition to customized and adapted software, ASTERIA's GDS also makes use of several third-party tools. These tools were provided as-is, usually from open source code, and were deployed to allow GDS design to be simple and quick. ASTERIA's third-party software includes:

- GitHub (JPL provided)
- Apache
- Debian
- Unison
- LDAP (JPL provided)

5 Link Performance

5.1 Link Analysis

The ASTERIA telecommunication system provides S-band downlink and uplink communication with the Morehead State University 21-m parabolic dish. ASTERIA telecommunication link margins are computed using link budget statistical techniques described in [10].

Each link's performance is computed using telecommunication link design software provided by the JPL Team Xc, a concurrent design facility for CubeSats [11]. The tool is an integrated STK-MATLAB-Excel software package¹³ that allows the user (in this case ASTERIA) to incorporate an orbit profile and to select mission specific spacecraft parameters. The user also selects the ground station (in this case the Morehead State University dish) from a database. Results for the ASTERIA/Morehead uplink and downlink are described in the following sections.

5.1.1 Uplink Performance

The uplink signal is a direct carrier BPSK modulated signal. The uplink performance is shown in Table 8 for the 32 Kbps data rate and in Table 9 for the 4 Kbps data rate. In each table, two cases are shown: the one at the left is at maximum range with ASTERIA at the edge of the ground station mask, and the one at the right is at minimum range with ASTERIA basically on top of the ground station.

It can be noticed that the link performance has plenty of margin in both cases.

¹³ STK refers to Systems Tool Kit, an astrodynamics computer program from Analytical Graphics, Inc. STK allows engineers and scientists to perform complex analyses of ground, sea, air, and space assets, and share results in one integrated solution. At the core of STK is a geometry engine for determining the time-dynamic position and attitude of objects and the spatial relationships among the objects. https://en.wikipedia.org/wiki/Systems_Tool_Kit

MATLAB (matrix laboratory) is a multi-paradigm numerical computing environment and proprietary programming language developed by MathWorks. MATLAB allows matrix manipulations, plotting of functions and data, and implementation of algorithms. <https://en.wikipedia.org/wiki/MATLAB>

Microsoft Excel is a software program that allows users to organize, format, and calculate data with formulas using a spreadsheet system. It features the ability to perform basic calculations, use graphing tools, create pivot tables, and create macros. <https://www.techopedia.com/definition/5430/microsoft-excel>

Table 8: Uplink design table (32 Kbps data rate).

Item	Symbol	Units	Uplink Max Range (Min)	Fav Tol	Adv. Tol	Var	Uplink Min Range (Mean)	Fav Tol.	Adv. Tol	Var
EIRP:										
Transmitter Power	P	dBW	17.00	0.00	0.00	0.00	17.00	0.00	0.00	0.00
Polarization Loss	L _i	dB	-0.50	0.00	0.00	0.00	-0.50	0.00	0.00	0.00
Transmit Antenna Gain (net)	G _t	dBi	51.00	0.60	-0.60	0.12	51.00	0.60	-0.60	0.12
Equiv. Isotropic Radiated Power	EIRP	dBW	67.50	0.60	-0.60	0.12	67.50	0.60	-0.60	0.12
Receive Antenna Gain:										
Frequency	f	Ghz	2.06	0.00	0.00	0.00	2.06	0.00	0.00	0.00
Receive Antenna Gain	G _r	dBi	7.00	2.00	-2.00	1.33	7.00	2.00	-2.00	1.33
Free Space Loss:										
Propagation Path Length	S	km	1,453.00	0.00	0.00	0.00	400.00	0.00	0.00	0.00
Free Space Loss	L _s	dB	-161.98	0.00	0.00	0.00	-150.77	0.00	0.00	0.00
Transmission Path and Pointing Losses:										
Transmit Antenna Pointing Loss	L _{pt}	dB	-1.00	1.00	-1.00	0.33	-1.00	1.00	-1.00	0.33
Receive Antenna Pointing Loss	L _{pr}	dB	-3.00	3.00	-3.00	3.00	-3.00	3.00	-3.00	3.00
Ionospheric Loss	L _{ion}	dB	0.00	0.00	0.00	0.00	0.00	0.00	0.00	0.00
Atmospheric Loss (H ₂ O and O ₂ losses)	L _{atmo}	dB	-0.42	0.00	0.00	0.00	-0.42	0.00	0.00	0.00
Loss due to Rain	L _{rain}	dB	-0.04	0.00	0.00	0.00	-0.04	0.00	0.00	0.00
Scintillation loss		dB	-0.68	0.00	0.00	0.00	-0.68	0.00	0.00	0.00
Implementation, additional losses		dB	-3.00	0.00	0.00	0.00	-3.00	0.00	0.00	0.00
Total Additional Losses		dB	-8.14	4.00	-4.00	3.33	-8.14	4.00	-4.00	3.33
Data Rate:										
Data Rate	R	bps	32,000.00	0.00	0.00	0.00	32,000.00	0.00	0.00	0.00
Data Rate	10 log (R)	dBbps	45.05	0.00	0.00	0.00	45.05	0.00	0.00	0.00
Boltzman's Constant:										
Boltzman's Constant	10 log (k)	dBW/(Hz*K)	-228.60	0.00	0.00	0.00	-228.60	0.00	0.00	0.00
System Noise Temperature:										
System Noise Temperature	T _s	K	907.00	2.00	-2.00	1.33	907.00	2.00	-2.00	1.33
System Noise Temperature	10 log (T _s)	dBK	29.58	0.00	0.00	1.25	29.58	0.00	0.00	1.25
E _b /N ₀		dB	58.35	0.00	0.00	6.04	69.56	6.60	-6.60	6.04
E _b /N ₀ required		dB	9.60	0.00	0.00	0.00	9.60	0.00	0.00	0.00
Performance Margin		dB	48.75	0.00	0.00	6.04	59.96	6.60	-6.60	6.04
Sigma			2.46	0	0	0	2.46	0	0	0
Margin - 3 Sigma			41.38	0	0	0	52.59	0	0	0

Table 9: Uplink design table (4 Kbps data rate).

Item	Symbol	Units	Uplink Max Range (Min)	Fav Tol	Adv. Tol	Var	Uplink Min Range (Mean)	Fav Tol.	Adv. Tol	Var
EIRP:										
Transmitter Power	P	dBW	17.00	0.00	0.00	0.00	17.00	0.00	0.00	0.00
Polarization Loss	L _i	dB	-0.50	0.00	0.00	0.00	-0.50	0.00	0.00	0.00
Transmit Antenna Gain (net)	G _t	dBi	51.00	0.60	-0.60	0.12	51.00	0.60	-0.60	0.12
Equiv. Isotropic Radiated Power	EIRP	dBW	67.50	0.60	-0.60	0.12	67.50	0.60	-0.60	0.12
Receive Antenna Gain:										
Frequency	f	Ghz	2.06	0.00	0.00	0.00	2.06	0.00	0.00	0.00
Receive Antenna Gain	G _r	dBi	7.00	2.00	-2.00	1.33	7.00	2.00	-2.00	1.33
Free Space Loss:										
Propagation Path Length	S	km	1,453.00	0.00	0.00	0.00	400.00	0.00	0.00	0.00
Free Space Loss	L _s	dB	-161.98	0.00	0.00	0.00	-150.77	0.00	0.00	0.00
Transmission Path and Pointing Losses:										
Transmit Antenna Pointing Loss	L _{pt}	dB	-1.00	1.00	-1.00	0.33	-1.00	1.00	-1.00	0.33
Receive Antenna Pointing Loss	L _{pr}	dB	-3.00	3.00	-3.00	3.00	-3.00	3.00	-3.00	3.00
Ionospheric Loss	L _{ion}	dB	0.00	0.00	0.00	0.00	0.00	0.00	0.00	0.00
Atmospheric Loss (H ₂ O and O ₂ losses)	L _{atmo}	dB	-0.42	0.00	0.00	0.00	-0.42	0.00	0.00	0.00
Loss due to Rain	L _{rain}	dB	-0.04	0.00	0.00	0.00	-0.04	0.00	0.00	0.00
Scintillation loss		dB	-0.68	0.00	0.00	0.00	-0.68	0.00	0.00	0.00
Implementation, additional losses		dB	-3.00	0.00	0.00	0.00	-3.00	0.00	0.00	0.00
Total Additional Losses		dB	-8.14	4.00	-4.00	3.33	-8.14	4.00	-4.00	3.33
Data Rate:										
Data Rate	R	bps	4,000.00	0.00	0.00	0.00	4,000.00	0.00	0.00	0.00
Data Rate	10 log (R)	dBbps	36.02	0.00	0.00	0.00	36.02	0.00	0.00	0.00
Boltzman's Constant:										
Boltzman's Constant	10 log (k)	dBW/(Hz*K)	-228.60	0.00	0.00	0.00	-228.60	0.00	0.00	0.00
System Noise Temperature:										
System Noise Temperature	T _s	K	907.00	2.00	-2.00	1.33	907.00	2.00	-2.00	1.33
System Noise Temperature	10 log (T _s)	dBK	29.58	0.00	0.00	1.25	29.58	0.00	0.00	1.25
E _b /N ₀		dB	67.38	0.00	0.00	6.04	78.59	6.60	-6.60	6.04
E _b /N ₀ required		dB	9.60	0.00	0.00	0.00	9.60	0.00	0.00	0.00
Performance Margin		dB	57.78	0.00	0.00	6.04	68.99	6.60	-6.60	6.04
Sigma			2.46	0	0	0	2.46	0	0	0
Margin - 3 Sigma			50.41	0	0	0	61.62	0	0	0

5.1.2 Downlink Performance

The downlink signal is a direct carrier OQPSK modulated signal. The downlink performance is shown in Table 10 for the 1 Mbps data rate and in Table 11 for the 10 Kbps data rate. As with the uplink tables, each downlink table shows maximum range performance to the left and minimum range to the right.

The downlink also has plenty of margin at both maximum and minimum range.

Table 10: Downlink design table (1 Mbps data rate).

Item	Symbol	Units	Downlink Max Range (Mean)	Fav Tol	Adv. Tol	Var	Downlink Min Range (Mean)	Fav Tol	Adv. Tol	Var
EIRP:										
Transmitter Power	P	dBW	0.00	0.00	0.00	0.00	0.00	0.00	0.00	0.00
Line Loss/Waveguide Loss	L _i	dB	-0.21	0.50	-0.50	0.08	-0.21	0.50	-0.50	0.08
Transmit Antenna Gain (net)	G _t	dBi	7.00	1.00	-1.00	0.33	7.00	1.00	-1.00	0.33
Equiv. Isotropic Radiated Power	EIRP	dBW	6.79	1.50	-1.50	0.42	6.79	1.50	-1.50	0.42
Receive Antenna Gain:										
Frequency	f	Ghz	2.27	0.00	0.00	0.00	2.27	0.00	0.00	0.00
Receive Antenna Diameter	D _r	m	21.00	0.00	0.00	0.00	21.00	0.00	0.00	0.00
Receive Antenna efficiency	η	n/a	0.60	0.00	0.00	0.00	0.60	0.00	0.00	0.00
Receive Antenna Gain	G _r	dBi	51.76	0.00	0.00	0.00	51.76	0.00	0.00	0.00
Free Space Loss:										
Propagation Path Length	S	km	1,453.00	0.00	0.00	0.00	400.00	0.00	0.00	0.00
Free Space Loss	L _s	dB	-162.82	0.00	0.00	0.00	-151.62	0.00	0.00	0.00
Transmission Path and Pointing Losses:										
Transmit Antenna Pointing Loss	L _{pt}	dB	-3.00	1.00	-1.00	0.33	-3.00	1.00	-1.00	0.33
Receive Antenna Pointing Loss	L _{pr}	dB	-1.00	0.50	-0.50	0.08	-1.00	-0.50	0.50	0.08
Ionospheric Loss	L _{ion}	dB	0.00	0.00	0.00	0.00	0.00	0.00	0.00	0.00
Atmospheric Loss (H ₂ O and O ₂ losses)	L _{atmo}	dB	-0.50	0.00	0.00	0.00	-0.50	0.00	0.00	0.00
Loss due to Rain	L _{rain}	dB	-0.10	0.00	0.00	0.00	-0.10	0.00	0.00	0.00
Scintillation loss		dB	-0.68	0.00	0.00	0.00	-0.68	0.00	0.00	0.00
Implementation, additional losses		dB	-4.00	0.00	0.00	0.00	-4.00	0.00	0.00	0.00
Total Additional Losses		dB	-9.28	1.50	-1.50	0.42	-9.28	0.50	-0.50	0.42
Data Rate:										
Data Rate	R	bps	1,000,000.00	0.00	0.00	0.00	1,000,000.00	0.00	0.00	0.00
Data Rate	10 log (R)	dBbps	60.00	0.00	0.00	0.00	60.00	0.00	0.00	0.00
Boltzman's Constant:										
Boltzman's Constant	10 log (k)	dBW/(Hz*K)	-228.60	0.00	0.00	0.00	-228.60	0.00	0.00	0.00
System Noise Temperature:										
System Noise Temperature	T _s	K	215.00	0.00	0.00	0.00	215.00	0.00	0.00	0.00
System Noise Temperature	10 log (T _s)	dBK	23.32	0.00	0.00	0.00	23.32	0.00	0.00	0.00
E _b /N ₀		dB	31.73	0.00	0.00	0.83	42.93	2.00	-2.00	0.83
E _b /N ₀ required		dB	6.20	0.00	0.00	0.00	6.20	0.00	0.00	0.00
Performance Margin		dB	25.53	0.00	0.00	0.83	36.73	2.00	-2.00	0.83
Sigma			0.91	0	0	0	0.91	0	0	0
Margin - 3 Sigma			22.79	0	0	0	33.99	0	0	0

Table 11: Downlink design table (10 Kbps data rate).

Item	Symbol	Units	Downlink Max Range (Mean)	Fav Tol	Adv. Tol	Var	Downlink Min Range (Mean)	Fav Tol.	Adv. Tol	Var
EIRP:										
Transmitter Power	P	dBW	0.00	0.00	0.00	0.00	0.00	0.00	0.00	0.00
Line Loss/Waveguide Loss	L _l	dB	-0.21	0.50	-0.50	0.08	-0.21	0.50	-0.50	0.08
Transmit Antenna Gain (net)	G _t	dBi	7.00	1.00	-1.00	0.33	7.00	1.00	-1.00	0.33
Equiv. Isotropic Radiated Power	EIRP	dBW	6.79	1.50	-1.50	0.42	6.79	1.50	-1.50	0.42
Receive Antenna Gain:										
Frequency	f	Ghz	2.27	0.00	0.00	0.00	2.27	0.00	0.00	0.00
Receive Antenna Diameter	D _r	m	21.00	0.00	0.00	0.00	21.00	0.00	0.00	0.00
Receive Antenna efficiency	η	n/a	0.60	0.00	0.00	0.00	0.60	0.00	0.00	0.00
Receive Antenna Gain	G _r	dBi	51.76	0.00	0.00	0.00	51.76	0.00	0.00	0.00
Free Space Loss:										
Propagation Path Length	S	km	1,453.00	0.00	0.00	0.00	400.00	0.00	0.00	0.00
Free Space Loss	L _s	dB	-162.82	0.00	0.00	0.00	-151.62	0.00	0.00	0.00
Transmission Path and Pointing Losses:										
Transmit Antenna Pointing Loss	L _{pt}	dB	-3.00	1.00	-1.00	0.33	-3.00	1.00	-1.00	0.33
Receive Antenna Pointing Loss	L _{pr}	dB	-1.00	0.50	-0.50	0.08	-1.00	-0.50	0.50	0.08
Ionospheric Loss	L _{ion}	dB	0.00	0.00	0.00	0.00	0.00	0.00	0.00	0.00
Atmospheric Loss (H ₂ O and O ₂ losses)	L _{atmo}	dB	-0.50	0.00	0.00	0.00	-0.50	0.00	0.00	0.00
Loss due to Rain	L _{rain}	dB	-0.10	0.00	0.00	0.00	-0.10	0.00	0.00	0.00
Scintillation loss		dB	-0.68	0.00	0.00	0.00	-0.68	0.00	0.00	0.00
Implementation, additional losses		dB	-4.00	0.00	0.00	0.00	-4.00	0.00	0.00	0.00
Total Additional Losses		dB	-9.28	1.50	-1.50	0.42	-9.28	0.50	-0.50	0.42
Data Rate:										
Data Rate	R	bps	10,000.00	0.00	0.00	0.00	10,000.00	0.00	0.00	0.00
Data Rate	10 log (R)	dBbps	40.00	0.00	0.00	0.00	40.00	0.00	0.00	0.00
Boltzman's Constant:										
Boltzman's Constant	10 log (k)	dBW/(Hz*K)	-228.60	0.00	0.00	0.00	-228.60	0.00	0.00	0.00
System Noise Temperature:										
System Noise Temperature	T _s	K	215.00	0.00	0.00	0.00	215.00	0.00	0.00	0.00
System Noise Temperature	10 log (T _s)	dBK	23.32	0.00	0.00	0.00	23.32	0.00	0.00	0.00
E _b /N ₀		dB	51.73	0.00	0.00	0.83	62.93	2.00	-2.00	0.83
E _b /N ₀ required		dB	6.20	0.00	0.00	0.00	6.20	0.00	0.00	0.00
Performance Margin		dB	45.53	0.00	0.00	0.83	56.73	2.00	-2.00	0.83
Sigma			0.91	0	0	0	0.91	0	0	0
Margin - 3 Sigma			42.79	0	0	0	53.99	0	0	0

5.2 Orbital Analysis

The STK software was used to simulate the orbital path of ASTERIA and to derive statistics on passes and on Doppler. Results of these analyses are discussed in the next two sections.

5.2.1 Passes Statistics

ASTERIA was deployed out of the International Space Station (ISS), and since it does not have an active propulsion system, it will remain in an orbit similar to the one of the ISS, while slowly decaying over two years. Hence, the orbit used for this analysis is of approximately 400 Km and 51.6 degree inclination. The analysis is developed for a year with the objective of inferring trends in the characteristics of the passes. Figure 34 shows a 2D map of the ASTERIA satellite orbit. The tracks covered by the satellite over time contribute to create the yellow shape on top of the site of the Morehead State University 21-m dish.

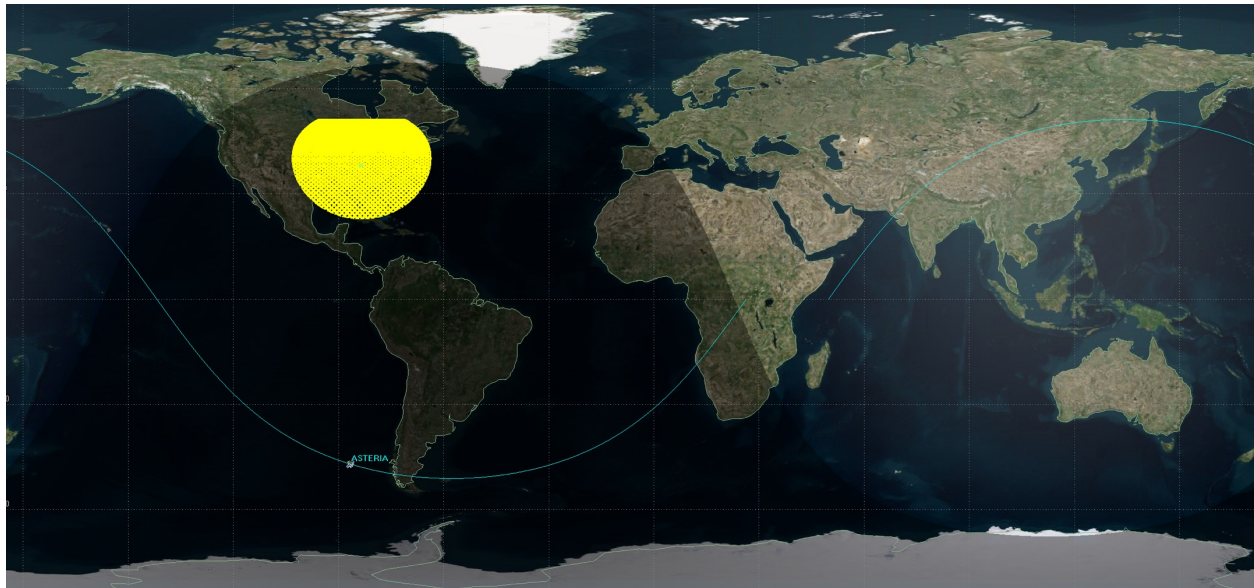


Figure 34: ASTERIA coverage map in 2D on a Mercator map.

In Figure 34, the yellow area comes from the overlapping of the tracking passes over the one year of simulation. The missing yellow area to the north is due to the 5-degree elevation constraint of the station.

Since the ASTERIA goal is to achieve very high pointing precision and to operate the optical instrument, the preference is for the telecommunication passes to happen in orbital day. Hence, the STK analysis in Figure 35 adds a daylight-only telecommunication constraint when computing the access availabilities. The orbital characteristics are such that there are intervals of time in which the figure shows no available passes; this happens because during those times the satellite is above the horizon at the ground station only during orbital night.

As a result of this analysis, the operational concept for ASTERIA was modified to include occasional passes in orbital night during these intervals. Figure 36 shows a more regular coverage between ASTERIA and the ground station when the added nighttime passes effectively removes the daylight-only constraint.

Figure 35 shows coverage holes caused by imposing the daylight-only constraint.

Figure 36 confirms there are no coverage gaps with the daylight-only constraint removed.

In terms of number of passes, the statistics show an average of six passes per day (in the unconstrained case) or three passes per day (when communication is restricted to daytime). Pass duration is approximately 8 minutes.

ASTERIA to MSU Access (one year simulation, daylight only)

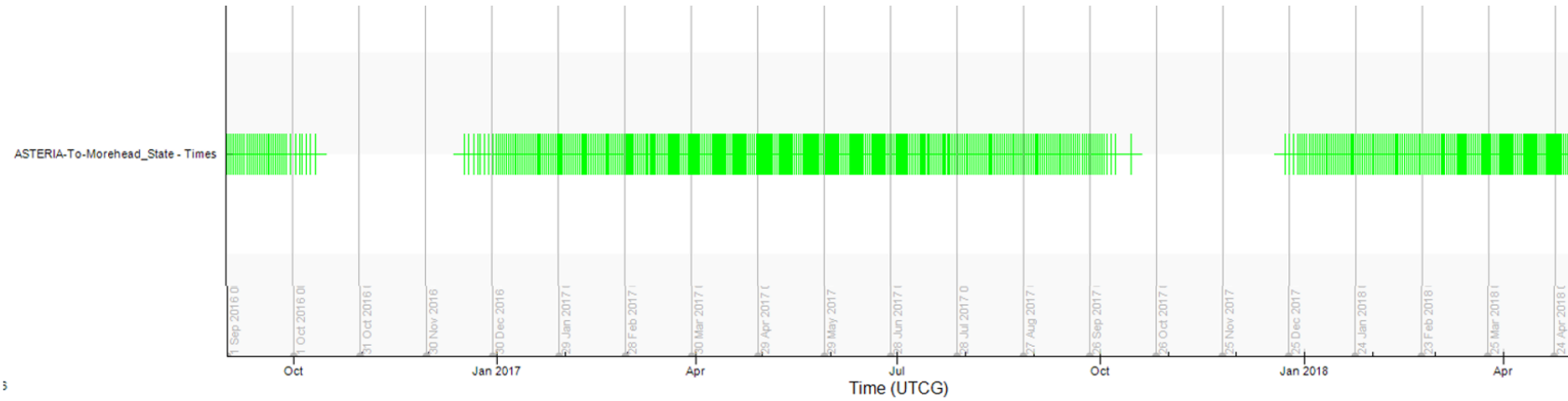


Figure 35: ASTERIA accesses simulated for one year (daylight-only tracking).

ASTERIA to MSU Access (one year simulation, daylight and nighttime)

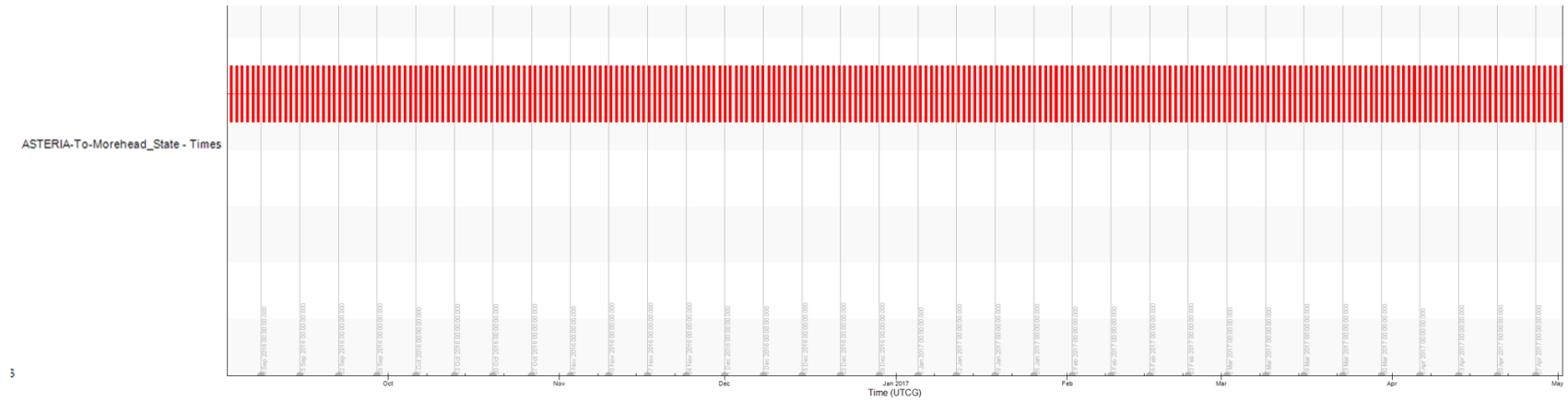


Figure 36: ASTERIA accesses simulated for one year (daylight and nighttime tracking).

5.2.2 Doppler Analysis

The orbital calculations are also used to estimate Doppler shift for uplink over the course of the ASTERIA mission. Doppler varies over the lifetime of the mission up to a maximum of ± 47 KHz. A more detailed analysis was conducted looking at some specific passes. Figure 37 and Figure 38 show the Doppler shift over telecommunications passes in early October and early November 2017. Doppler rate causes the received frequency to vary most rapidly in the middle of a pass. A test (prior to flight) was conducted with the radio that confirmed it could handle the maximum rate.

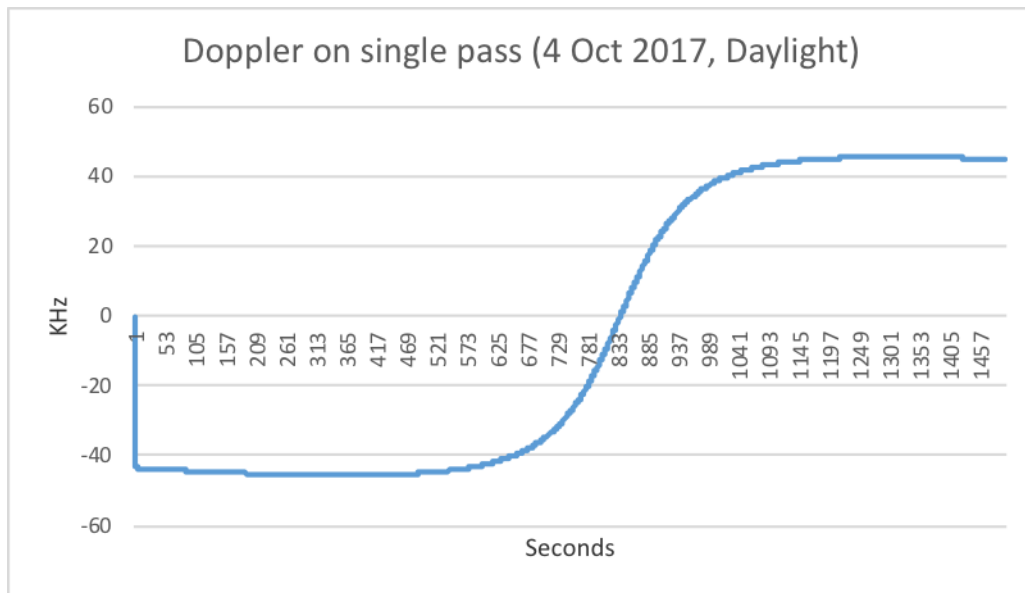


Figure 37: Simulated Doppler shift during the 4 October 2017 telecommunication contact.

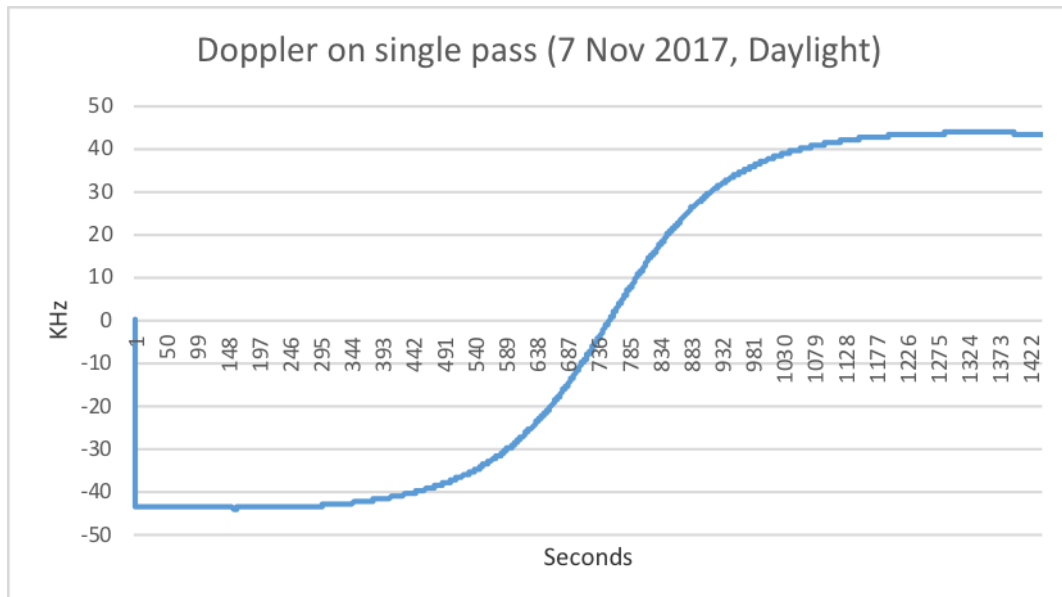


Figure 38: Simulated Doppler shift during the 7 November 2017 telecommunication contact.

In addition, the tracking and acquisition bandwidths of the radio were measured at hot and cold during the spacecraft test in the thermal vacuum chamber. The thermal vacuum chamber test was performed by thermally cycling the spacecraft between +40°C (hot limit) and –25°C (cold limit). The bandwidth results at hot and cold for the two uplink rates are shown in Table 12. The bandwidth in all cases is larger than the anticipated maximum Doppler shift.

Table 12: Tracking and acquisition bandwidth for the ASTERIA radio over temperature.

Bandwidth calculation (KHz)						
Data rate: 32 Kbps						
	Hot case			Cold case		
	Different values of carrier threshold			Different values of carrier threshold		
	–90 dBm	–100 dBm	–110 dBm	–90 dBm	–100 dBm	–110 dBm
Tracking (lower)	714	614	94	2366	2322	86
Acquisition (lower)	106	60	54	134	72	66
Tracking (upper)	1270	1160	50	2090	1120	80
Acquisition (upper)	90	70	48	100	84	68
Data rate: 4 Kbps						
	Hot case			Cold case		
	Different values of carrier threshold			Different values of carrier threshold		
	–90 dBm	–100 dBm	–110 dBm	–90 dBm	–100 dBm	–110 dBm
Tracking (lower)	350	200	156	226	168	100
Acquisition (lower)	80	80	88	94	92	88
Tracking (upper)	230	150	150	180	160	140
Acquisition (upper)	86	84	92	92	92	90

5.3 Spectrum Considerations and License Process

ASTERIA is a JPL mission, and the license process was conducted through the National Telecommunications and Information Administration (NTIA). The Stage 4 NTIA filing was submitted in April 2016, and the license was granted in August 2016. Figure 39 shows the radio spectrum and its compliance with respect to the NTIA mask in red.

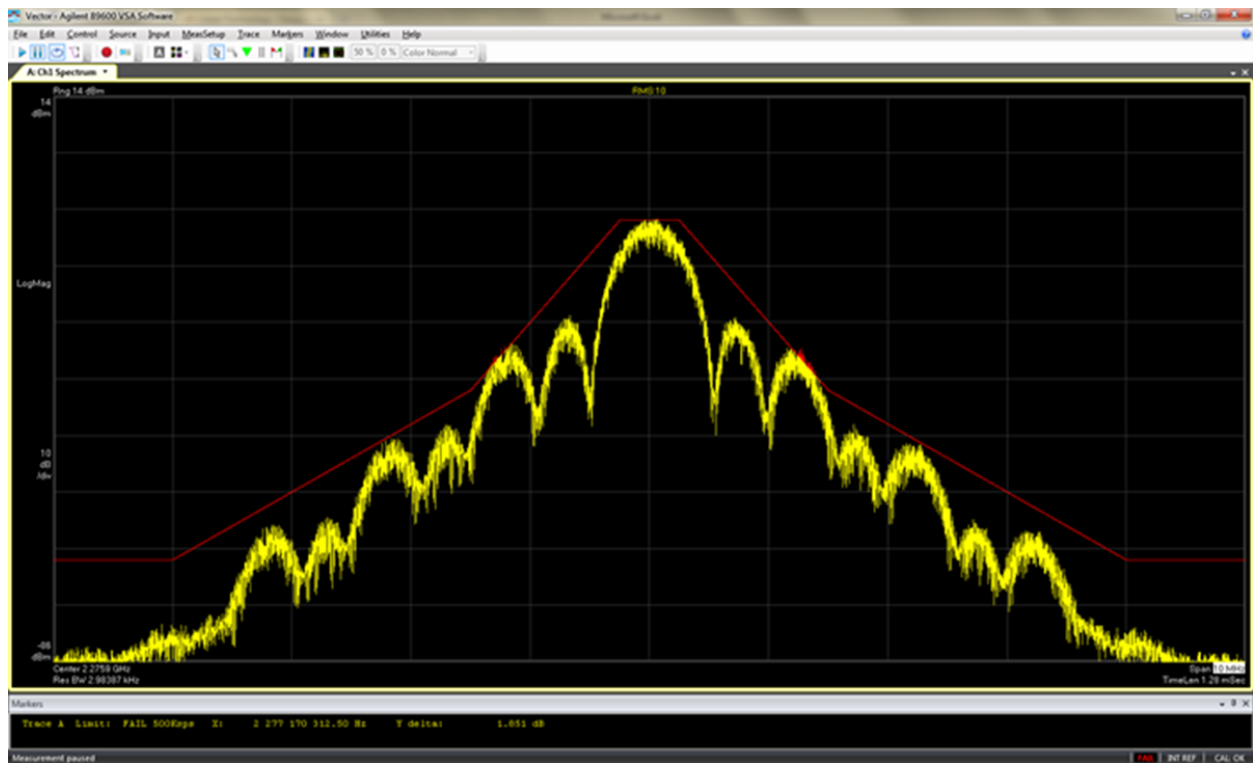


Figure 39: ASTERIA measured radio spectrum. The red line indicates the NTIA mask.

6 Flight Operations

From before launch to the end of flight, there has been one team that operates ASTERIA, the Mission Operations Team (also referred to as the operations team). This team's process recognizes that flight is a continuing cycle of planning, sequence generation and review, and data downlinking and analysis activities. Typically, planning and sequencing for the next cycle or cycles occur at the same time as downlinking and analysis continues in the present cycle. The outcome of analysis leads to more planning for later mission times. The nature of this small project's operations results in roles (such as within planning) being taken by individual team members, often with a particular team member serving in multiple roles.

With an emphasis on telecom activities, after an overview this section begins with a description of ASTERIA planning. Normal operations planning includes the constraints of flight rules and consideration of contingency planning in case off-nominal events occur during execution. The section continues with sequencing and then with execution. It ends with a discussion of the major flight rules that affected all three parts of the team process.

Some materials for this section have been taken from [5], [8], and [9].

6.1 Overview of the Operations Cycle

The life cycle of ASTERIA command products revolves around planned activities. Operationally, ASTERIA launched with a list of activities to complete checkout and the technology demonstration mission. In the extended mission, science or engineering activities have been proposed by the science lead or by Project members. Table 13 shows the activity plan for a prelaunch operational readiness test (ORT).

Table 13: ASTERIA ORT activities and activity leads.

ID	Name	Lead	Stakeholders
1	Spacecraft Acquisition and Health Check	A. Donner	A. Babuscia
2	Parameter Update	A. Donner	B. Campuzano
3	Radio Checkout	A. Babuscia	R. Bocchino
4	XACT Checkout	C. Pong	R. Bocchino
5	Piezo Stage Checkout	C. Pong	B. Campuzano
6	Camera System Checkout	M. Smith	C. Pong, M. Knapp, D. Kessler
7	Pointing Control System Checkout/Tuning	C. Pong	L. Day
8	Thermal Control System Checkout/Tuning	C. Smith	J. Luu, C. Pong, B. Campuzano

Each ASTERIA spacecraft activity has an activity lead and one or more activity stakeholders. An activity stakeholder has an interest in the outcome of the activity. Stakeholders may include mission management and team members. Almost always the activity lead is a primary stakeholder.

Figure 40 shows an overview of six stakeholder functions for ASTERIA activities, as well as the life cycle of the activities. As the figure shows, each command product starts with a planned activity. During execution of planned activities, products are made by the activity lead for the activity, and unique product IDs are assigned to the products. After the IDs are assigned, the activity lead will add them to the testing configuration repository (repo), where the testbed operator will pull them, run the products on the testbed, and document the test run for the Command Approval Meeting (CAM). During the CAM, the Mission Manager will review the products and approve them for flight, at which point they will be added to the flight configuration repo.

After they have been tested and approved, the spacecraft operator will query flight products from the flight repository, execute them in planned passes, and downlink the resulting products. Each stakeholder will review the data products for spacecraft health and safety, and the activity lead will then review and deliver results of the activity (if applicable). Upon results review, further activities may be fed back into the activity plan, and approved commands may be re-used by later activities.

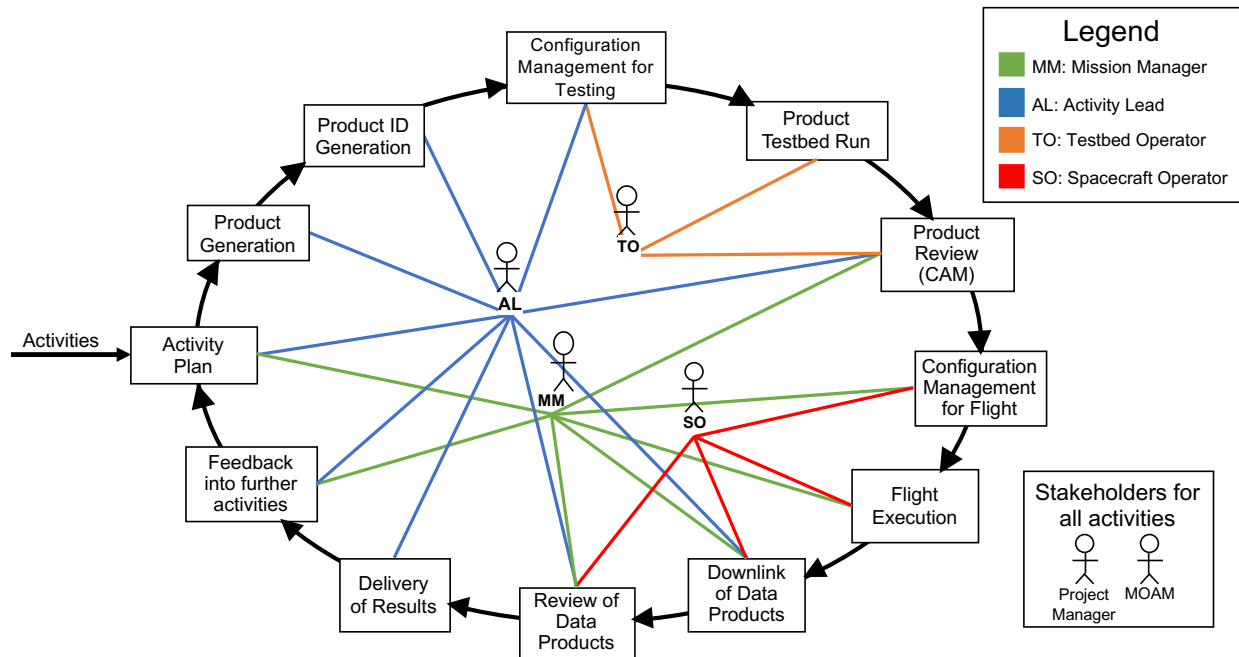


Figure 40: ASTERIA Command Product Life Cycle.

During nominal execution of activity plans, the following documents are generated:

1. Uplink Approval Form

This form follows the activity products from generation through command approval. It logs any test issues, the hashes of the repo commits¹⁴, and comments from the activity lead, the test lead, and the Mission Manager prior to approval. Approved waivers to flight rules are noted during the CAM on the uplink approval form.

2. Pass Plan

As part of the planned activity, the pass plan for the team member with the role of spacecraft operator is generated. This is a checklist that the operator follows during the nominal pass that defines the order of product uplink, the go/no-go scenarios for the product, and any other data the spacecraft operator should know prior to the pass.

3. Post-Pass Report

After each pass, the spacecraft operator will generate a post-pass report that is sent to the entire team. This allows the activity lead to know the status of their activity after the pass.

¹⁴ The specialized terms related to the correctness and security of the uplink approval form include:

“hash” or SHA hash is a family of cryptographic hash functions published by the National Institute of Standards and Technology (NIST) as a U.S. Federal Information Processing Standard (FIPS). A cryptographic hash (sometimes called “digest”) is a kind of “signature” for a text or a data file.

https://en.wikipedia.org/wiki/Secure_Hash_Algorithms

“repo” is a github repository. Git is an online version control system incorporating git repositories typically used for code. It is used to track changes in computer files and to coordinate work on these files among multiple people.

<https://en.wikipedia.org/wiki/Git>

“commit”. Each commit to a git repository algorithmically creates a unique SHA-1 hash for the commit, uniquely identifying the particular commit to the repository.

6.2 Operations Planning

6.2.1 Deployment and Initial Acquisition

ASTERIA's planned day and time of deployment from the ISS were provided to the team by NanoRacks, along with approximate deployment velocities. That data, in combination with the known trajectory of the ISS, allowed the team to create a pre-planned pass list with Morehead State University based on the most-likely available post-deployment passes. Figure 41 shows the planned pass list for ASTERIA deployment. The green-highlighted box shows the planned first-signal pass, and the yellow-highlighted box shows the actual first signal received.

Initial acquisition was planned to occur a few days after deployment, on November 22. This was due to expecting to receive a TLE with detailed trajectory information. In fact, as discussed in Section 7, the TLE was received sooner than expected, allowing earlier than planned first contact (November 22 at 20:22); the first verified spacecraft signal was received at approximately 02:15:12 UTC on 22 November 2017.

Activities for ASTERIA initial contact were designed to be minimal. Initial contact was to be used to monitor spacecraft state post-deployment and to send a single no-op (no operation) command to verify commandability. Subsequent passes were to be used to update post-deployment parameters and thresholds.

6.2.2 Planning and Sequencing Following Initial Acquisition

After initial acquisition was achieved, the normal telecom planning for ASTERIA has consisted of two activities:

1. Pass scheduling with MSU
2. Spacecraft sequencing for passes

For nominal pass scheduling with MSU, the pass list is updated in a two-week cadence, with passes that are requested from the ASTERIA team being confirmed or denied by the Morehead team. In the event of unexpected spacecraft behavior, contingency passes may be scheduled depending on station availability. The pass list may go through several iterations before being confirmed if there are station conflicts or down time.

Once a confirmed pass list is generated, the spacecraft operations team may sequence spacecraft pointing to improve telecom characteristics for the pass. This is an optional activity—throughout much of operations the spacecraft was in sun point mode during telecom passes. Sequenced passes ensure that the spacecraft antenna is pointing at the ground station and that the radio is on for the pass. An unsequenced pass may be missed due to planned radio duty cycling.

6.2.3 Flight Rules

ASTERIA launched with 43 flight rules. Flight rules were generated during the spacecraft buildup and through lessons learned from the ASTERIA ORTs. During normal mission activities, any deviation from the flight rules requires approval by the Mission Operations Assurance Manager (MOAM), the Project Manager, and the Mission Manager, and any such deviation is logged in the uplink approval.

Uplink sequence products are always evaluated for compliance to flight rules. Included in the uplink approval form are any flight rule violations, including waivers. Some examples of telecom-related flight rules with their rationales are:

- Only run sequences in nominal mode. Doing this allows for the safe mode response to recover the spacecraft from a sequence command error or from a payload anomaly.

- Do not allow the spacecraft to be in a non-Sun-pointed attitude, including eclipse, for longer than 40 consecutive minutes. This limit prevents a specific fault monitor from tripping that resets the spacecraft.
- Do not operate the camera and the radio at the same time. This restriction ensures a power-positive state during observations and also prevents electromagnetic interference (EMI) between the two subsystems).

During ASTERIA mission operations, it was deemed necessary to change some flight rules. Changes were approved by the Mission Manager or the Project Manager with configuration management (CM) in the operations document repository for ASTERIA.

6.2.4 Contingency Planning

In the event of an off-nominal pass, the ASTERIA spacecraft operator will log the status of the spacecraft but continue to follow the pass plan. Most off-nominal states of the spacecraft have default spacecraft operator behaviors, such as pre-approved commands for spacecraft safe-mode recovery, or reset recovery. With the use of pre-approved recovery products, the ASTERIA spacecraft may be put in a nominal operational mode in as few as one or two passes.

If the off-nominal event is determined to be due to a more serious condition, the Mission Manager must inform the Project Manager, who will inform project stakeholders. A quick-response (Tiger) team may be formed to assess mission impact and recovery scenarios while the operations team continues its work. The Tiger team may include experts from the affected pre-launch design and test areas and will input its analysis and recommendations to project management and the operations team.

6.3 Execution

Telecom monitoring for ASTERIA is done by the spacecraft operator in collaboration with the MSU station operator. During tracks, real-time data from the AMERGINT modem is monitored by the spacecraft operator, and S-band band signal strength is monitored by the MSU station operator. Typically, the spacecraft operator will view the spectrum analyzer input to the modem, the in-phase/quadrature (I/Q) plot, and the input power to the modem. During tracks, some settings may be changed to improve telecom performance. Especially during early operations, the tracking bandwidth and tracking center frequency were changed to account for Doppler. A typical operator view of ASTERIA telecom data during tracking may be seen in Figure 42.

In addition to monitoring the incoming telecom data, the spacecraft operator is also responsible for monitoring the modem state, connectivity, and for changing modem settings such as the downlink data rate during nominal operations.



Pass Planning



DOY	Start_EST	Transition_EST	End_EST	Start_PST	Transition_PST	End_PST	Type	Duration	Duration_Day	Max_Elev	Selected?	
324	20-Nov-2017 02:15:37		20-Nov-2017 02:24:39	19-Nov-2017 23:15:37		19-Nov-2017 23:24:39	Night	9.02	0.00	10.09		
324	20-Nov-2017 03:52:02		20-Nov-2017 04:02:44	20-Nov-2017 00:52:02		20-Nov-2017 01:02:44	Night	10.70	0.00	33.37		
324	20-Nov-2017 05:28:37	20-Nov-2017 05:35:29	20-Nov-2017 05:38:51	20-Nov-2017 02:28:37	20-Nov-2017 02:35:29	20-Nov-2017 02:38:51	Night-->Day	10.23	3.37	22.65		
325	20-Nov-2017 20:30:58		20-Nov-2017 20:41:14	20-Nov-2017 17:30:58		20-Nov-2017 17:41:14	Night	10.27	0.00	22.57		
325	20-Nov-2017 22:07:04		20-Nov-2017 22:17:49	20-Nov-2017 19:07:04		20-Nov-2017 19:17:49	Night	10.75	0.00	33.84		
325	20-Nov-2017 23:45:10		20-Nov-2017 23:54:13	20-Nov-2017 20:45:10		20-Nov-2017 20:54:13	Night	9.05	0.00	10.17		
325	21-Nov-2017 01:23:09		21-Nov-2017 01:31:46	20-Nov-2017 22:23:09		20-Nov-2017 22:31:46	Night	8.63	0.00	8.43		
325	21-Nov-2017 02:59:47		21-Nov-2017 03:10:04	20-Nov-2017 23:59:47		21-Nov-2017 00:10:04	Night	10.28	0.00	20.97		
325	21-Nov-2017 04:36:09	21-Nov-2017 04:45:55	21-Nov-2017 04:46:57	21-Nov-2017 01:36:09	21-Nov-2017 01:45:55	21-Nov-2017 01:46:57	Night-->Day	10.80	1.03	46.58		
325	21-Nov-2017 06:14:26	21-Nov-2017 06:18:37	21-Nov-2017 06:20:09	21-Nov-2017 03:14:26	21-Nov-2017 03:18:37	21-Nov-2017 03:20:09	Night-->Day	5.70	1.53	2.54		
326	21-Nov-2017 19:39:26		21-Nov-2017 19:48:33	21-Nov-2017 16:39:26		21-Nov-2017 16:48:33	Night	9.12	0.00	11.41		
326	21-Nov-2017 21:14:34		21-Nov-2017 21:25:33	21-Nov-2017 18:14:34		21-Nov-2017 18:25:33	Night	10.98	0.00	64.19		
326	21-Nov-2017 22:32:13		21-Nov-2017 23:01:33	21-Nov-2017 19:32:13		21-Nov-2017 20:01:33	Night	9.39	0.00	15.20		
326	22-Nov-2017 00:30:31		22-Nov-2017 00:38:58	21-Nov-2017 21:30:31		21-Nov-2017 21:38:58	Night	8.45	0.00	7.81		
326	22-Nov-2017 02:07:31		22-Nov-2017 02:17:16	21-Nov-2017 23:07:31		21-Nov-2017 23:17:16	Night	9.75	0.00	14.62		
326	22-Nov-2017 03:43:49		22-Nov-2017 03:54:46	22-Nov-2017 00:43:49		22-Nov-2017 00:54:46	Night	10.96	0.00	81.38		
326	22-Nov-2017 05:21:02	22-Nov-2017 05:29:05	22-Nov-2017 05:29:31	22-Nov-2017 02:21:02	22-Nov-2017 02:29:05	22-Nov-2017 02:29:31	Night-->Day	8.48	0.43	8.69		
327	22-Nov-2017 20:22:17		22-Nov-2017 20:33:14	22-Nov-2017 17:22:17		22-Nov-2017 17:33:14	Night	10.94	0.00	60.85	Yes	Acq/LS/downlink/param
327	22-Nov-2017 21:59:24		22-Nov-2017 22:09:33	22-Nov-2017 18:59:24		22-Nov-2017 19:09:33	Night	10.15	0.00	18.56	Yes	Acq/LS/downlink/param
327	22-Nov-2017 23:37:44		22-Nov-2017 23:46:17	22-Nov-2017 20:37:44		22-Nov-2017 20:46:17	Night	8.55	0.00	8.14	Yes	Acq/LS/downlink/param
327	23-Nov-2017 01:15:09		23-Nov-2017 01:24:22	22-Nov-2017 22:15:09		22-Nov-2017 22:24:22	Night	9.20	0.00	10.97		
327	23-Nov-2017 02:51:31		23-Nov-2017 03:02:20	22-Nov-2017 23:51:31		23-Nov-2017 00:02:20	Night	10.81	0.00	40.73		
327	23-Nov-2017 04:28:13		23-Nov-2017 04:38:08	23-Nov-2017 01:28:13		23-Nov-2017 01:38:08	Night	9.91	0.00	17.95		
...												
336	02-Dec-2017 14:54:00		02-Dec-2017 15:01:02	02-Dec-2017 11:54:00		02-Dec-2017 12:01:02	Day	7.04	7.04	4.65	Yes	File system LS
336	02-Dec-2017 16:27:51		02-Dec-2017 16:38:49	02-Dec-2017 13:27:51		02-Dec-2017 13:38:49	Day	10.96	10.96	61.98	Yes	Downlink PCS data
336	02-Dec-2017 18:04:58	02-Dec-2017 18:12:34	02-Dec-2017 18:15:08	02-Dec-2017 15:04:58	02-Dec-2017 15:12:34	02-Dec-2017 15:15:08	Day-->Night	10.16	7.60	18.48	Yes	Downlink PCS data
337	02-Dec-2017 19:43:18	02-Dec-2017 19:45:13	02-Dec-2017 19:51:53	02-Dec-2017 16:43:18	02-Dec-2017 16:45:13	02-Dec-2017 16:51:53	Day-->Night	8.58	1.92	8.17		
337	02-Dec-2017 21:20:43		02-Dec-2017 21:29:57	02-Dec-2017 18:20:43		02-Dec-2017 18:29:57	Night	9.24	0.00	11.09		
337	02-Dec-2017 22:57:04		02-Dec-2017 23:07:54	02-Dec-2017 19:57:04		02-Dec-2017 20:07:54	Night	10.83	0.00	41.33		
337	03-Dec-2017 00:33:46		03-Dec-2017 00:43:40	02-Dec-2017 23:33:46		02-Dec-2017 21:43:40	Night	9.90	0.00	17.74		
337	03-Dec-2017 14:05:13		03-Dec-2017 14:05:39	03-Dec-2017 11:05:13		03-Dec-2017 11:05:39	Day	0.43	0.43	-0.56		
337	03-Dec-2017 15:35:44		03-Dec-2017 15:46:17	03-Dec-2017 12:35:44		03-Dec-2017 12:46:17	Day	10.56	10.56	29.04	Yes	Downlink PCS data
337	03-Dec-2017 17:12:07	03-Dec-2017 17:22:14	03-Dec-2017 17:22:46	03-Dec-2017 14:12:07	03-Dec-2017 14:22:14	03-Dec-2017 14:22:46	Day-->Night	10.64	10.12	28.20	Yes	Data download
337	03-Dec-2017 18:50:19	03-Dec-2017 18:54:52	03-Dec-2017 18:59:14	03-Dec-2017 15:50:19	03-Dec-2017 15:54:52	03-Dec-2017 15:59:14	Day-->Night	8.92	4.55	9.49		
338	03-Dec-2017 20:28:09		03-Dec-2017 20:36:56	03-Dec-2017 17:28:09		03-Dec-2017 17:36:56	Night	8.78	0.00	8.97		
338	03-Dec-2017 22:04:42		03-Dec-2017 22:15:10	03-Dec-2017 19:04:42		03-Dec-2017 19:15:10	Night	10.48	0.00	24.55	Yes	Start Thermal checkout (1 of 3)
338	03-Dec-2017 23:41:07		03-Dec-2017 23:51:47	03-Dec-2017 20:41:07		03-Dec-2017 20:51:47	Night	10.66	0.00	35.37		
338	04-Dec-2017 01:20:10		04-Dec-2017 01:24:00	03-Dec-2017 22:20:10		03-Dec-2017 22:24:00	Night	3.83	0.00	0.70		

Early mission, passes occur at night. Attempt 3 passes to obtain 2 (radio duty cycle)

Bias passes toward late evening EST instead of early morning EST for logistical simplification

Daytime passes become available in early December

Passes can have a lighting transition (day-to-night or night-to-day)

Avoid low-elevation passes where possible

During ACS, PCS, and thermal checkouts, spacecraft activities occur out of view

Time gap for data analysis before starting next activity

Figure 41: Deployment pass planning from the ASTERIA Operational Readiness Review.



Figure 42: Real time telecom monitoring by spacecraft operator during initial ASTERIA acquisition.

6.4 Lessons Learned

This section highlights general findings with particular emphasis on how pre-launch design and testing influenced the operations phase.

- Validating the system-level functionality, behavior, and robustness was the main objective of the ASTERIA mission scenario test (MST) campaign. MSTs took place over a two-week period and provided a forum for relatively long duration FSW testing on the system testbed. One lesson learned is that MSTs offer high value during the crucial final system integration phase. Contributing significantly to the value of the MSTs was the use of a fully functional and flight-like GDS, including ground station modem, front-end processor, and GDS software for end-to-end communication with the vehicle over the spacecraft radio.
- Another lesson learned is the value of designing flexibility and extensibility into the system with an eye toward operations. By uplinking new parameters, the ASTERIA team has been able to configure which fault monitors are enabled or disabled, which fault responses are linked to which monitors, the limits at which fault conditions are announced, and how long a faulted condition must persist before it triggers a response. This flexibility allowed for an in-flight tuning of the fault protection system to address new off-nominal behavior seen in flight.
- Verification before launch of the ability to update FSW on orbit has proved to have critical value. This verification provided a fallback capability for future updates to address corner cases¹⁵ or space environment-related issues that we were unable to test before launch. One of the updates addressed a problem uncovered in the FSW interface between the radio and flight computer. Until corrected, this problem would lead to an expired watchdog timer, which would trigger a flight computer reset. An FSW update increased the robustness of the radio interface, decreasing the need for fault protection to intervene, and improved operational efficiency.
- The ASTERIA flight computer runs the Linux OS, and the FSW incorporates an ability to issue low-level commands directly to the shell. This flexibility has brought several key benefits during mission operations including an ability to diagnose anomalies via command line queries¹⁶ (e.g., ls and grep) and use compression (gzip) to increase effective downlink data volume.
- A final lesson learned is the value of continual process improvement during operations. As the mission has progressed, the team has developed various tools and processes to increase efficiency with less staffing. This includes a GitHub-based uplink approval and CM process, automated tools for generating observation and engineering sequences, and scripts to parse and organize downlink data.

¹⁵ In engineering, a corner case (or pathological case) involves a problem or situation that occurs only outside of normal operating parameters—specifically one that manifests itself when multiple environmental variables or conditions are simultaneously at extreme levels, even though each parameter is within the specified range for that parameter. https://en.wikipedia.org/wiki/Corner_case

¹⁶ The unix or linux command ls lists files and directories. The name grep comes from /g/re/p (globally search a regular expression and print); gzip comes from GNU (GNU's Not Unix), and gzip refers to a file format and software application used for file compression. <https://en.wikipedia.org/wiki/Ls> <https://en.wikipedia.org/wiki/Grep>, <https://en.wikipedia.org/wiki/Gzip> <https://en.wikipedia.org/wiki/GNU>

7 In-flight Performance

7.1 *Spacecraft Deployment*

Spacecraft deployment from the ISS occurred nominally at 12:25:01 UTC on 20 November 2017. Because ASTERIA was deployed by itself—as opposed to in a cluster with other CubeSats—identification by the JSpOC was relatively quick, and a TLE set was available within 12 hours of deployment. First contact with ASTERIA actually occurred at approximately 02:15 UTC on 22 November 2017. Data downlinked in the mission’s opening days confirmed that the deployment proceeded nominally, starting with a 30-minute timer after ejection from the ISS, followed by solar array deployment, detumble, and Sun acquisition. Initial tip-off rates were less than 1 degree per second in all three axes, and the spacecraft slewed and settled into a Sun-pointed attitude within 150 seconds of the XACT powering on.

7.2 *Telecommunication Acquisition*

As discussed in Section 1, spacecraft tracking is carried out by JSpOC, which produces a TLE set that contains the orbital ephemerides for ASTERIA. Right after deployment, the TLE were used to identify ground station contact opportunities. The acquisition for ASTERIA was particularly challenging due to the following aspects:

1. ASTERIA was relying on only one ground station.
2. The MSU station has a very small beamwidth, as a result of having such a large dish.
3. The ASTERIA antennas are regulated by a switch, so there was no omnidirectional coverage of the spacecraft during acquisition.
4. The radio did not support a beacon mode, and it needed to receive an uplink signal in order to activate the downlink.
5. The radio was on a duty cycle for which it was on for 30 minutes and off for 10 minutes.

As a result of all these constraints, acquisition was deemed a very difficult task for the ASTERIA satellite, and the operations team was planning to dedicate several passes just to acquire the signal. Luckily, the system worked even better than expected. The signal from ASTERIA was acquired at the very first actual available opportunity, which was the second time that the spacecraft was in visibility with the ground station from the moment of deployment. The team later determined from telemetry post-processing that the duty cycle had the radio off at the first Morehead visibility.

After acquisition was performed, the team effort focused on performing radio checkout operations as described in the next section.

7.3 *Radio Checkout and Link Performance Achieved*

Following first acquisition, the operations team devoted several passes to perform radio checkout operations. Radio checkout operations included two main activities:

1. Ensuring the health of the telecom subsystem, in particular the radio, by monitoring the key health telemetry parameters and the spectrum.
2. Performing a switch to high data rates and ensuring the health of the telecom subsystem in the high data rates configuration.

For the crucial first activity, the key telecommunication telemetry parameters provided in the ASTERIA real-time telemetry (with values updated every 28 seconds) are the following:

1. Antenna: this value is either 1 or 2 depending on which particular antenna the spacecraft is using to communicate. Antenna 1 is the primary antenna, and it is located on the side opposite to the solar panels. Antenna 2 is located on the opposite side of the spacecraft. Expected default value after deployment and after radio re-boot is 1.
2. Radio temperature of the Memory Signal Processor (MSP): this is the temperature of the radio processor, and the flight allowable temperature range is -25 deg to 60 deg Celsius.
3. Radio lock: the value is 1 if the radio is locked, zero otherwise. Given that this value is from real-time telemetry, we expect this value to be almost always 1, except for the few cases in which the value is sampled less than 28 seconds before lock is achieved.
4. Radio oscillator temperature: the flight allowable range for this sensor is also -25 to 60°C .
5. Radio voltage of the power amplifier: if everything is normal, this value is expected to be between 3 and 5 V.

During the second and the third of the ASTERIA communication passes (contacts), values were monitored by the team while it was performing other checkout operations. Table 14 lists the values during Pass 2 and Pass 3.

Table 14: Real-time telecommunication telemetry values during Passes 2 and 3.

Telemetry value	Pass 2 (average)	Pass 3 (average)	Flight allowable range
Antenna	1	1	1
MSP temperature	23.3	23.5	-25 to 60°C
Lock	1	1	1
Oscillator temperature	21	21.6	-25 to 60°C
PA voltage	4.5	4.5	3–5 V

It can be seen that values were reasonable and well within the expected ranges. With this, in Pass 4, the team attempted a change in uplink and downlink data rates. Table 15 lists telemetry values during Pass 4, and these were also within the expected ranges.

Table 15: Real-time telecommunication telemetry values during Pass 4.

Telemetry value	Pass 4 (average)	Flight allowable range
Antenna	1	1
MSP temperature	23.7	-25 to 60°C
Lock	1	1
Oscillator temperature	22	-25 to 60°C
PA voltage	4	3–5 V

With this normal telemetry, the activity lead authorized the change of data rates. A command was sent to the spacecraft to switch to high data rates from low, while the ground transmitter and receiver were reconfigured for 1 Mbps downlink and 32 Kbps uplink. However, the spectrum of the received signal at Morehead just before the change of data rate had indicated a low E_b/N_0 (average 15 dB-Hz). As a result, the ASTERIA and Morehead teams were not able to re-establish contact with the spacecraft downlink when the switch occurred.

It is important to note that, despite this initial failure, the status of the ASTERIA downlink was not considered critical because the radio is set up to power cycle every 30 minutes and to restart in the default low-data-rate configuration. Hence, the operations team knew that at the following contact opportunity, the radio would be deterministically at the low-data-rate state, making it possible to re-establish communication. In fact, during Pass 5, contact was established, and radio telemetry is shown in Table 16.

Table 16: Real-time telecommunication telemetry values during Pass 5.

Telemetry value	Pass 5 (average)	Flight allowable range
Antenna	1	1
MSP temperature	23.6	-25 to 60°C
Lock	1	1
Oscillator temperature	22	-25 to 60°C
PA voltage	4	3–5 V

The average E_b/N_0 was 22 dB-Hz, enough to switch to high data rates. The improvement was mostly due to the different antenna angle. Again the activity lead commanded the switch to high data rates, and the change was successful. Contact was re-established with ASTERIA at the high data rate. The successful change of data rates and Morehead station lock to the high-rate downlink closed the radio checkout phase of the mission. However, there were still some questions to be resolved in regards to the ASTERIA-Morehead geometry and issues with the performance of the end-to-end communication system:

1. The spectrum was shifting in frequency faster than expected with this causing frequent loss of lock during the pass. This was found to be due to both Doppler and spacecraft rotation.
2. Downlink E_b/N_0 was lower than expected. Troubleshooting by the ASTERIA team and the ground station team at Morehead State University found three main causes for this:
 - a. The high level of uplink power was saturating the ASTERIA receiver.
 - b. The rotation of the spacecraft was causing variation in spacecraft antenna pointing.
 - c. Though not determined immediately, the LNA at the ground station was failing. The failure was discovered during the extended mission phase. Replacing the LNA resulted in a 3 dB increase in the received E_b/N_0 .

The fixes implemented were the following:

1. The downlink receiver bandwidth was increased by a factor of 10 to reduce the loss of lock.
2. The uplink signal from the ground station was reduced by approximately 9 dB in order to avoid receiver saturation.
3. The spacecraft pointing system was commanded to point the antenna at the ground station to limit the loss of contact due to spacecraft rotation. Before this fix, spacecraft pointing was mostly used for attitude control and science, while the telecommunication system was mostly relying on the wide beamwidth of its patch antenna and not on a finer pointing requirement.

These fixes were implemented sequentially over a series of passes to see how they affected the link. Results showed that all three fixes improved the length and quality of the telecommunication passes. Specifically:

1. Pass length substantially improved, from 2–3 minutes to an average of 8 minutes.
2. E_b/N_0 moved to a reliable average of approximately 18 dB at high data rates (21 dB after the ground station LNA replacement in August 2018).

After radio checkout operations, the operations team moved on to perform other subsystems checkout and then to normal operations. During all this time, the telecom subsystem was monitored to identify anomalies and to characterize performances. Specifically, the following parameters were monitored:

1. Real-time telemetry values: they remained in the expected ranges, and no anomalies were detected. Figure 43, Figure 44, Figure 45, Figure 46, and Figure 47 show telemetry data values during a typical pass. It can be seen that the antenna selected is Antenna 1 and that the spacecraft is in lock during the pass, as expected. The temperatures for both the processor and

the oscillator are increasing as expected due to the radio operating in full duplex mode for some minutes while these measurements were being taken. Lastly, the power amplifier voltage is stable at 4 V.

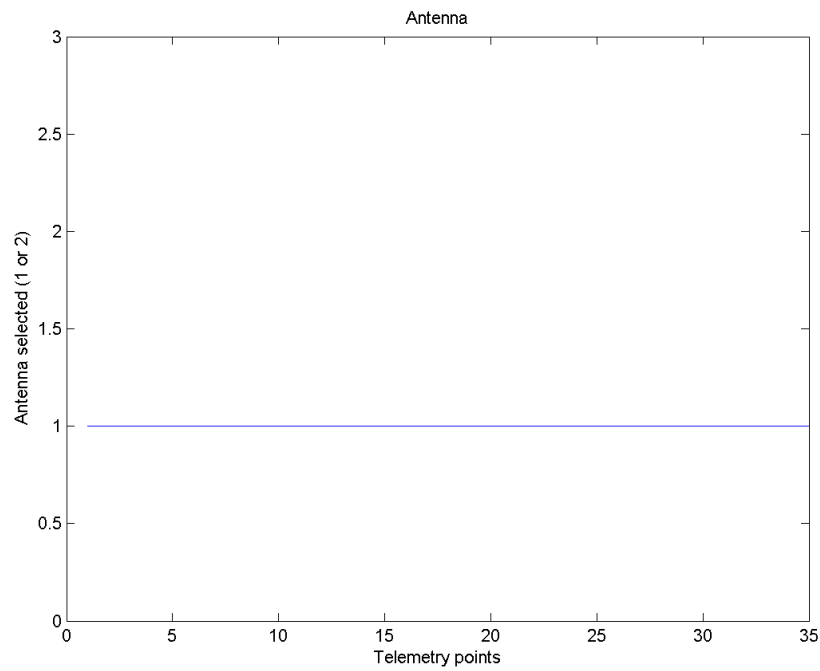


Figure 43: Real-time telemetry values during Pass 30 (Antenna 1 used).

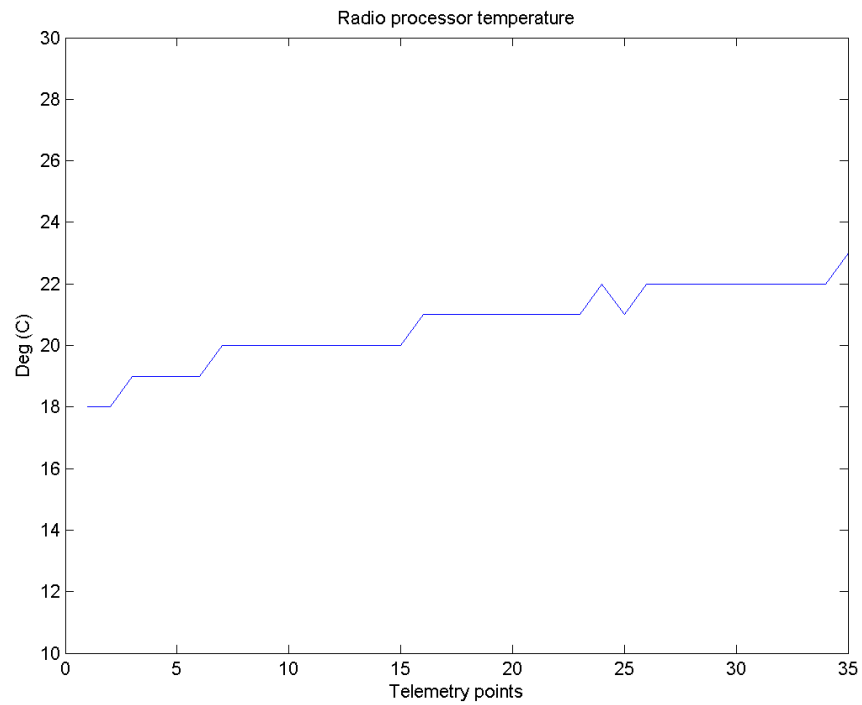


Figure 44: Real-time telemetry values during Pass 30 (radio processor temperature).

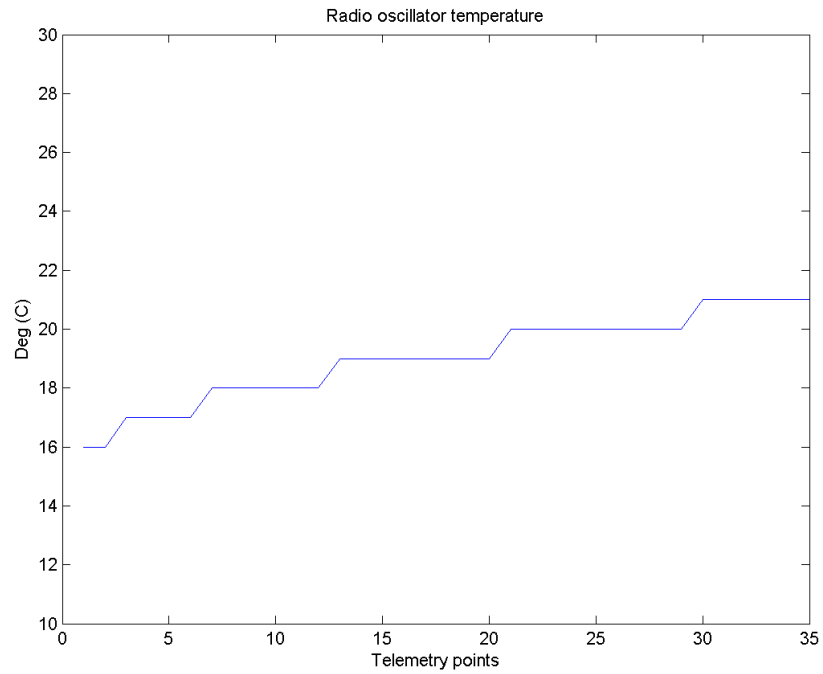


Figure 45: Real-time telemetry values during Pass 30 (oscillator temperature).

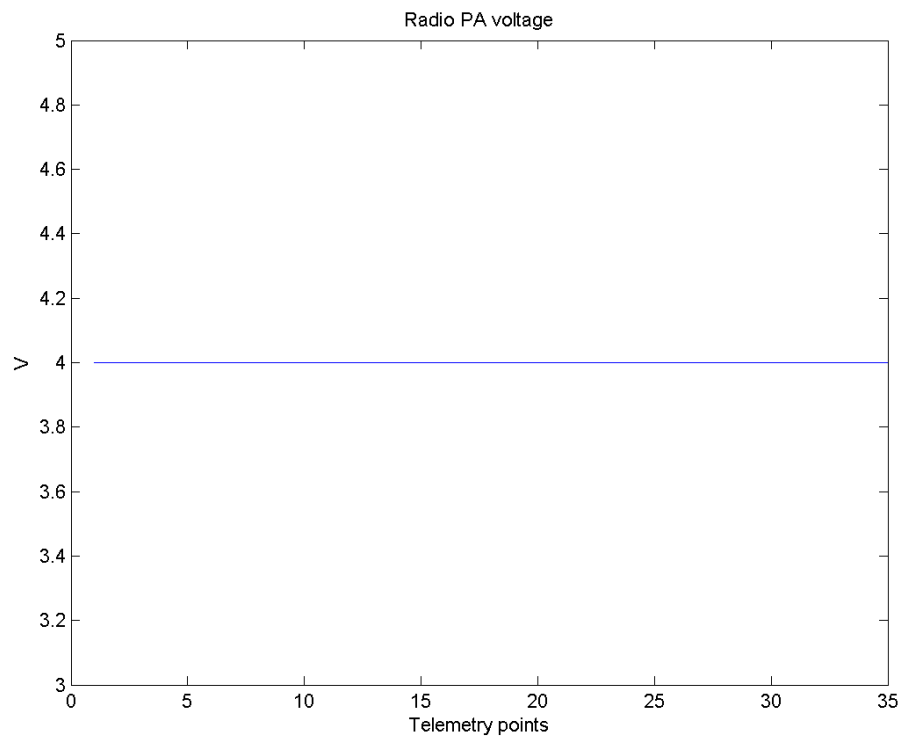


Figure 46: Real-time telemetry values during Pass 30 (power amplifier voltage).

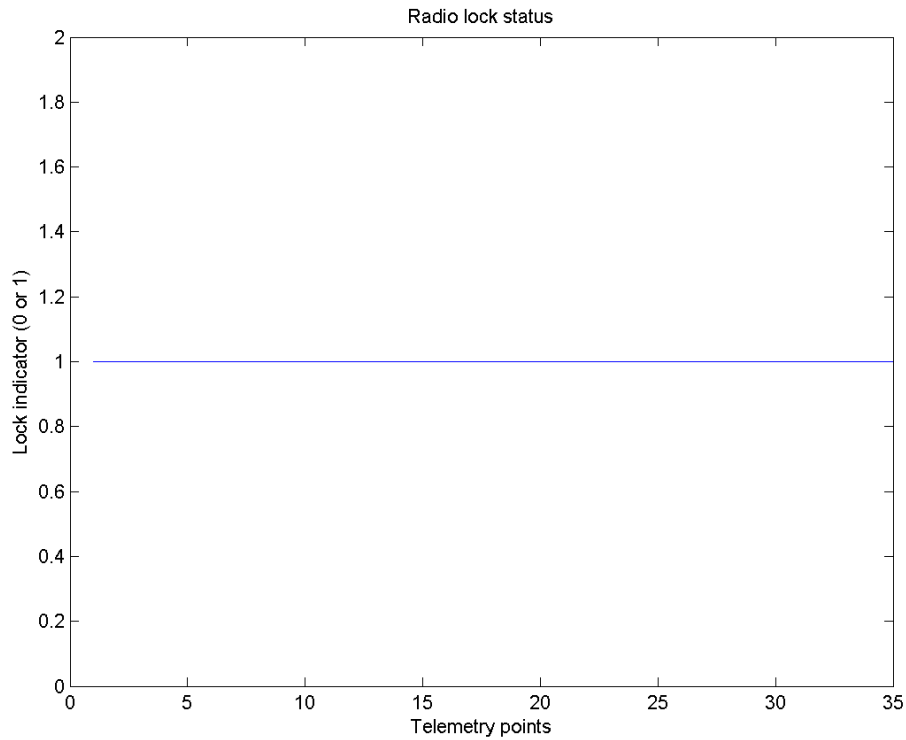


Figure 47: Real-time telemetry values during Pass 30 (lock status).

Mission data in Figure 48 and Figure 49 was updated as of the last week of July 2018. Since then the ASTERIA spacecraft has been on its second extended mission collecting data. The spacecraft will survive in orbit and could continue to operate until atmospheric entry, estimated to be late 2019.

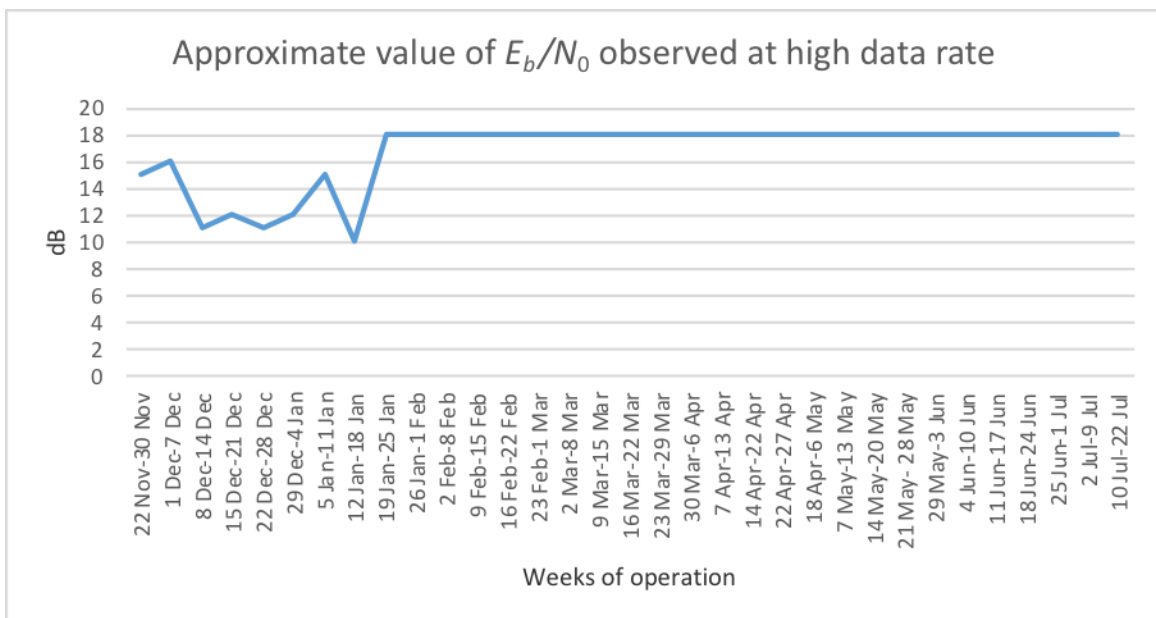


Figure 48: Approximate value of E_b/N_0 for high-rate downlink per weeks of operation.

Initially, the high-rate (1 Mbps) downlink E_b/N_0 was very unstable. Then, it stabilized around 18 dB as can be seen toward the middle of the plot. In the extended mission (beyond the right edge of Figure 48), in mid-August 2018, the value increased to approximately 21 dB after the change of LNA at the ground station.

The E_b/N_0 values in Figure 48 are as read by the operators in real time from the AMERGINT receiver. They are much lower than the predicted values in Section 5. The ASTERIA team does not know the reason for this discrepancy but speculates it comes from a combination of factors: lack of precise pointing of the spacecraft antenna, reflections around the antenna, and also unexpectedly large ground station losses. The high-rate downlink would not lock at an indicated 15 dB in Pass 4 but did lock at an indicated 18 dB in Pass 5. This suggests an empirical E_b/N_0 threshold for 1 Mbps as received at the Morehead tracking station.

Normal ASTERIA radio operation is shown in Figures 12 through 14. An unexpected radio reset or “crash” occurs when an unexpected input or output in the radio software or flight software interacts to reset the radio to its idle mode (Figure 12) and the FSW to go to System Safe Mode.

Radio crashes tend to happen when spacecraft pointing is bad, such as when the spacecraft is spinning during orbital night in safe mode. The passes occurred at night during the high-crash period in March 2019. One radio crash (which puts the spacecraft into safe mode and slowly spins at night) can trigger a cluster of crashes because most contacts have poor pointing. In short, the initial crash was likely random, but the orbital/pass geometry at the time made it worse.

Figure 49 shows the number of radio crashes per week during normal operations. This count does not include regular radio resets due to software resets.

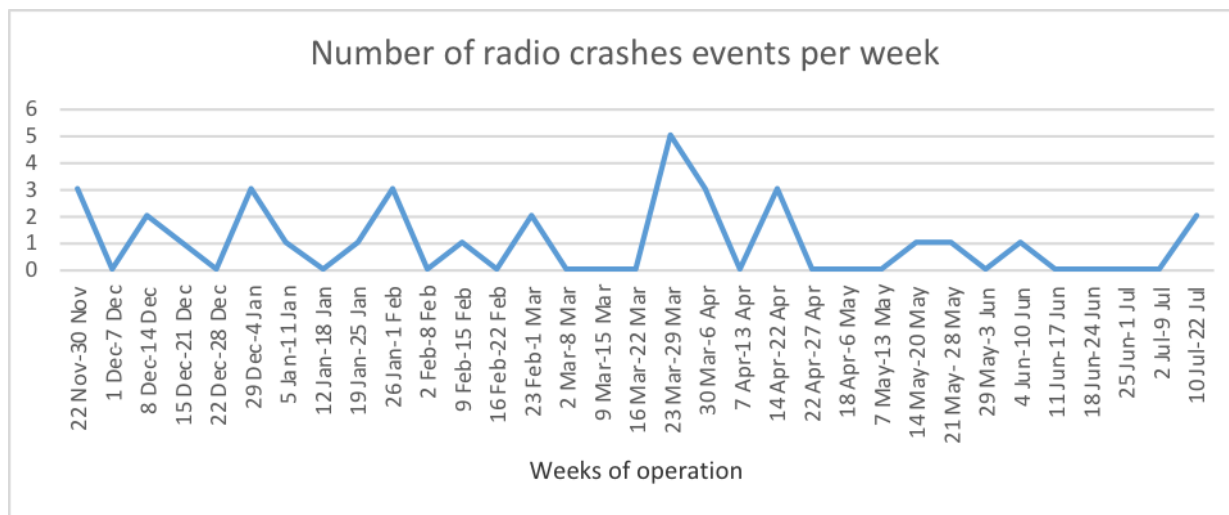


Figure 49: Number of radio crash events per week of operations.

8 References

- [1] Calla Cofield, “Planet-Hunter CubeSat Images Los Angeles,” JPL News (website), May 16, 2019, <https://www.jpl.nasa.gov/news/news.php?feature=7402>
- [2] Calla Cofield, “Astrophysics CubeSat Demonstrates Big Potential in a Small Package,” JPL News (website), April 12, 2018, <https://www.jpl.nasa.gov/news/news.php?feature=7097>
- [3] Lauren Hinkel and Mary Knapp, “Tiny ASTERIA satellite achieves a first for CubeSats,” MIT News (website), August 15, 2018, <http://news.mit.edu/2018/mit-nasa-cubesat-asteria-exoplanet-transit-0815>
- [4] Calla Cofield, “ASTERIA Wins Small Satellite Mission of the Year Award,” JPL News (website), August 14, 2018, <https://www.jpl.nasa.gov/news/news.php?feature=7213>
- [5] Matthew W. Smith, et al., “On-Orbit Results and Lessons Learned from the ASTERIA Space Telescope Mission,” *Proceedings of the AIAA/USU Conference on Small Satellites*, SSC18-I-08.
- [6] Christopher M. Pong, “On-Orbit Performance & Operation of the Attitude & Pointing Control Subsystem on ASTERIA,” *Proceedings of the AIAA/USU Conference on Small Satellites*, SSC18-PI-34.
- [7] Robert L. Bocchino Jr., et al., “F Prime: An Open-Source Framework for Small-Scale Flight Software Systems,” *Proceedings of the AIAA/USU Conference on Small Satellites*, SSC-18-XII-04.
- [8] Ronald G. Eaglin, “21-M Space Tracking Antenna,” Space Science Center, Morehead State University,
[https://www.moreheadstate.edu/getattachment/College-of-Science/Earth-and-Space-Sciences/Space-Science-Center/Satellite-Tracking,-Telemetry-Control-Services/satellite-\(2\).pdf.aspx?lang=en-US](https://www.moreheadstate.edu/getattachment/College-of-Science/Earth-and-Space-Sciences/Space-Science-Center/Satellite-Tracking,-Telemetry-Control-Services/satellite-(2).pdf.aspx?lang=en-US)
- [9] Amanda Donner, et al., “ASTERIA Operations Demonstrates the Value of Combining the Mission Assurance and Fault Protection Roles on CubeSats,” 69th International Astronautical Congress, IAF, Bremen, Germany, October 1–5, 2018.
- [10] Joseph H. Yuen, “Deep Space Telecommunications Systems Engineering,” Springer US, 1983.
- [11] Pez Zarifian, et al., “Team Xc: JPL’s Collaborative Design Team for Exploring CubeSat, NanoSat, and SmallSat-based Mission Concepts,” IEEE Aerospace Conference, Big Sky, MT, 2015.

9 Abbreviations, Acronyms, and Nomenclature

6U	CubeSat with 6 10×10×10 cm cubic units
ACS	Attitude Control System
ADCS	Attitude Determination and Control System
ADV	adverse tolerance (in link budget tables)
AL	activity lead
AM	ante-meridien
AIAA	American Institute of Astronautics and Aeronautics
AMMOS	Advanced Multimission Operations System
ANSI	American National Standards Institute
ANT	antenna
API	application programming interface
Apr	April
ASTERIA	Arcsecond Space Telescope Enabling Research in Astrophysics
AZ	azimuth
β	beta (angle)
BCH	Bose-Chaudhuri-Hocquenghem codes
BCT	Blue Canyon Technology
BPSK	binary phase shift keying
C, C++	programming languages
CAD	computer aided design
CAM	Command Approval Meeting
CCSDS	Consultative Committee for Space Data Systems
C&DH	command and data handling
CIC	Cell-Interconnect Coverglass
cm	centimeter
CM	configuration management
CMD	command
CMF	command file
CMOS	complementary metal-oxide-semiconductor
COM	communication, command
COTS	commercial off the shelf
CRS	Commercial Resupply Services
CSR	CubeSat Radio
CSR-SDR-SS	CubeSat Radio-Software Defined Radio-S/S band (Vulcan designation)
CSV	comma-separated values
dB	decibel

dB _i	decibel with respect to isotropic antenna
dB _K	decibel with respect to 1 K
dB _m	decibel with respect to 1 mW
dB _W	decibel with respect to 1 watt
dBW/Hz	decibels referenced to watts per hertz
Dec	December
deg	degree
DESCANSO	Deep Space Communication and Navigations Systems Center of Excellence
E_b/N_0	Bit Energy (E_b) divided by Spectral Noise Density (N_0)
EIA	Electronic Industries Alliance
EIRP	equivalent isotropic radiated power
EL	elevation
EMI	electromagnetic interference
ENG	engineering
EOL	end of life
EOM	end of mission
EPS	Electrical Power System
EST	Eastern Standard Time
EVR	event verification record
F	frequency
F'	F prime
FAV	favorable tolerance (in link budget tables)
Feb	February
FEC	forward error correction
FIPS	Federal Information Processing Standard
FM1, FM2	flight model 1 or 2
FOV	field of view
FPGA	field-programmable gate array
FSW	flight software
g	gram
g	acceleration equal to Earth surface force of gravity (9.8 m/s^2)
G_t, G_r	antenna transmit gain, receive gain (in link budget tables)
GDS	Ground Data System
GEVS	General Environmental Verification Standard
GHz	gigahertz
GPIO	general purpose input/output
GPS	Global Positioning System
G_{rms}	G, root-mean-square (unit of acceleration)

GSE	ground support equipment
G/T	ratio of antenna gain to receiver noise temperature
H ₂ O	moisture loss (in link budget table)
HORZ	horizontal polarization
Hz	Hertz
ISS	International Space Station
ICD	interface control document
IMG	image
IMU	inertial measurement unit
I/Q	in-phase and quadrature signal components
I-CH	in-phase channel
J	jack
Jan	January
JEM	Japanese Experiment Module
JPEG	Joint Photographic Experts Group, also file extension for lossy graphics file
JPG	file extension for a lossy graphics file
JPL	Jet Propulsion Laboratory
JSON	JavaScript object notation
JSPOC	Joint Space Operations Center
Jul	July
Jun	June
K	Kelvin
Kbps	kilobits per second
kg	kilogram
KHz	kilo-Hertz
km	kilometer
Ku-band	frequency band from 12 GHz to 18 GHz
L1	Level 1 (requirement)
LDAP	Lightweight Directory Access Protocol
LEO	Low Earth Orbit
LGA	low gain antenna
LHCP	left hand circularly polarized
LNA	low noise amplifier
m	meter
Mar	March
MHz	mega-Hertz
mm	millimeter
MM	mission manager

Mbps	megabits per second
MMCX	Micro Miniature CoaXial connector
MOAM	Mission Operations Assurance Manager
MOC	Mission Operations Center
MOS	Mission Operations System
MSP	memory signal processor
Msp/s	megasymbols per second
MST	Mission Scenario Test
MSU	Morehead State University
NASA	National Aeronautics and Space Administration
NIST	National Institute of Standards and Technology
NoOp	no operation
NORAD	North American Aerospace Defense Command
Nov	November
NRZ	non return to zero
NRZ-L	non return to zero level
NTIA	National Telecommunications and Information Administration
O ₂	oxygen loss (in link budget tables)
OCT	October
OpenMCT	Open Mission Control Technologies (open source software)
OQPSK	offset quadrature phase shift keying
ORR	Operational Readiness Review
ORT	Operational Readiness Test
OVC	over voltage current protection
OS	Operating System
PA	power amplifier
PCS	Pointing Control System
PDT	Pacific Daylight Time
PID	proportional derivative integral
PNG	portable network graphics (extension for a lossless graphics file)
POL	polar axis
PPM	parts per million
P-POD	Poly-Picosatellite Orbital Deployer
pppd, PPPD	point-to-point protocol daemon
PRT	platinum resistance thermometer
PST	Pacific Standard Time
PWR	power
Q-CH	quadrature channel

R	data rate (in link budget tables)
REPO	repository
RF	radio frequency
RHCP	right hand circularly polarized
RT, RLT	real time
RMS	root mean square
RS	Reed Solomon (coding or encoded)
RS-232	ANSI Recommended Standard 232
RS-422	ANSI Recommended Standard 422
RS-433	ANSI Recommended Standard 433
RS-485	ANSI Recommended Standard 485
RT400	Real Time 400
RT Logic	Kratos Real Time Logic (company)
RX	receive or receiver
S-band	frequency band that includes ASTERIA's receive/transmit frequencies (2090 to 2280 MHz)
S/C	spacecraft
S/S	S-band uplink / S-band downlink
SCET	spacecraft event time
SCID	spacecraft ID
SDR	software defined radio
SHA	secure hash algorithm
SO	spacecraft operator
SPI	serial peripheral interface
S/S	S-downlink/S-uplink
SSPA	solid state power amplifier
STK	Systems Tool Kit (formerly Satellite Tool Kit)
T400	RT Logic modem
TAR	Tape ARchiving (in Unix, etc.)
TCL	Tool Command Language
TCP	transfer control protocol
TDL	tactical downlink
TGZ	compressed TAR archive file (.tgz)
THM	thermal
TLE	NORAD Two-line element
TO	testbed operator
TOL	tolerance (in link budget tables)
T/R	transmit/receive
T _s	system noise temperature (in link budget tables)

TX	transmit
UHF	ultra high frequency (ranges between 300 MHz and 3 GHz)
USB	universal serial bus
UTC	Universal Time Coordinated
UTCG	Universal Time code generator
UTJ	Ultimate Triple-Junction
V	volt
V_{dc}	voltage direct current
Var	variance (in link budget tables)
VERT	vertical polarization
VSWR	voltage standing wave ratio
W	Watt
WISE	Wide-field Infrared Survey Explorer
WTCCS	WISE Telemetry Command and Communications System
XACT	Flexible Attitude Control Technology